Energy Research and Development Division
FINAL PROJECT REPORT

INTEGRATING BIOENERGETICS, SPATIAL SCALES, AND POPULATION DYNAMICS FOR ENVIRONMENTAL FLOW ASSESSMENTS

Prepared for: California Energy Commission
Prepared by: University of California, Santa Barbara

MARCH 2011
CEC-500-2013-139

PREPARED BY:

Primary Author(s):
Roger Nisbet
Kurt Anderson
Laurie Pecquerie
Lee Harrison

University of California, Santa Barbara
Department of Ecology, Environment, and Marine Biology
Santa Barbara, CA 93106

Contract Number: UC MRA-061

Prepared for:

California Energy Commission

Joe O'Hagan
Contract Manager

Linda Spiegel
Office Manager
Energy Generation Research Office

Laurie ten Hope
Deputy Director
ENERGY RESEARCH AND DEVELOPMENT DIVISION

Robert P. Oglesby
Executive Director

ACKNOWLEDGEMENTS

The authors wish to thank Alison Amenta for literature review on Chinook, Leah Johnson and John Williams for very helpful discussions. We also thank Allison Kolpas and Jonathan Sarhad for providing technical assistance and Margaret Simon for assisting with computational tasks and report preparation. Steven Lindley, Jill Lancaster, Andrew Paul, and three anonymous reviewers provided extremely helpful comments that improved the quality of this report. We also thank Cincin Young for patiently assisting us with budget and final report submission.

PREFACE

The California Energy Commission Energy Research and Development Division supports public interest energy research and development that will help improve the quality of life in California by bringing environmentally safe, affordable, and reliable energy services and products to the marketplace.

The Energy Research and Development Division conducts public interest research, development, and demonstration (RD&D) projects to benefit California.

The Energy Research and Development Division strives to conduct the most promising public interest energy research by partnering with RD&D entities, including individuals, businesses, utilities, and public or private research institutions.

Energy Research and Development Division funding efforts are focused on the following RD&D program areas:

- Buildings End-Use Energy Efficiency
- Energy Innovations Small Grants
- Energy-Related Environmental Research
- Energy Systems Integration
- Environmentally Preferred Advanced Generation
- Industrial/Agricultural/Water End-Use Energy Efficiency
- Renewable Energy Technologies
- Transportation

Integrating Bioenergetics, Spatial Scales, and Population Dynamics for Environmental Flow Assessment is the final report for the Research on Instream Flow Determinations for Hydropower Applications in California project (contract number UC MRA-061) conducted by Universiy of California, Santa Barbara. The information from this project contributes to Energy Research and Development Division's Energy-Related Environmental Research Program.

For more information about the Energy Research and Development Division, please visit the Energy Commission's website at www.energy.ca.gov/research/ or contact the Energy Commission at 916-327-1551.

ABSTRACT

Approximately half of California's hydropower dams are scheduled to be relicensed over the next 15 years. The number of projects, the cost of the licensing process, and the increased appreciation of stream ecosystem complexity highlight the need for better methods of assessing and mitigating the ecological impacts of stream flow alterations from hydropower operations.

This goal of this research was to advance new approaches for assessing the ecological impacts of flow alterations. The research objectives were to formulate and evaluate a full life cycle model for Pacific salmon based on the Dynamic Energy Budget theory and to perform simulations to guide simplified representations of flow-mediated dispersal of benthic macroinvertebrates that comprise the major food source of young salmon. The full life cycle model was based on a theory predicting how physiological processes and transitions between life stages vary among taxonomically similar species. These predictions were tested using literature data from five Pacific salmon species. Observed patterns at the embryo and spawning adult stages were well captured by the model and supported the validity of modeling all the different life stages of Pacific salmon using a common framework. The flow simulations used a validated hydraulic model of the two-dimensional flow field through a restored region of the Merced River. A particle tracking module described the transport of benthic macroinvertebrates. Model performance was well approximated with a much simpler one-dimensional model, although the model overestimated average dispersal distances. The project team identified two areas of immediate potential application of the Dynamic Energy Budget model. It could be extended to describe the effects of oxygen stress on embryonic development and growth of the youngest fish. It could also be used with temperature data to reconstruct histories of food availability from scales or otoliths, which are small carbonate structures from the inner ear.

Keywords: *Oncorhynchus* species, life cycle, intra/inter-specific comparison, bioenergetics, dynamic energy budget, hydrology, modeling, macroinvertebrates, dispersal, drift transport, spatial dynamics, length scale

Please use the following citation for this report:

Nisbet, Roger; Kurt Anderson; Laurie Pecquerie; Lee Harrsison. (University of California, Santa Barbara). 2011. ***Integrating Bioenergetics, Spatial Scales, and Population Dynamics for Environmental Flow Assessment.*** California Energy Commission. Publication number: CEC-500-2013-139.

TABLE OF CONTENTS

LIST OF FIGURES

LIST OF TABLES

EXECUTIVE SUMMARY

Introduction

Riverine systems are characterized by dynamic feedbacks among system components, a high degree of spatial and temporal variability, and connectivity between habitats. A major challenge is to identify ways of recognizing these characteristics in practical methodology for environmental flow assessment. This is especially true as significant portions of non-federal hydropower projects in California face relicensing by the Federal Energy Regulatory Commission. These permits are issued for 30 to 50 years so it is critical that the best science inform the relicensing process.

Some of this report's authors and others have recently proposed that process-oriented ecological models that consider dynamics across scales and levels of biological organization can contribute to flow regime management (*Frontiers in Ecology and Environment* 4: 309-318, 2006). In that review they also identified areas where further research is required before process-based ecological models that simulate the biological and ecological processes and temporal variability that operate to link the ecosystem together will make an effective contribution to environmental flow assessments. This report summarizes progress on research that addressed two of these areas: (1) improving bioenergetic-based (energy flow through living organisms) models for the study of population dynamics; and (2) testing models of the effects of spatial variability on population responses to changes in flow regime.

Previous bioenergetic approaches usually focused on the impact of the environmental conditions on a single life stage. Yet performance at a given life stage is known to impact subsequent life stages and hence the dynamics of the population. This issue is particularly relevant for anadromous fish species with largely unobservable ocean stages. Anadromous fish species such as salmon are born in fresh water but spend most of their lives in the sea and return to fresh water to spawn.

Changes to flow regimes can also have profound effects on both the spatial structure and total availability of physical habitat. Theory describing explicit links between population dynamics of target species and changes in physical habitat at different spatial scales is available but is seldom applied.

Project Purpose

The overarching goal of this research was to contribute to new conceptual frameworks based on process-based models that differ from and are complementary to habitat-based metrics. In a one-year project it was not possible to develop tools ready for application in the Federal Energy Regulatory Commission relicensing and decision-making processes. Researchers hoped to propose an essential first step in using recent advances in theory as the basis for new decision-making tools.

There were two broad objectives. The first objective was to formulate and evaluate a full life cycle model for Pacific salmon based on Dynamic Energy Budget theory. This theory would describe the uptake and use of energy and nutrients and the consequences for maintenance,

growth, maturation and reproduction throughout an animal's life cycle. This work would include:

- Synthesizing data from five salmon species to test the assumptions and predictions of the Dynamic Energy Budget model.
- Using the information from the data synthesis to parameterize the model for Chinook salmon (*Oncorhynchus tshawytscha*).
- Calculating the sensitivity of salmon population growth rates to changes in food delivery rates that in turn are influenced by changes in flow regime.

The second objective was to perform simulations that could guide appropriate representations of flow-mediated dispersal and resulting distributions of benthic macroinvertebrates that comprise the major food source of salmon. This work would include:

- Using a two-dimensional hydraulic model of a restored section of the Merced River to describe the transport and settlement of macroinvertebrates that are the primary food source for young salmon.
- Evaluating the validity of models based on one-dimensional approximations of Merced River hydrology in describing flow variability and resulting transport and distribution of macroinvertebrates.
- Exploring the influence of macroinvertebrate transport in a variable flow environment on dispersal distributions and related characteristic length scale calculations for the Merced River.

Project Results

The team formulated a full life cycle model. Dynamic Energy Budget theory makes predictions on how rates of physiological processes and transitions between life stages vary among taxonomically similar species. These predictions were tested using literature data from five salmon species: pink, chum, sockeye, Coho and Chinook. Observed patterns at the embryo stage and the spawning adult stage were well captured by the model. Initial discrepancies between data and model predictions for several variables were resolved by adjusting one parameter value. The findings supported the validity of modeling all the different life stages of Pacific salmon in a common framework.

The simulation results for Chinook broadly agreed with experimental studies on Chinook growth and development rates. However, the fecundity patterns that were initially predicted did not match the field data. Further work will refine the parameter estimates with additional model assumptions relating to food availability and allocation of energy to reproduction.

The methodology for calculating the sensitivity of salmon population growth rate to changes in food delivery rate was put in place, but the calculations required completion of the next round of parameter estimation for Chinook, as well as a more detailed description of survival.

A hydraulic model (MIKE 21 FM) of the two-dimensional flow field through the lower 1.7 kilometer (km) of a restored region of the Merced River was calibrated and validated. A particle tracking module was added to describe the transport of benthic macroinvertebrates. The transport component was parameterized using a mix of literature data and measurements from previous studies in the Merced region. The trajectories of simulated macroinvertebrates were dominated by the high velocity core under all discharge conditions. The model generated distributions of dispersal distances qualitatively consistent with literature observations using assumptions on dispersion.

The two dimensional (2D) flow environment was collapsed into a one dimensional (1D) representation that allowed its use in population dynamic models for benthic invertebrates previously developed by two members of the project team. Simulations suggested that distributions of macroinvertebrates would show a strong inverse relationship with flow velocity whose strength is set by other model parameters, especially the rate at which drift dispersal is initiated and the rate at which dispersers settle to the benthos. Surprisingly, these parameters had minimal effects on benthic distributions over the range of parameters examined.

Estimates of dispersal distributions from the 1D and 2D models were compared and were qualitatively similar. One characteristic length scale (the average dispersal distance) was overestimated in the 1D model under most parameter combinations. This result was likely due to an incomplete representation of how dispersion in the 2D model influenced settlement in the 1D model.

The outcomes from this one-year project represented incremental progress toward the broad goal of developing applicable process-based models. The project team identified two areas of immediate potential application of the Dynamic Energy Budget model. It could be extended to describe the effects of oxygen stress on embryonic development and the growth of the youngest fish. It could also be used in conjunction with temperature data to reconstruct histories of food availability from scales or otoliths. The flow model could be extended to allow improved representations of food delivery to young salmon by including additional flow complexity and macroinvertebrate behavior.

The immediacy of assessments in California of many dam-induced alterations to flow and the short duration of this research project implied that the primary outcome of the research would be limited to incremental improvements in instream flow needs methodology. Many habitat-based methods require metrics such as weighted usable area that attempt to measure habitat quantity and/or quality as a proxy for management concerns such as fish population density or viability. The new research complemented this in two distinct ways:

- The bioenergetic modeling sidestepped the problems of identifying "suitable" habitat by focusing directly on growth of young fish as well as estimating the consequences in later life stages of stress in early life. This approach facilitated new ways of directly estimating food availability for fish.
- A high-resolution temperature and flow model for the Sacramento River could be coupled to the Chinook embryo Dynamic Energy Budget model to examine how (for

example) operation of Shasta Reservoir impacts incubating winter-run Chinook eggs in the reaches of the Sacramento River below the dam.

Contiguity of habitat will have a major impact and the response length calculations could guide appropriate choices for the size of "minimal" habitat units for habitat-based evaluations.

Project Benefits

Hydroelectric power supplies a substantial portion of California's electricity and approximately half of California's hydropower dams are scheduled to be relicensed over the next 15 years. This project developed new approaches for assessing the ecological impacts of stream flow alterations on Pacific salmon. The ecological impacts of hydropower dams will be a key consideration in decisions about whether to relicense these dams. Hydropower does not produce greenhouse gases so the continued operation of California's dams will help to mitigate climate change.

CHAPTER 1:
Ecological dynamics and instream flow assessments

Instream flow assessments (IFAs) have traditionally relied on simple hydrological and habitat-association methods to predict how changes in flow will affect the viability of instream populations and communities. Common are hydrological methods that allocate discharge based on historic averages or physical habitat models that link habitat "suitabilities" for target species with hydraulic models that simulate availability of physical habitat as it varies across discharge (e.g., PHABSIM; Anderson et al. 2006b,Locke et al. 2008). These traditional IFA methods only explicitly consider the tolerance of individuals in target populations to general flow and habitat variables (see Figure 2 in Anderson et al. 2006 – reproduced below as Figure 1). Yet preserving the viability of managed populations is fundamental to modern IFA thinking. This requires explicitly linking changes in the flow regime and habitat availability with population dynamics, as viability necessitates that additions of new individuals to the population exceed losses over the long term.

Figure 1: Instream Flow Assessment Methods

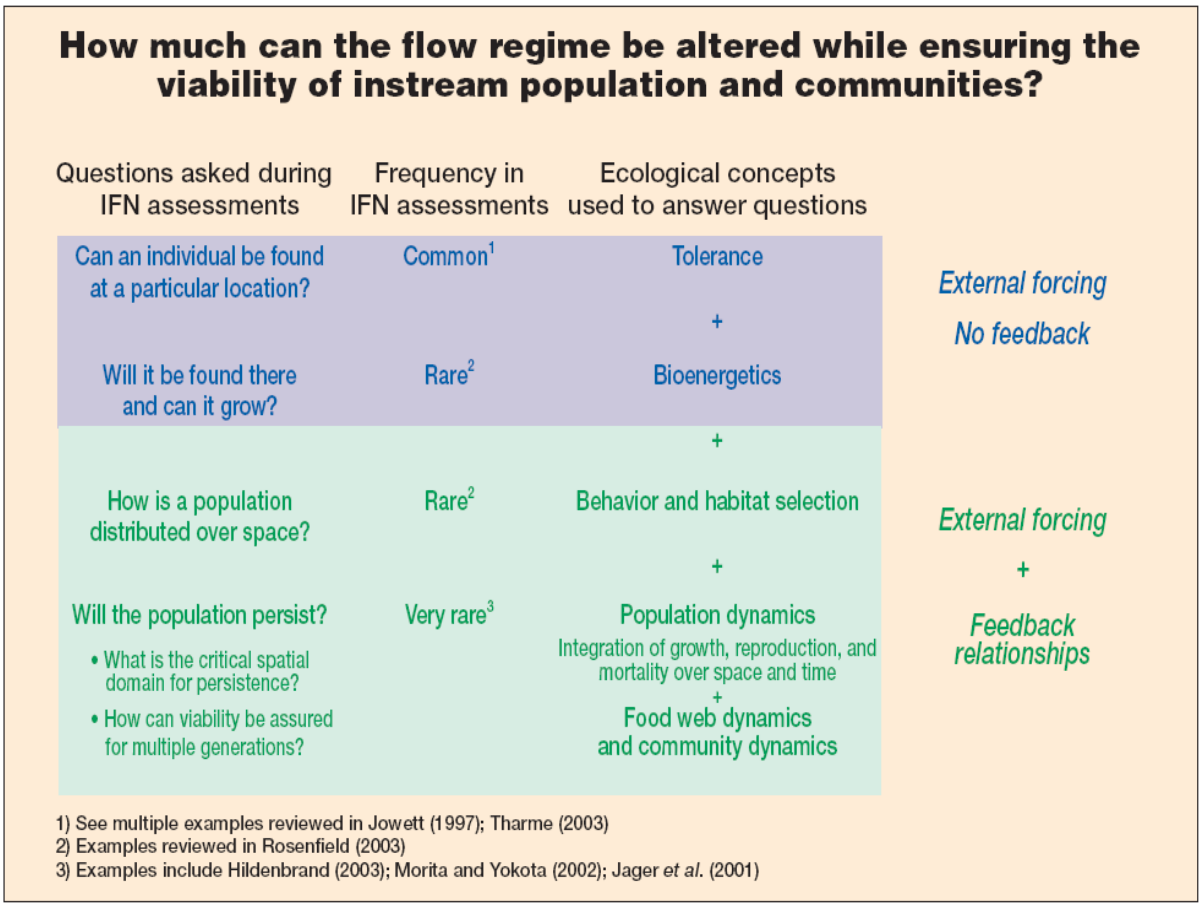

Source: From figure 2 in Anderson et al. 2006

Figure 1 shows how IFN methods based on ecological ideas of tolerance and bioenergetics treat all aspects of the biotic and abiotic environment other than the focal organism as external forcing mechanisms, and lack feedbacks between system components. Some habitat selection methods and most population and community dynamics models allow consideration of external forcing by the physical environment, as well as feedbacks between biotic and abiotic components. Dynamic models that integrate rate processes are best equipped for investigating population viabilities under changing flow regimes.

In a review of ecological dynamics pertinent to IFA methodology, Anderson et al. (2006) argued that assessing flow-related changes in viability involves considering feedbacks among dynamic physical and ecological processes that may change in strength, both temporally and spatially. Furthermore, they argue that an important impediment to progress is the lack of a methodological framework to integrate ecological dynamics into IFAs. These recommendations are echoed in a recent publication of the Instream Flow Council (Locke et al. 2008). Figure 14-2 of Locke et al. (also reproduced below as Figure 2) lucidly summarizes the many steps involved in connecting flow to population change, thereby highlighting the complexity of the connections between the point of management action (control of flow regime) and the themes of management concern such as population viability.

Anderson et al. (2006) advocated four research questions whose resolution will markedly advance our ability to address the range of issues involved in assessing instream flow needs. Here, we restate these recommendations: (1) models of fish bioenergetics must be improved to integrate the temporal and spatial variation experienced over the entire lifetime of a fish; (2) tools that integrate models of large-scale physical habitat processes with population dynamic models must be more fully developed to address landscape-level persistence; (3) methods must be advanced to disentangle the combined effects of spatial and temporal variability on population and community responses to changes in the flow regime; and (4) understanding how river and instream ecological states emerge from transient rather than long-term responses to temporal variability, and how these responses are altered by the presence of spatial variability, is crucial. These recommendations are consistent with more recent recommendations on research priorities by Locke et al. (2008).

The grand aim of developing completely new process-based methodology for IFAs as outlined by Anderson et al. and Locke et al. will require an enormous sustained effort. However, complements to habitat based methods can both serve to address immediacy of assessments in California of many dam-induced alterations to flow and provide incremental improvements towards some of the goals outlined above. The work we report here has been conducted in this spirit. In the short-term, we propose conceptual frameworks that differ from and are complementary to habitat-based metrics that attempt to measure habitat quantity and/or quality as a proxy for management concerns such as fish population density or viability. Our work relates to two of the links identified in the Figure from Locke et al.: habitat-to-individual and

Figure 2: Links to Mechanistically Understanding Instream Flow Needs

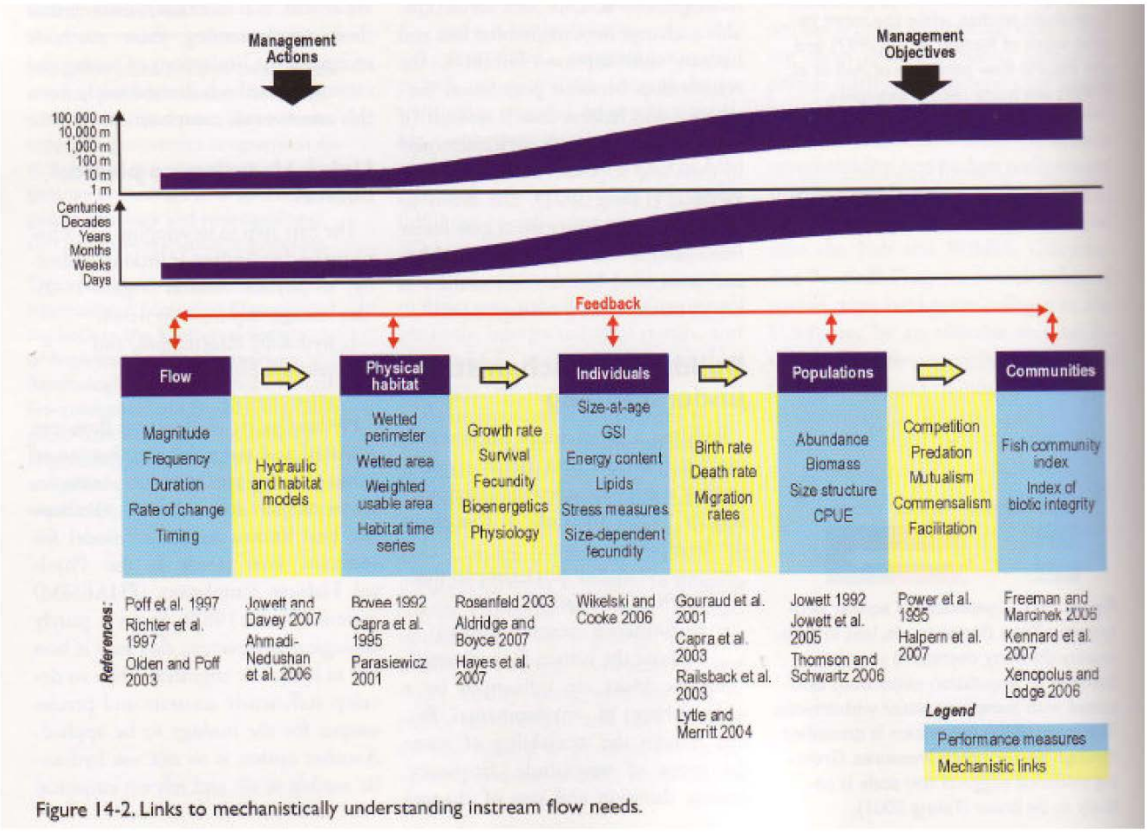

Figure 14-2. Links to mechanistically understanding instream flow needs.

Source: From figure 14.2 of Locke et al., 2008.

individual-to-population. In a one-year project, we did not aim to develop new tools ready for application in the FERC relicensing and decision-making processes. Rather, the research reported here is an essential first step in using recent advances in theory as the basis for these new decision-making tools. We focus on two distinct themes:

1. Dynamic energy budget models of salmonids. Changes in energy balances directly affect fish growth, mortality, and reproduction, which are key components of viability. Standard bioenergetics modeling links flow-related factors such as swimming costs or rates of drift provision to individual habitat choice or habitat quality, but ignore population-level consequences of changes in growth, fecundity, and survivorship (Rosenfeld 2003).

   Dynamic energy budget (DEB) models provide an alternative means of linking fish bioenergetics to population viability (Kooijman 2010b; Nisbet et al. 2000a). DEB models describe rates at which individuals distribute food energy among the competing demands of physiological maintenance, growth, reproduction, and survival; these costs in turn depend on both the state of the organism and its environment. They have the

potential to provide superior measures of "suitable" habitat by simultaneously describing embryonic and growth of young fish as well as estimating the consequences in later life stages of stress in early life.

In this study, we focus on parameterizing a DEB model using data from various salmon species. Interspecific scaling of physiological parameters in DEB models is well understood (Kooijman 2010), opening the possibility of using data on a range of salmon species to provide a baseline "null" model that can be altered for specific applications. Although not described in this report, DEB models describe many other aspects of metabolic organization, with important future application being models of the effects of oxygen stress in redds, and, more broadly, changes in water quality during downstream migrations.

2. Spatial scales of hydrodynamic and ecological processes. Assessments of weighted usable area in habitat-based methods such as PHABSIM have at their center characterizations of spatial variability in fish habitat and its response to temporal changes in the flow regime. However, as we have stated before, these methods do not explicitly link such variability to changes in fish viability. This leaves us with the problem of how to predict the responses of instream populations to temporal and spatial variability in flow and other environmental variables.

   The spatial scales over which variability in habitat and other processes regulate population dynamics can be described by characteristic length scales. These length scales emerge as properties of a community of organisms interacting dynamically with their environment (see Table 2 of Anderson et al. (2006) that lists many potentially relevant spatial scales, reproduced below as Figure 3). Characteristic length scales are especially important for streams and rivers, since longitudinal transport of materials and organisms may influence population dynamics and community patterns. By quantifying the effects of spatial variability on processes important to instream populations, length scales can provide a useful means to compare the spatial scales of management effects to those that are relevant to preserve viability.

   Previous research on spatial scales demonstrates that both population viability and spatial variation in population density are not likely to simply reflect the weighted sum or integral of "suitable" habitat (Speirs and Gurney 2001; Anderson et al. 2005; Pachepsky et al. 2005; Lutscher et al. 2006; Lutscher et al. 2007; Nisbet et al. 2007; Anderson et al. 2008). However, characteristic length scales are likely to reflect a strong influence of flow conditions (Speirs and Gurney 2001; Anderson et al. 2005; Diehl et al. 2008), particularly as mediated by dispersal in the drift.

These themes define two broad objectives:

1. To formulate and evaluate a full life cycle model for Pacific salmon based on Dynamic Energy Budget (DEB) theory. This work to include:

- Synthesis of data from five salmon species to test the assumptions and predictions of the DEB model
- Use of information from the data synthesis to parameterize the model for Chinook salmon (*Oncorhynchus tshawytscha*)
- Calculations of sensitivity of salmon population growth rate to changes in food delivery rate that in turn are influenced by changes in flow regime

2. To perform simulations that can guide appropriate representations of flow-mediated dispersal and resulting distributions of benthic macroinvertebrates that comprise the major food source of salmon. Specifically:
    - To use a two-dimensional hydraulic model of a restored section of the Merced River to describe the transport and settlement of macroinvertebrates that are the primary food source for young salmon
    - To evaluate the validity of models based on one-dimensional approximations of Merced River hydrology in describing flow variability and resulting transport and distribution of macroinvertebrates
    - To explore the influence of macroinvertebrate transport in a variable flow environment on dispersal distributions and related characteristic length scale calculations for the Merced River

Beyond our two immediate areas of focus, we anticipate that the research will have longer-term value as a contribution to the development of a process-based methodology. Our work relates to items 1) and 3) from Anderson et al. reiterated above, as well as to two of the links identified in Locke et al.: habitat-to-individual and individual-to-population. As such it can lay the foundation for further work, especially work that takes account of some of the key feedback mechanisms inherent in linking individual and population level dynamics.

The rest of this document is organized into three chapters. In chapter 2, we describe a parameterized DEB model for salmon. In chapter 3, we describe simulations of hydrodynamics and food delivery rates in the Robinson Reach using both at 2D flow model and a 1D approximation. We end in Chapter 4 with a set of conclusions and recommendations for future research.

Figure 3: Ecological Feedback Processes

Table 2. Ecological feedback processes set the characteristic length scales that determine system responses to spatial environmental variability; examples of ecological factors that could influence characteristic length scales are listed below

Parameter	*Ecological factor*	*Factor effects*	*Example references*
(a) Nutrient spiraling			
Uptake length	Consumers	Increase nutrient transport by reducing periphyton mats	Mulholland *et al.* 1994
	Zones of slow water passage	Capture nutrient molecules, increase uptake	Mulholland *et al.* 1994, 1997
	Discharge	Increases downstream displacement	Meyer and Likens 1979; Fisher *et al.* 1998
Turnover length	Primary production rate	Production during succession leads to high retention of nutrients in biomass	Grimm 1987
	Consumers	Transport nutrients through dispersal; reduce turnover rate in periphyton; assimilating and egesting nutrients	Wallace *et al.* 1982; Grimm 1988; Mulholland *et al.* 1994
	Top consumers	Large nutrient inputs by fish death	Gresh *et al.* 2000
(b) Response length			
Emigration rate	Predation	Emigration rates increase in response to predator density, may decrease if response is hiding; predators redistribute to areas of high prey (or drift) density	Englund *et al.* 2001; Grossman *et al.* 2002
	Resource availability	Rates increase with decreased biomass; depress biomass high densities; track biomass	Kohler 1985; Hart and Robinson 1990; Roll *et al.* 2005
	Physical habitat	Dislodgement and sloughing; presence of flow refugia	Allan 1987; Peterson 1996; Winterbottom *et al.* 1997
	Growth	Cell division and photosynthetic activity, size lead to sloughing in diatoms; good condition trout fry less dispersive	Müller-Haeckel 1971; Elliott 1987b
	Parasitism	Parasites induce increased and decreased drift rates in their hosts	Vance 1996; Wellnitz *et al.* 2003
	Competition	Aggressive interactions and density increases emigration	Hildrew and Townsend 1980; Walton *et al.* 1977
	Grazing	Dislodgement by foraging	Lamberti and Moore 1984
Dispersal length	Current velocity	Proportional to velocity; response may be both passive and active; may not track variation because of active swimming	Elliott 1971; Cambell 1985; Lancaster *et al.* 1996
	Condition	Older trout fry in good condition return to bottom faster than young and/or poor condition fry	Elliott 1987b
Mortality rate	Grazing and predation	Consumption by grazers or predators may lead to density-dependent mortality rates	Kratz 1996; Diehl *et al.* 2000; Englund *et al.* 2001
	Competition	Density-dependent population regulation from competition for habitat or food	Elliott 1987a; Marchant and Hehir 1999
	Parasitism	May include increased or decreased secondary exposure to predators	Vance 1996; Kohler and Wiley 1997; Wellnitz *et al.* 2003
	Emersion	Lack of photosynthesis	Poff and Ward 1990
	Dessication	Reduction in primary producer biomass	Stanley and Fisher 1992

Full citations for references are provided in Web Appendix A

From Anderson et al. (2006) Table 2

CHAPTER 2:
Modeling the life cycle of Pacific salmon using Dynamic Energy Budget theory

2.1 Abstract

To determine the response of Pacific salmon populations to environmental change, we need to understand impacts on all life stages. An integrative approach is particularly challenging for Pacific salmon that use river, estuarine and marine environments. Here, a bioenergetic model is developed that predicts development, growth and reproduction of a Pacific salmon, from an egg to a reproducing female and its eggs, in a dynamic environment. This model uses Dynamic Energy Budget (DEB) theory to predict how parameters vary among five species of Pacific salmon: pink, sockeye, Coho, chum and Chinook. Supplemented with a limited number of assumptions on anadromy and semelparity, the model reproduces the differences in egg size, fry size and fecundity among these five species. The model is then calibrated on available data on development, growth and reproduction for Chinook salmon. The main life history traits of this species are well reproduced, from the egg to the adult stages. This model can thus be used to test the impact of different river conditions during the early life stages on the following life stages and to make projections of long-term populations growth rates under these environmental conditions.

2.2 Introduction

The *Oncorhynchus* genus of the Salmonidae family includes more than 15 species of salmon and trout distributed throughout the Pacific, in Asian, Oceanian and North American rivers and lakes. Two major features characterize the salmon species of this genus (Quinn 2005): *anadromy*, i.e., their ability to migrate to the ocean after rearing as young juveniles in rivers and migrate back to the same river to spawn, and *semelparity* – i.e., they only spawn once in their lifetime and die few days later. These specificities make Pacific salmon species particularly sensitive to anthropogenic factors – such as river uses (e.g., dams, irrigation), but also other stresses such as temperature fluctuations, oxygen depletion or pollution at critical stages in their life cycle – especially as spawning adults and as eggs and young juveniles. The primary aim of the work reported in this chapter, already detailed in chapter 1, is to develop theory that is relevant to instream flow assessments, while recognizing that any impacted populations experience multiple stresses. Here, we explore the feasibility of an integrative approach that includes the full life cycle of salmon in order to generate projections of the effects of environmental change on long-term population growth rates.

Bioenergetic approaches have been developed previously to study the impact of environmental conditions on salmonids (Stewart and Ibarra 1991; Brodeur et al. 1992; Cech and Myrick 1999; Ballantyne et al. 2003; Beauchamp et al. 2004; Madenjian et al. 2004; Aydin et al. 2005), but these approaches are often specific to a particular size range of individuals and it has been shown that the transfer of these models to other size ranges and/or other species often result in biased predictions when compared to data (Trudel et al. 2004; Trudel et al. 2005; Peterseni et al. 2008).

However, instream flow conditions that are impacted by dams influence the status of several species and for each species there are distinct, well-documented subpopulations. Given limited resources for empirical work, this points to a need to investigate the extent to which models and model parameters are in some sense "transferable" among species and subpopulations. This effort can ensure that limited experimental and field work can be used cost-effectively by focusing effort on those species and habitat specific properties that turn out not to be "transferable".

We characterize the life cycle of Pacific salmon species using Dynamic Energy Budget (DEB) theory (Nisbet et al. 2000b; Kooijman 2010a). Kooijman and collaborators developed a "standard" DEB model that, to our knowledge, is the simplest model that describes the full life cycle of an organism in a variable environment (Sousa et al. 2010). DEB theory implies rules for covariation of parameter values among species (see for example, Kooijman 2010, table 8.1). These rules are referred to as "body size scaling relationships". Their validity is here evaluated for the main life history traits of five species of Pacific salmon that occur in North America: pink (*Oncorhynchus gorbuscha*), sockeye, (*O. nerka*), coho (*O. kisutch*), chum (*O. keta*), and Chinook (*O. tshawytscha*).

The standard DEB model and the body size scaling relationships yield a null model for the life cycle of Pacific salmon. The remaining discrepancies between model predictions and observations can then be interpreted in terms of differences in life-history strategy and specific adaptations of these species to their environment. These differences can be included in species-specific DEB models.

We first identify which characteristics are common to Pacific salmon species and in particular which events characterize their life cycle. We then present the standard DEB model for a "generalized Pacific salmon". We describe the body-size scaling relationships and their predictions for several life-history traits for species of the same genus but different maximum sizes. We compare these predictions with data that we reviewed from the existing literature on Pacific salmon. We discuss which rules should complement the standard DEB model to model the life cycle of pacific salmons in a more realistic way and point out two future model applications with potential for informing management decisions on changes in flow regime.

2.3 Generic characteristics of Pacific salmon

2.3.1 Features common to salmonid species

When compared to other freshwater fish, salmonids, which includes salmon, trout and char, share four characteristics highlighted by Quinn (2005):

- salmonids grow rapidly but do not live long,
- salmonids are generalists and can occupy a large variety of freshwater and oceanic habitats. In rivers, they can feed on insects and zooplankton, and large individuals could feed on fish and larger invertebrates. At sea, their diet is composed of

zooplankton, macro-invertebrates (krill, squid) and small schooling fish (anchovy, herring, sand lance…),

- female salmonids have very large eggs (diameter > 4mm), but they produce fewer eggs at a given size relative to other freshwater fishes (Wootton 1984; Quinn 2005).

- female salmonids display parental care (egg burial and nest protection).

2.3.2 Specific features of Pacific salmon life cycle

Pacific salmon species exhibit three distinctive properties (Quinn 2005):

- *Anadromy*. They migrate from freshwater to saltwater and back, requiring two metamorphoses at the transitions between habitats and two substantial migrations, in particular the upstream migration to spawn, that they seem to perform without feeding, though a recent paper showed that they are able to feed on salmonids eggs, which might provide a non-negligible source of energy during this migration Garner et al. 2009.

- *Homing*. They have the ability to return to their natal rivers, thereby generating some genetic isolation between populations of the same species and permitting local adaptations to their specific environment. Specific adaptations include thermal tolerance and optimum temperature, timing of smolt, and spawning migrations. Substantial differences in life-history traits are observed among populations of the same species.

- *Semelparity*. They typically have only one reproductive event in their lifetime. Furthermore, Pacific salmon spawn in the fall, while most freshwater fishes spawn in spring in temperate regions. But as for other life-history traits, spawning timing can vary between species and populations and occur as early as July for sockeye in Alaska and as late as February for chum and coho in Washington, and year-round for Chinook in the Sacramento River.

2.3.3 Common life events among Pacific salmon

We distinguish five life events that are common among Pacific salmon species and well described in the literature. In particular, we consider the life cycle of a *female* Pacific salmon for which the connections between traits in eggs and later life stages are more easily observable. In addition, female seem to display less diverse life histories than males.

1. Eggs are normally spawned in the fall in freshwater. They are buried in a redd (gravel nest) that provides protection from predators during winter and spring.

2. In spring, when the larvae have exhausted their yolk, they emerge from the gravels as fry and start feeding. Individuals can spend few weeks to few years in rivers and lakes.

3. After undergoing substantial physiological and morphological changes, individuals migrate to the ocean as smolts. The timing of the migration is specific to the species and the population. Individuals can then spend one to several years in the ocean.
4. Similarly, after undergoing substantial physiological and morphological changes, individuals migrate back, normally to their natal river, and stop feeding as they enter freshwater. The timing of this migration is also specific to the population. Some populations enter their natal rivers several months prior spawning.
5. After migrating upstream a substantial distance, females built nests, spawn, protect their nest from disturbance from other females and die few days later.

2.4 Methods

2.4.1 Standard DEB model

The "standard" DEB model (Sousa et al. 2010) is the simplest model that describes assimilation, maintenance, development, growth and reproduction of an organism throughout *all* stages of its life cycle, in a dynamic environment. Four state variables define an individual, the structural mass M_V (C-moles), the reserve mass M_E (C-moles), the cumulative mass invested into maturity M_H and the reproduction energy buffer M_{ER} (C-moles). There are two forcing variables that characterize the environment, the temperature T (K) and the food density M_X (C-moles). For clarity, we mention that the terms "structure" and "reserve" have very precise meanings in DEB theory that differ from other subdisciplines (Kooijman 2010a; Sousa et al. 2010); however this subtlety is not important for the present work.

The principal metabolic processes in the model are illustrated in Figure 4. Assimilation is the process of transforming food into reserves. **Somatic** maintenance is the expenditure of energy to sustain living tissue and involves primarily the processes of degradation and reconstruction of structure. Growth is the production of new structure. Development is increase in complexity. Maturity maintenance is the expenditure of energy required to maintain this level of complexity.

The state variables, the parameters and the equations of the standard DEB model are given in Tables 1 and 2. Somatic maintenance is taken to be proportional to structural mass. Maturity maintenance is taken to be proportional to the amount of energy invested into development. The standard DEB model further assumes isomorphic growth, i.e., that the individual does not change in shape throughout ontogeny. If the organism is not an **isomorph** throughout **ontogeny**, surface-areas relate to volume in different ways and correction functions are added to surface area specific processes to reflect changes in how surface areas relate to volume. Temperature impacts all rates through a simple **Arrhenius function**.

The life cycle is described by three life stages: embryo, juvenile and adult. An embryo is characterized by an initial amount of reserve that is used throughout the embryo stage to fuel development, growth and maintenance processes. Once the individual has invested a particular threshold of energy into development, the individual is complex enough to start feeding, which marks "birth", the transition between the embryo and the juvenile stage.

During the juvenile stage, reserve is continuously used to fuel metabolic processes and replenished if food is available. Once the organism has invested enough energy to reach his maximum level of complexity, the energy previously invested into development is redirected to the reproduction buffer, which defines "puberty", the transition between the juvenile and adult stage. As with other terminology, the term "puberty" has an unconventional meaning in DEB theory; we use it here to retain consistency with the cited publications on the standard model.

During the adult stage, the amount of energy available for gamete production is described by the standard DEB model. The rules for the production and the release of these gametes into the environment are, by contrast, typically species-specific. The standard DEB model provides nonetheless a method to calculate the amount of energy required to produce one or several viable eggs with identical growth and development potentials as the mother, i.e., with the same parameters (Kooijman 2009). Using a simple rule that relates the condition of the offspring at birth to that of the mother (maternal effect), this method does not require additional parameters. With further calculations, it can be used to determine the fecundity of the female, i.e., the number of eggs that a female individual can produce at the time of spawning.

Table 1: State Variables, Forcing Variables and Parameters of the Standard DEB model. Rates are Given at the Reference Temperature T_1 = 293K (=20°C)

Symbol	Value	Units	Description
M_E		mmol	Reserve mass
M_V		mmol	Structure mass
M_H		mmol	Cumulated mass invested into development
M_{ER}		mmol	Reproduction buffer
X		mmol	Food density
T		K	Temperature
$f(X)$			Scaled functional response
$c(T)$			Temperature correction factor
$\{\dot{F}_m\}$	6.51	$cm^{-2}.d^{-1}$	Specific searching rate
T_A	8000	K	Arrhenius temperature
$\{\dot{J}_{EAm}\}$	$0.0413\,z$	$mmol.cm^{-2}.d^{-1}$	Maximum surface-area-specific assimilation rate
$[\dot{J}_{EM}]$	0.033	$mmol.cm^{-3}.d^{-1}$	Volume-specific somatic maintenance rate
$[M_V]$	4	$mmol.cm^{-3}$	Volume-specific structural mass
$\dot{v}$	0.02	$cm.d^{-1}$	Energy conductance
κ	0.8		Fraction of utilized reserve to growth + maintenance
y_{VE}	0.8		Yield of structure from reserve in growth
$\dot{k}_J$	0.002	d^{-1}	Maturity maintenance rate coefficient
M_H^b	$0.00005\,z^3$	mmol	Maturity threshold at birth
M_H^p	$0.3\,z^3$	mmol	Maturity threshold at puberty
κ_R	0.95		Fraction of the reproduction buffer fixed into eggs
δ_M	0.15		Shape coefficient

$L_m = \frac{\kappa\{\dot{J}_{EAm}\}}{[\dot{J}_{EM}]}$	1	cm	Maximum volumetric length
$g = \frac{\dot{v}[M_V]}{\kappa\{\dot{J}_{EAm}\}y_{VE}}$			Energy investment ratio
$K = \frac{\{\dot{J}_{EAm}\}}{y_{EX}\{\dot{F}_m\}} =$		mmol	Saturation coefficient

Table 2: Equations of the Standard DEB model.

Notations are described in Table 1.

$$\frac{d}{dt}M_E = \dot{J}_{EA} - \dot{J}_{EC} \quad (1.1)$$

$$\frac{d}{dt}M_V = \dot{J}_{VG} = (\kappa\dot{J}_{EC} - \dot{J}_{EM})y_{VE} \quad (1.2)$$

$$\frac{d}{dt}M_H = (1-\kappa)\dot{J}_{EC} - \dot{J}_{EJ} \quad \text{if } M_H < M_H^p \quad \text{, else } \frac{d}{dt}M_H = 0 \quad (1.3)$$

$$\frac{d}{dt}M_{ER} = 0 \quad \text{if } M_H < M_H^p \quad \text{, else } \frac{d}{dt}M_{ER} = (1-\kappa)\dot{J}_{EC} - \dot{J}_{EJ} \quad (1.4)$$

$$\text{with} \quad \dot{J}_{EA} = c(T)f(X)\{\dot{J}_{EAm}\}L^2 \quad \text{if } M_H \geq M_H^b \quad \text{else } \dot{J}_{EA} = 0 \quad (1.5)$$

$$\dot{J}_{EC} = c(T)\{\dot{J}_{EAm}\}L^2\frac{ge}{g+e}\left(1+\frac{L}{gL_m}\right) \quad (1.6)$$

$$\dot{J}_{EM} = c(T)[\dot{J}_{EM}]L^3 \quad (1.7)$$

$$\dot{J}_{EJ} = c(T)\dot{k}_J M_H \quad (1.8)$$

$$f(X) = \frac{X}{X+K} \quad (1.9)$$

$$c(T) = \exp\left(\frac{T_A}{T_1} - \frac{T_A}{T}\right) \quad (1.10)$$

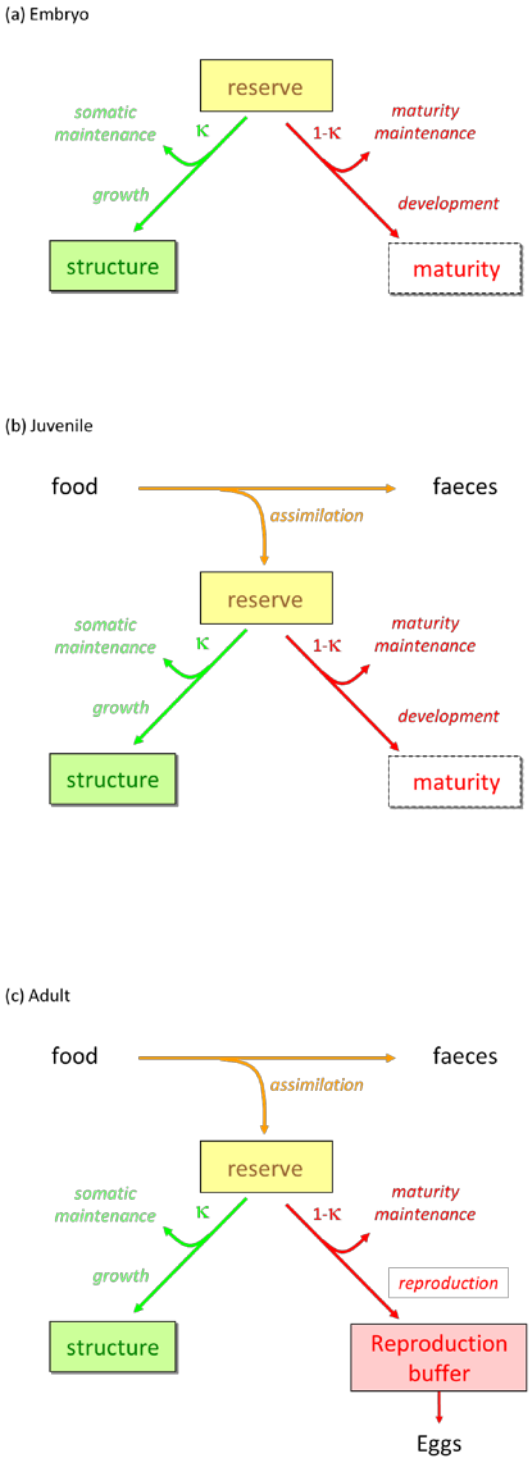

Figure 3: Schematic Representation of the Three Life Stages of a Standard DEB Model. An Embryo (a) Uses Reserve to Grow and Develop. At "birth" a Juvenile (b) Starts Feeding and at "Puberty" an Adult (c) Starts Allocating Energy to Reproduction.

2.4.2 A generic DEB model for Pacific salmon

Link between state variables and data

Many biological quantities that are relatively easy to measure, such as body mass and respiration rate have contributions from different components or processes in the model. The weight of an individual has contributions from reserves and structure, carbon dioxide production has contributions from somatic maintenance, but also from the overheads on assimilation and growth. These measured quantities are therefore not natural variables in process-based models such as the standard DEB model.

The state variables of the standard DEB model are, however, not readily measurable. For example, reserve and structure cannot be directly measured apart in most applications. Each cell is composed of both reserve and structure. The abstraction underlying the DEB concept of reserve and structure is designed to capture common patterns across taxa in a simple and generic way. But for specific applications, defining how they relate to quantities that can be easily measureable is a difficult task that needs particular attention (Kooijman et al. 2008; Lika et al. 2011).

We now discuss the relationships between quantities used in our data analysis and the variables in the DEB model.

Length. The physical length L_w (cm) i.e., the length that is measured is assumed proportional to the cube root of structural biomass. For salmon, two types of length are measured: Fork length in all stages and often postorbital-hypural length in spawning adults.

Weight. The total dry weight W and wet weight W_w of an individual are given by

$$W = w_V M_V + w_E (M_E + M_{ER}) \ , \tag{1.11}$$

$$W_w = \frac{w_V}{\kappa_{WV}} M_V + \frac{w_E}{\kappa_{WE}} (M_E + M_{ER}), \tag{1.12}$$

with κ_{WV} and κ_{WE} the fraction of water in structure and reserve respectively.

Fecundity. The number of eggs per female is given by

$$F = \frac{\kappa_R M_{ER}}{M_E^0} \quad , \tag{1.13}$$

with M_E^0 the initial amount of reserve per egg and κ_R the fraction of the reproduction buffer fixed in eggs. The method to calculate M_E^0 is given in Kooijman (2009).

Link between the different life events of a Pacific salmon and DEB stage transitions

All stage transitions are assumed to be triggered by attaining a threshold value for the maturity variable. Thus, the lengths at which an individual reaches these different thresholds can vary with its food history, and different phenotypes can be generated according to the environment experienced by the individual throughout ontogeny. In the present work, we evaluate the effect

of this model property in combination with the concept of time windows for migration and/or maturation decision as developed in life-history models (Mangel 1994; Mangel and Satterthwaite 2008).

We distinguish three types of life events:

1. Transitions that are linked solely to the state of the individual, e.g., birth, where the individual starts feeding. These transitions are similar to those considered in the standard DEB model and may be relatively easily to observe, e.g., the individual starts feeding when it emerges from the gravel. But the transition between the juvenile and the adult stage, i.e., the start of allocation of energy to the reproduction buffer, is usually unobserved.

2. Change in habitats that occur at a particular date or season, e.g., the migration to the ocean or the migration back to the river, that only involve a change in the environmental conditions experienced by the individual. These events are particularly well documented in the salmon literature. In salmon species, transitions between habitats are particularly drastic and hence the states of the individuals that perform these migrations between habitats are particularly well described, in terms of age, length, weight and fat content for instance.

3. Decisions made prior to these changes in habitats that are triggered by the state of the individual *at a particular time in the year*, e.g., the decision to undergo smolting may occur months before the migration to the ocean. These transitions are not easily observable. Observations, when available, are usually made after the transition, e.g., after a change in habitat or after metamorphosis. However, these decision events have been the focus of experimental studies (Beckman et al. 2007) and life history models (Mangel 1994; Mangel and Satterthwaite 2008).

We therefore define the following life stages and transitions in our Pacific salmon DEB model (Fig. 2):

Embryo stage: similarly to the standard DEB model, the embryo can experience constant or seasonal temperatures.

Birth: the individual reaches a maturity threshold and starts feeding. For salmon, we define birth at the time at emergence from the gravel when fry start to feed actively. For salmon – and in most fish species – birth is more easily observable (and restricted in time). In a DEB-sense birth is different from hatching: yolk-sac larvae are not actively feeding and rely on endogenous source of energy so they are still considered as "embryo".

Juvenile stage: is split into two stages, the *river* and the *ocean* stage. The feeding and assimilation processes are different between these two stages. Maintenance rates could potentially be also different.

The *decision to migrate to the ocean* is made during the river stage at a particular date (i.e., time windows). If the individual have reached a particular maturity threshold at this particular date, the individual undergo these morphological and physiological changes associated with

smolting. At a particular date, the individual enter the ocean and the food environment changes.

Puberty: occurs in the ocean. The individual reaches a maturity threshold and starts allocating energy to the reproduction buffer. This transition cannot be compared with observations.

Adult stage: The individual allocates energy to the reproduction buffer.

At a particular date, a *decision is made to migrate back to the river to spawn*. As a first approximation, we consider that an organism needs to reach a particular threshold of energy stored in the reproduction buffer at a particular time in the year, and if this threshold is not reached, the individual spends another year in the ocean. Once the decision is made to migrate back to the river, the adults enter the river at a particular time and stop feeding. We compare the simulations with data on the state of the individuals that migrate back to the river: length, weight, and fecundity data. The features of the migration upstream are not considered in the present study but can easily be taken into account in a more detailed model. In particular, starvation and migration costs are be related to the length of the organisms. Maintenance processes could also be switched off and explain the rapid death of the individuals after spawning. Similarly, the cost of nest protection are not detailed but can be related to the length of the female as well.

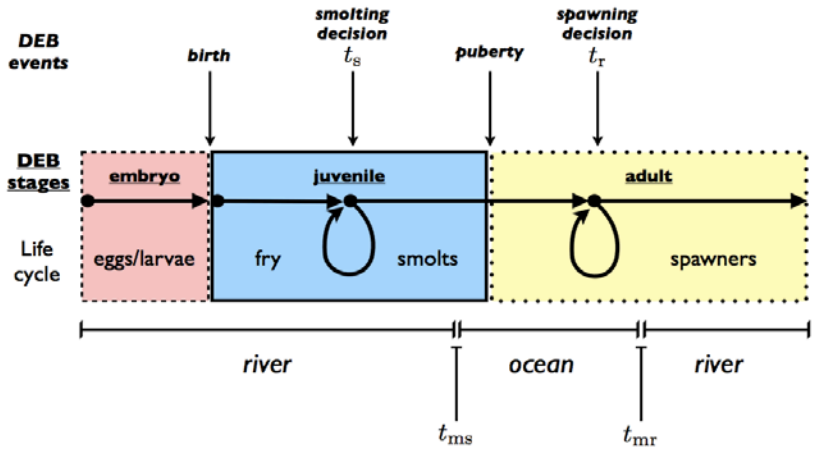

Figure 4: Schematic Representation of the Life Cycle of a Pacific Salmon and Link with DEB Life Stages and Events.

Time windows for smolting decision (ts) and spawning decision (tr) prior to smolt migration (tms) and spawning migration (tmr) were added to a standard DEB model. If the individual does not reach the required maturity threshold MHs at ts, the individual stays in the river until the next time window in the year cycle for smolting, and then migrates and enters the ocean at tms. Once in the ocean, if the individual does not reach MERr, the reproduction buffer threshold, at tr the individual stays an extra year or more in the ocean and then migrates back to the river at tmr and spawns

2.4.3 Body size scaling relationships

By modeling the life cycle of all Pacific salmon species using a single DEB model, we assume that the different species of Pacific salmon may only differ by *i)* their parameters and *ii)* the environmental conditions they experience. Predicting how these parameters are expected to vary between species is one of the powerful properties of DEB theory. The reasoning is detailed

by Kooijman (2010), and the essential ideas are explained in an ecological context by Nisbet et al. (2000). As a first approximation, some parameters representing metabolic processes are expected to be constant between related species and some will covary with their maximum size. The remaining discrepancies between model predictions and species performances (e.g., growth rate or reproduction investment) can then be explained by evolutionary processes.

As a consequence, interspecific differences in respiration rates, maximum feeding and reproduction rates, length of embryonic and juvenile stages for instance follow naturally from DEB theory as these traits can be written as functions of DEB parameters that either do not depend on body size, or are proportional to maximum length.

Our species comparison of Pacific salmon is therefore based on their differences in length at spawning. If predictions compare well with patterns observed in the data, this approach would then inform how to borrow parameter values for species where specific data are sparse.

The methodology for inter-species comparisons is detailed in chapter 8 of Kooijman (2010), with Table 8.1 particularly helpful. Use is made of the "zoom factor" z, which is the ratio of the maximum (structural) lengths of the compared species 1 and 2, species 1 taken as the reference species.

$$z = \frac{L_{m2}}{L_{m1}} \tag{1.14}$$

Only three primary parameters of the standard DEB model (Table 2.1) covary with the zoom factor, the maximum surface-area-specific assimilation rate $\{\dot{J}_{EAm}\}$, and the maturity thresholds at birth M_H^b and at puberty M_H^p:

$$\{\dot{J}_{EAm}\}_2 = z\{\dot{J}_{EAm}\}_1 \tag{1.15}$$

$$M_{H2}^b = z^3 M_{H1}^b \tag{1.16}$$

$$M_{H2}^p = z^3 M_{H1}^p \tag{1.17}$$

No other primary parameters are expected to vary among species of the same genus.

2.4.4 Simulations and comparison with data

We first simulated our model for five different species that only differed by their zoom factor; the environment they experience was the same. We then asked the following question: do the patterns found in the literature follow qualitatively the predictions of the standard DEB model for the five different species of Pacific salmon?

Second, we considered the predictions of the standard DEB model for a particular species, but this time considering that variability among individuals can be generated as they experienced different temperature or different food conditions. The parameters for all conspecific individuals have the same values. We here evaluate the ability of the model to generate different phenotypes among individuals with reduced genetic variability (i.e., individuals that

share the same primary parameters). We compare these simulation results with patterns observed for Chinook (*O. tshawytscha*).

For inter-species comparisons, we mostly used comparisons of species that co-occur in the northern latitudes, mostly in British Columbia (Beacham and Murray 1990; Groot and Margolis 1991; Beacham and Murray 1993; Groot et al. 1995; Quinn 2005). We consider the average female sizes at spawning given by Quinn (2005), which ranks by increasing order: 1) pink (52.2 cm), 2) sockeye (55.3 cm), 3) coho (64.3 cm), 4) chum (68.3 cm), and 5) Chinook (87.1 cm). The ranking is the same in Beacham and Murray (1993) but reported sizes are smaller. We analyzed the data according to this rank and compare the average traits per species with the simulations of the standard DEB model for five individuals with different zoom factors.

For comparisons at the intra-species level on Chinook, we prioritized interpretation of experimental studies where temperature conditions and food conditions were kept constant. For practical reasons of experiment duration, these experimental studies mostly concerned the embryo and the juvenile stage of Chinook. For the ocean and spawning adult stage, we used studies that reviewed average patterns observed in populations.

We present our analysis of the literature data by life stages and how the state of the organism at one stage transition is connected to the state of the individual at the previous stage transition.

2.5 Results

2.5.1 Patterns and variability in Pacific salmon life history traits

We first describe patterns by pairs of life-history traits when data per species are pooled together. We then compare how average life-history traits rank among species (summarized in Table 2.3) and we finally analyze the variability of these life-history traits within species.

Embryo stage

Length and weight at emergence are strongly correlated with egg wet weight when we pooled data per species in Beacham and Murray 1990 (Fig. 6 a,b). We also observed a classic allometric relationship between length and weight at emergence ($W = 0.0072L^{3.205}$, $r^2 = 0.7$, Fig. 6c).

When comparing average *egg* wet weights per species, species rank as follow: sockeye, pink, coho, chum and Chinook (Fig. 6a). When comparing length at emergence by species, this rank is well conserved, except that Chinook and chum are not significantly different in length at emergence. When comparing weight at emergence, the rank is also well conserved but here, coho and chum have no significant differences in average weight at emergence (Fig. 6b).

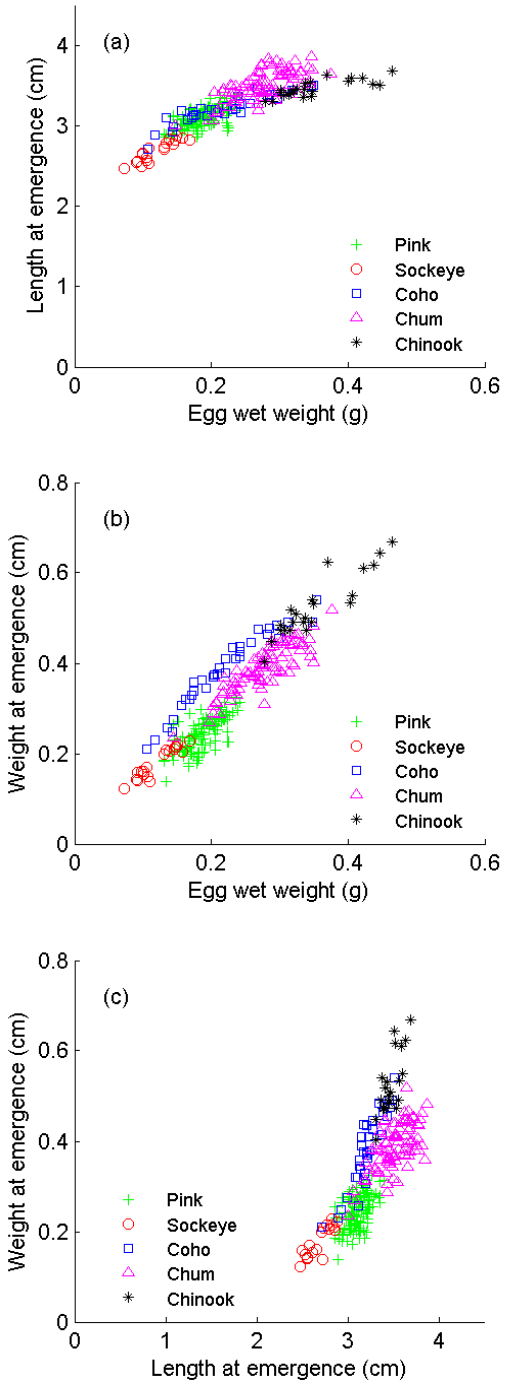

Figure 5: Length and Weight at Emergence. (a) Length at Emergence and (b) Weight at Emergence as a Function of Egg Wet Weight. (c) Weight-Length Relationship at Emergence.

Data from Beacham and Murray (1990).

When comparing the variability of these traits within species, coho has the largest variability in egg weight, and length and weight at emergence. In addition, coho is slightly heavier at emergence for a given egg weight compared to other species (Fig. 6b).

The variability within species of the weight-length relationship at emergence is particularly interesting. Sockeye, coho and Chinook have very similar weight-length relationships at emergence, and limited variability around this relationship. In contrast, pink and chum have a slightly different weight-length relationship at emergence, i.e., individuals weigh less at a given size, but the variability around this relationship is larger (Fig. 6c).

Age at emergence decreases when temperature increases (Fig. 7) from 333 days at 2°C for pink to 54 days at 15°C for coho. Although coho is found to grow faster than the other four species at all temperatures, the ranking of these other species varies with temperature. At 5°C, sockeye and Chinook have the same development rate and develop more slowly than pink and chum. At 11°C, sockeye and pink develop more slowly than chum and Chinook. But the differences in development rates are reduced as the temperature increases: from 83 days at 2°C to 25 days at 15°C between pink and coho.

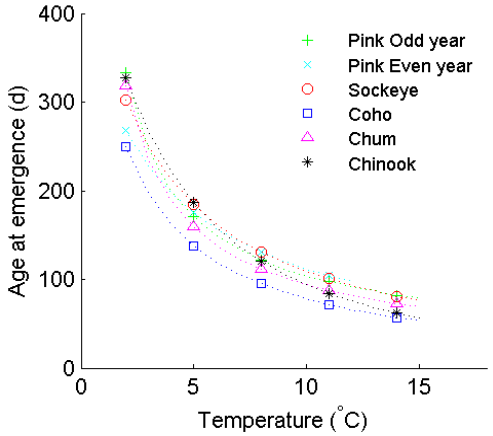

Figure 6: Embryo Stage: Age at Emergence as a Function of Temperature.

Data from Beacham and Murray (1990)

River stage

When considering the compilation of data performed by Quinn(2005), the species rank as follows: 1) pink (3.2cm), 2) chum (4cm), 3) sockeye (8cm), 4) coho (10.5cm). As Quinn (2005) gives a large range of smolt sizes for Chinook (6-12 cm), we do not assign it a rank.

Ocean stage

Similarly, we are looking for datasets that relate the state of the individual at smolting to the state of the individual when returning back to the river (length and age). As mentioned in the Methods section, if we look at the rank of length at spawning in females, species rank as

follows: 1) pink (52.2 cm), 2) sockeye (55.3 cm), 3) coho (64.3 cm), 4) chum (68.3 cm), and 5) Chinook (87.1 cm).

Similarly to the juvenile stage, individuals that grow fast during the ocean stage migrate back to their natal river at a younger age and at a smaller size in indeterminate spawners, i.e., species for which age at maturity can be variable: sockeye, coho, chum and Chinook (Weatherley and Gill 1995). In contrast, pink always migrate after a year spent in the ocean (Weatherley and Gill 1995).

Adult spawning stage

In Beacham and Murray 1993, two different tables provide fecundity and length data. Table 1 in their report provides fecundity average per population for a given standardized length over all populations of a given species and Appendix 1 provides the actual average length per population per species. Unfortunately, sockeye fecundity data and average pink egg weight per population were not available. Therefore, we used both tables to analyze fecundity and egg weight pattern as a function of female length among and within species (Fig. 8).

Fecundity (Fig. 8a,b) and egg weight (Fig. 8c,d) both increase with female length in salmon species. When data are not pooled by species-specific length at spawning (Fig. 8b), the relationship between fecundity and length is well described by a weighted sum of L^3 and L^2 terms as is predicted by DEB theory. When comparing reproductive weight (Fig. 2.5e), length at spawning is a better descriptor, and the reproductive weight is proportional to L_{sp}^3, with L_{sp} the length at spawning when data are not pooled by species-specific length at spawning, i.e., for coho, chum and Chinook.

When comparing average fecundity per species, species rank as follows (Fig. 8a): 1) pink, 2) chum and coho, 4) sockeye and 5) Chinook (Beacham and Murray 1993). Interestingly, as the length at spawning is a better covariate for the reproductive weight than for fecundity, the rank between species for the reproductive weight becomes the same as the length at spawning: pink < sockeye < coho < chum < Chinook.

Nota bene: In Quinn (2005), the relationship between the average species length at spawning and fecundity is somewhat different from Beacham and Murray (1993), i.e., the fecundity averages are similar, but average female lengths are larger in Quinn (2005). The patterns among species are the same, i.e., sockeye and chum have on average a larger and a lower fecundity, respectively when compared with the other salmon species and these differences are reduced when comparing the total reproductive weight (fecundity x egg wet weight).

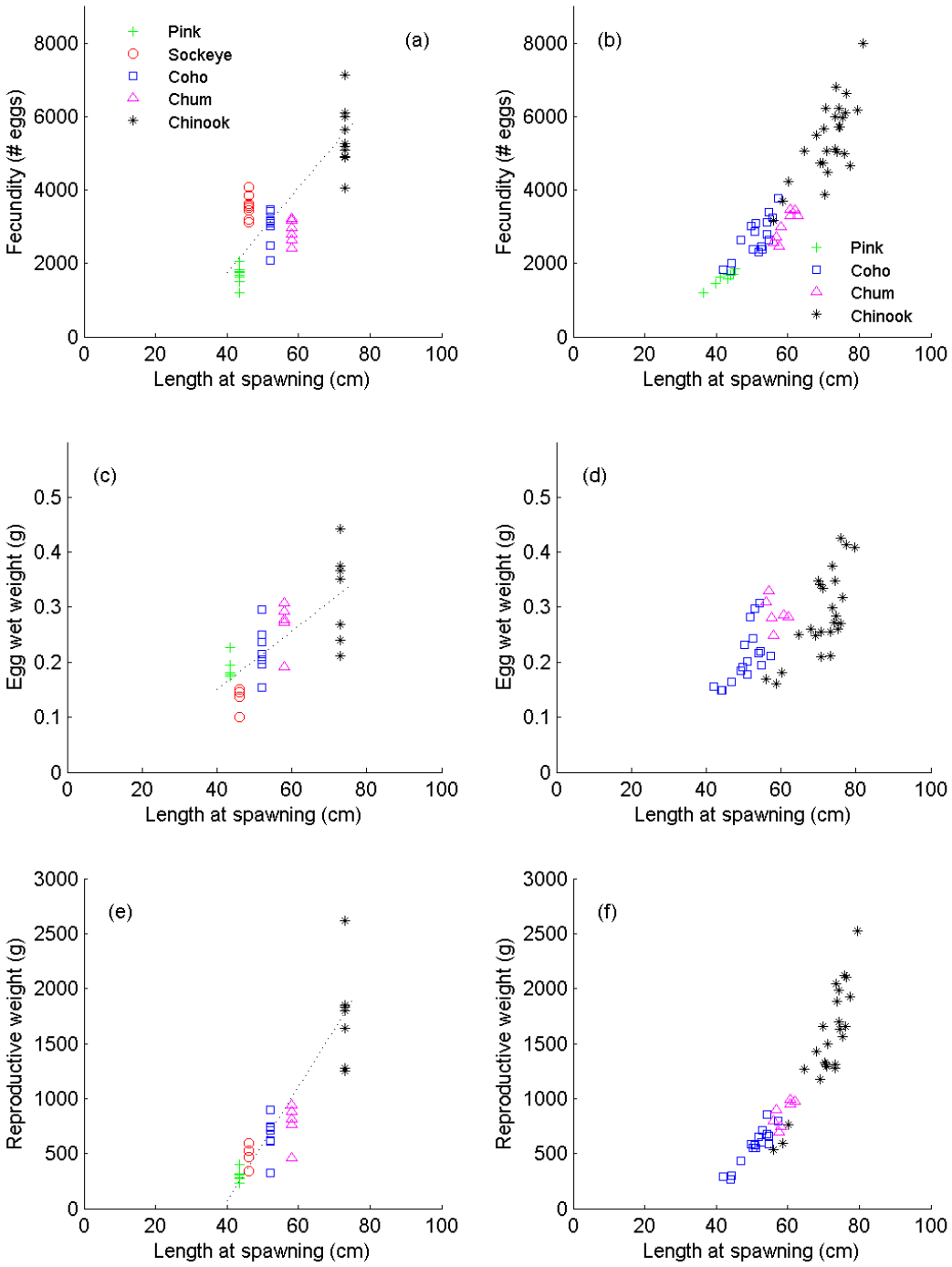

Figure 7: Adult Stage: Fecundity (a,b), Egg Wet Weight (c,d) and Reproductive Weight [e,f (Fecundity x Egg Weight)] as a Function of Female Length at Spawning.

Data from Beacham and Murray1993: Left panel, standardized length at spawning, Table I. Right panel, Table Appendix 1.

2.5.2 Comparisons with body-size scaling relationships predictions

We summarize our findings in Table 3 and detail the results by stage in the following sections.

Table 3: Comparisons of Rank in Traits Among Pacific Salmon Species and Body-Size Scaling Relationships

Life-history traits	Observations	Agreement between model predictions and observations
Female length at spawning	pink < sockeye < coho < chum < chinook Beacham and Murray 1993; Quinn 2005	Reference for our comparison
Reproductive material	pink < sockeye < coho < chum < chinook Beacham and Murray 1993; Quinn 2005	Yes
Fecundity	pink < coho ≈ chum < sockeye < chinook	Yes, if M_H^b in sockeye is smaller than predicted by simple body-size scaling relationships
Egg wet weight	sockeye < pink < coho < chum < chinook Beacham and Murray 1990	Yes, if M_H^b in sockeye is smaller
Fry length	sockeye < pink < coho < chum ≈ chinook Beacham and Murray 1993; Quinn 2005	Yes, if M_H^b in sockeye is smaller
Age at emergence	Rank depends on temperature level Beacham and Murray 1990 coho < chum < pink < chinook ≈ sockeye at 5°C coho < chum ≈ chinook < pink ≈ sockeye at 10°C	No, simple body-size scaling relationship do not explain why coho has a much faster development than other species.

Embryo stage

As observed in the pooled data, the standard DEB model supplemented with body-size scaling relationships reproduces quite well the relationships observed between egg wet weight and length and weight at emergence, respectively (Fig. 9b,d,e): larger eggs produce larger and heavier individuals at emergence.

If we recognize that the maturity threshold at birth (initiation of feeding, i.e., emergence) for sockeye and pink are switched (sockeye < pink) instead of the predicted rank by body-size scaling relationships (pink < sockeye), the standard DEB model also predicts well the rank in egg wet weight and length and weight at emergence for all five species (Fig. 9b,d,f).

The standard DEB model also predicts an increase in the variability of egg weight and length at emergence with an increasing zoom factor. We observe this pattern in the study by Beacham and Murray (1993) for egg weight (Fig. 8c), but as mentioned earlier, the variability of length and egg weight was largest for coho in an earlier study by Beacham and Murray (1990). To further test this prediction, studying the variability at the population level would be interesting.

For the age at emergence as a function of temperature, simple body-size scaling relationships did not capture the observed pattern (Fig. 10). More specifically, coho was found to grow faster than the other four species at all temperatures (Beacham and Murray 1990). Furthermore, the ranking of the four other species varies with temperature. At 5°C, sockeye and Chinook have the same development rate and develop more slowly than pink and chum. At 11°C, sockeye and pink develop more slowly than chum and Chinook. Interestingly, the differences in development rates are reduced as the temperature increases: from 83 days at 2°C to 25 days at 15°C between pink and coho. This latter pattern is reproduced in our simulations (Fig. 10).

Spawning adult

The standard DEB model supplemented with body-size scaling relationships predicts well the relationship between the reproductive weight and female length at spawning (Fig. 8f and 11e, f), both in terms of general form and rank between species.

When we supplement the model with the assumption that the threshold at birth in sockeye is smaller than for pink, the higher fecundity and smaller egg size of sockeye is also well predicted. (Fig. 11b, d). The relationship between length and the reproduction buffer compares well with the observed pattern (Fig. 8f and 11f).

2.6 Concluding remarks

At the inter-species level, the body-size scaling relationships implied by DEB theory provide us with a simple, but successful way to compare and reproduce the relationships between life-history traits among the different Pacific salmon species. The correct predictions for the various life-history-traits provide strong support for the general assumptions underlying DEB theory (van der Veer et al. 2003). We found that although sockeye produce smaller eggs than expected for their size, female sockeye invest similar energy into reproduction compare to other salmon species (Fig. 8a,b). Furthermore, by assuming that the energy required to reach emergence in sockeye is smaller than in other Pacific salmon species, we assume that a strong selection toward smaller egg size operates to increase survival rates in redds. Quinn et al. (1995) found that among sockeye populations in Alaska, egg weight was correlated with the size composition of incubation gravels, assuming that fine substrates may limit oxygen uptake during egg development. This selection may hold when comparing sockeye with other Pacific salmon species.

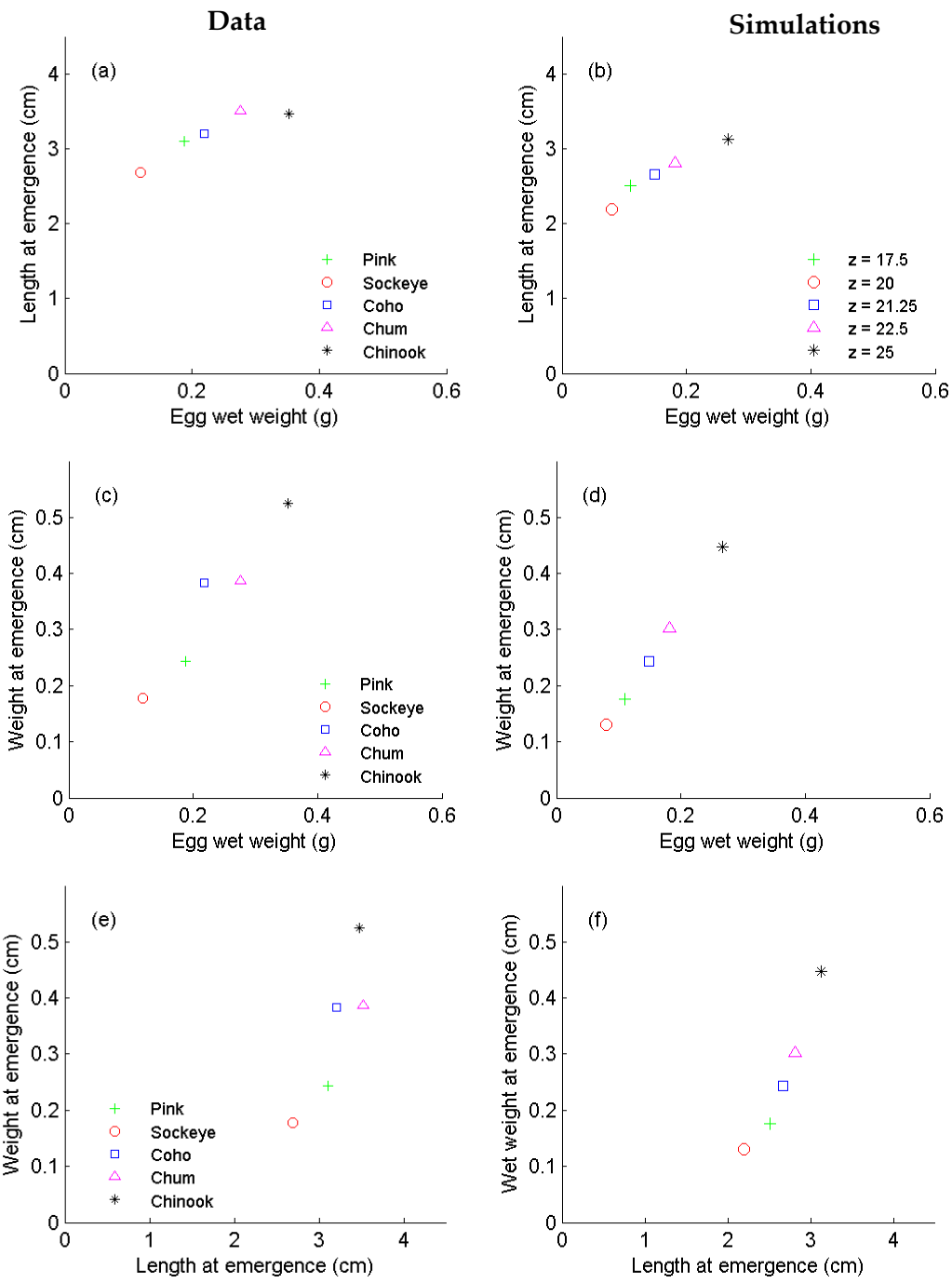

Figure 8: Embryo Stage. Length at Emergence as a Function of Egg Wet Weight. (a) Average Per Species, (b) Simulations for Different Zoom Factors (M_H^b) For Sockeye is Smaller Than Predicted by Body-Size Scaling Relationship).

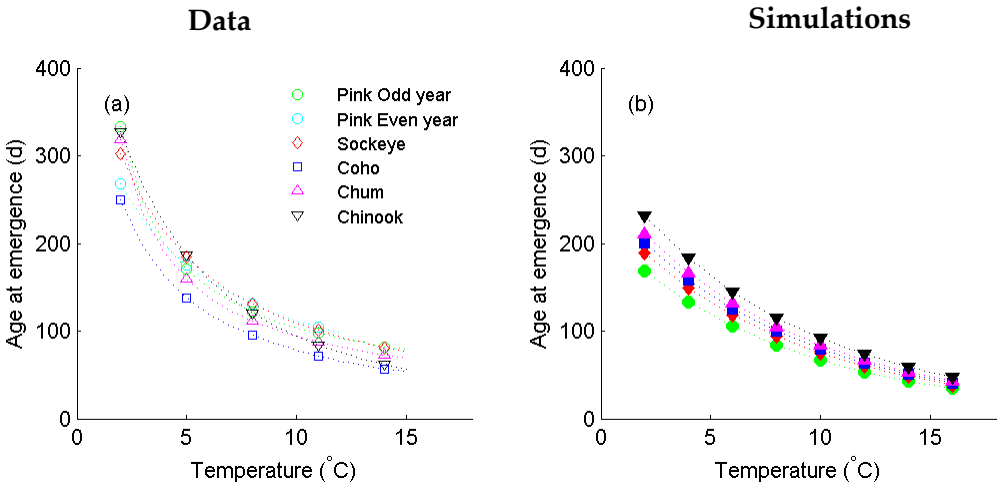

Figure 9: Embryo Stage. Age at eEmergence as a Function of Temperature. (a) Open Symbols: Data From Beacham and Murray (1990). (b) Filled Symbols: Simulations.

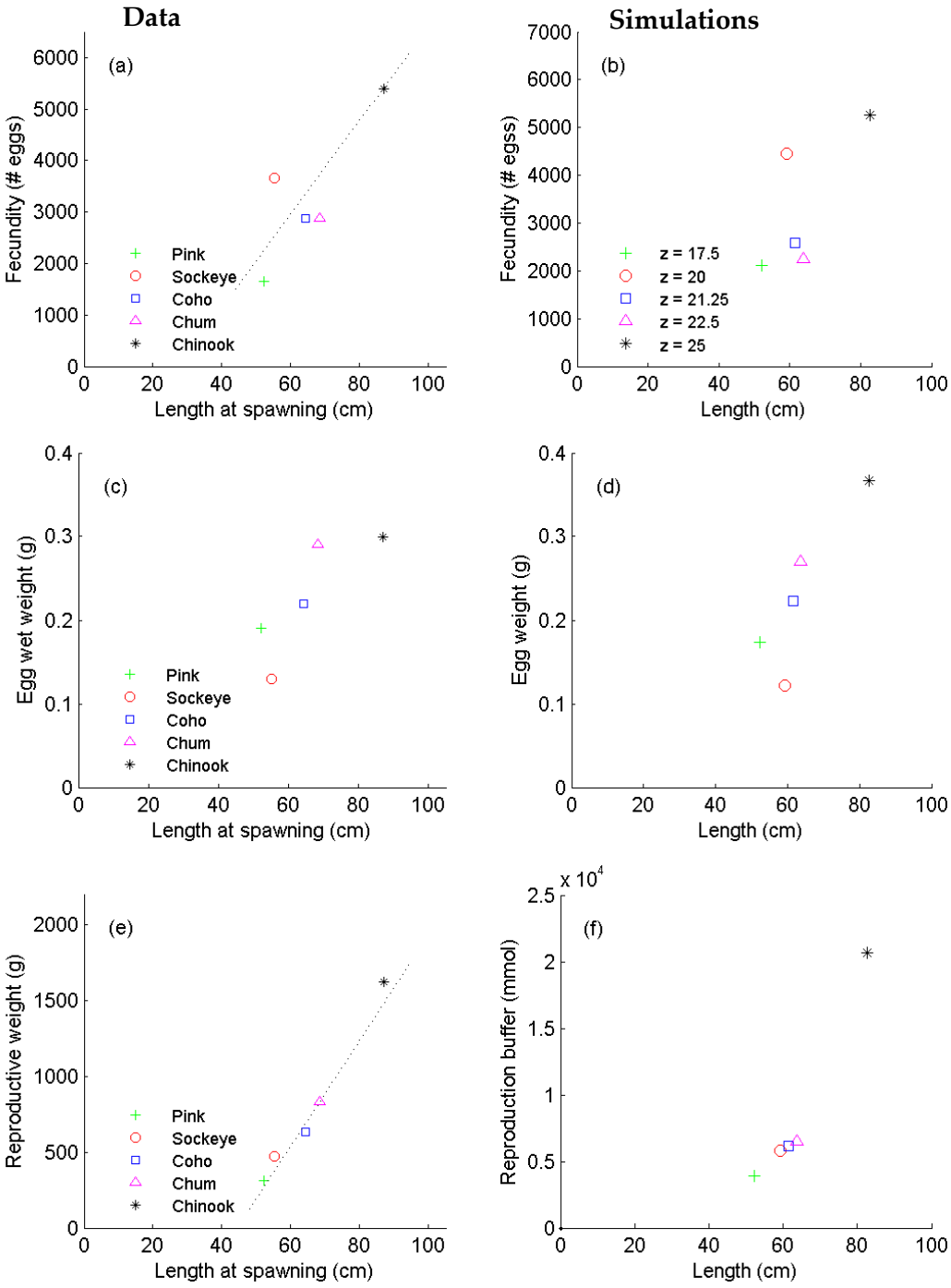

Figure 10: Adult Stage. Fecundity (Top Panel), Egg Wet Weight (Mid-Panel) and Reproductive Weight (Fecundity * Egg Weight, Lower Panel) as a Function of Length: (a), (c), (e) Average Per Species

Data from Quinn2005, (b), (d), (f) simulations for different zoom factors. Parameter M_H^b of species 2 is set to 0.9 M_H^b species 1.

2.6.1 Development, growth and reproduction patterns within a particular species: Chinook (O. tshawytscha)

As the standard DEB model successfully captures the main patterns among life-history traits in the five species of Pacific salmon occurring in North-America, we now analyze in more details the qualitative predictions of the standard DEB model for Chinook (Table 4). The objective of this analysis was again to guarantee that the patterns between life-history traits were well captured by a standard DEB model supplemented with a limited number of assumptions concerning the timing of migrations and the spawning strategy (i.e semelparity).

Table 4: Patterns Within Species and Comparisons with Qualitative Predictions of the Pacific Salmon DEB Model

Life stage	Patterns	Observations	Agreement between model predictions and observations
Embryo	1) Length at emergence as a function of egg wet weight	Larger eggs produce larger fry Beacham and Murray 1990	Yes, Larger eggs have more initial reserve M_E^0 and if $k = \dot{k}_J / \dot{k}_M < 1$, larger eggs produce larger fry at emergence
	2) Weight-Length relationship at emergence	Allometric Beacham and Murray 1990	Yes
	3) Age at emergence as a function of egg wet weight	In chinook, age at emergence slightly increases with egg weight at 10C or stay constant at other temperatures) Rombough 1985	No, If temperature is constant and $k < 1$, age at emergence decreases with egg size
	4) Length at emergence as a function of temperature	In chinook, length at emergence decreases with temperature Rombough 1985	No, temperature affects rates in the same way thus has no effect on size at stage transition
	5) Age at emergence as a function of temperature	Age at emergence decreases with temperature Beacham and Murray 1990	Yes
Adult	6) Female length and age as a function of growth history during the ocean stage	Individuals that grow faster return at a smaller size and a younger age for species with on ocean stage that can be longer than an year Parker and Larkin 1959; Quinn 2005	Yes, with addition of time windows
	7) Female condition as a function of the duration and/or distance of the spawning migration	Female condition decreases with the length of the spawning migration Rand and Hinch 1998	Yes, Individuals use their reserve and do not feed during spawning migration
	8) Female condition as a function of female length at spawning	Larger individuals are in better condition after spawning migration	Yes, larger individuals mobilize their reserve at a slower rate than the smaller individuals
	9) Fecundity as a function of female length	Fecundity increases with length Beacham and Murray 1993; Quinn 2005	Yes, large individuals allocate more energy per unit of structure to the reproduction buffer
	10) Egg wet weight as a	Egg weight increases with female length	Yes, if we assume that larger female are in better condition (ie have larger scaled

Life stage	Patterns	Observations	Agreement between model predictions and observations
	function of female length	Beacham and Murray 1993	reserve density) than smaller females after their spawning migration

We then summarize the main life-history traits of an ocean-type Chinook that migrated to the ocean few months after emerging from the gravels (Table 5). These values are used in the parameter estimation procedure.

Table 5: Average Life-History Traits of a Female Chinook Salmon

Stage	Season	Age (d)	Length (cm)	Weight (g)	Fecundity (# eggs)	Temperature (°C)	References
Egg	Fall	0		0.3			Beacham and Murray (1990)
Fry	Spring	126	3.7	0.52		7.3	Rombough (1985)
Smolt	Fall	267	9	8.90		12.3	Zabel and Achord (2004); Quinn (2005); Shrimpton *et al.* (2007)
Spawning	Fall	5 * 365	87.1	8770	5400	NA	Quinn (2005)

Embryo stage

The model reproduces well the decrease in age at emergence with increasing temperature (Fig. 12). It also reproduces well the decrease in dry weight during embryo development and that this decrease in dry weight is faster at higher temperatures (Fig. 13b) as observed in the experiment performed at different temperature by Rombough [(1985), Fig.16a]. The model also captures well the growth in length during the embryo stage at different temperatures (Fig. 14c,d).

Although the slight decrease in length at emergence as the temperature increases (Fig.13c) is not captured by the standard DEB model (Fig. 13d), the increase in age and weight at emergence as a function of egg weight is well captured by the model (Fig. 14).

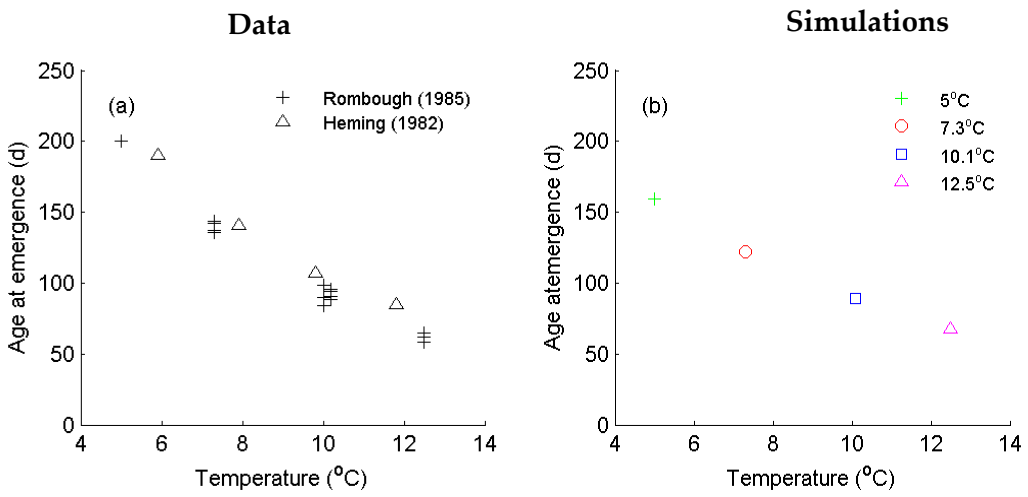

Figure 11: Chinook Embryo Stage. (a,b) Age at Emergence as a Function of Temperature.

Data from Rombough 1985 and Heming 1982.

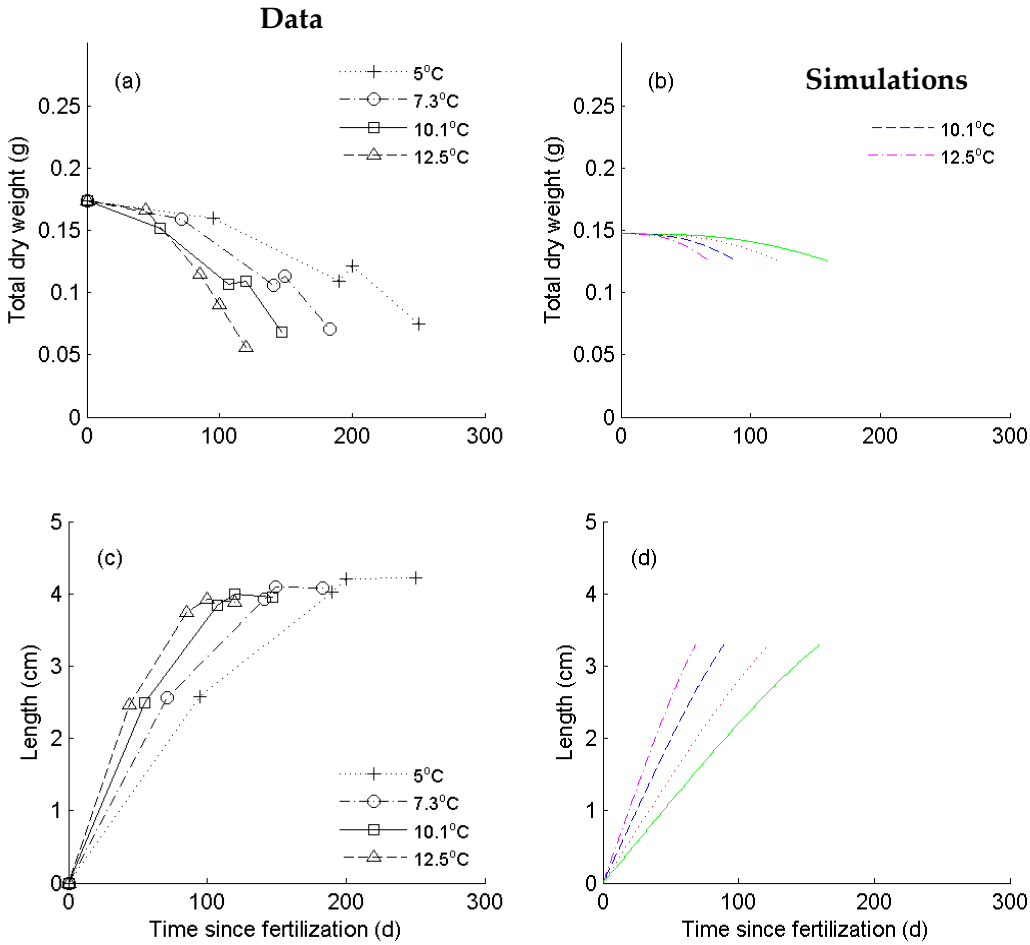

Figure 12: Chinook Embryo Stage. (a,b) Total Dry Weight as a Function of Time, (c, d) Growth in Length.

Data from Rombough 1985.

River stage

The growth pattern in controlled conditions (Fig. 15a,b) and the weight-length relationship obtain from field data during the river stage (Fig. 15c,d) are well captured by the model. We present here simulations for different food levels to show that part of the variability observed in the weight-length relationship can be captured by considering different food conditions.

Ocean stage and returning adults

The average growth pattern is well predicted by the model (Fig. 16a,b). Change in food quality between the river and the ocean stage enabled us to capture the differences in growth rates between these two stages. The model also predicts an allometric weight-length relationship (Fig. 16c,d) and that large females have a higher fecundity (Fig. 16e,f). However, the model predicts a weight-at-length and a fecundity–at-length that is too small compared to the observations.

Concerning the size of the egg at a given female length, if we consider that individuals experienced the same average food environment, the standard DEB model does not predict variation in egg size with the length of the female (not shown), as observed for a large number of Chinook populations (Beacham and Murray 1993). However, large females may produce larger eggs if their reserve density is larger than smaller females.

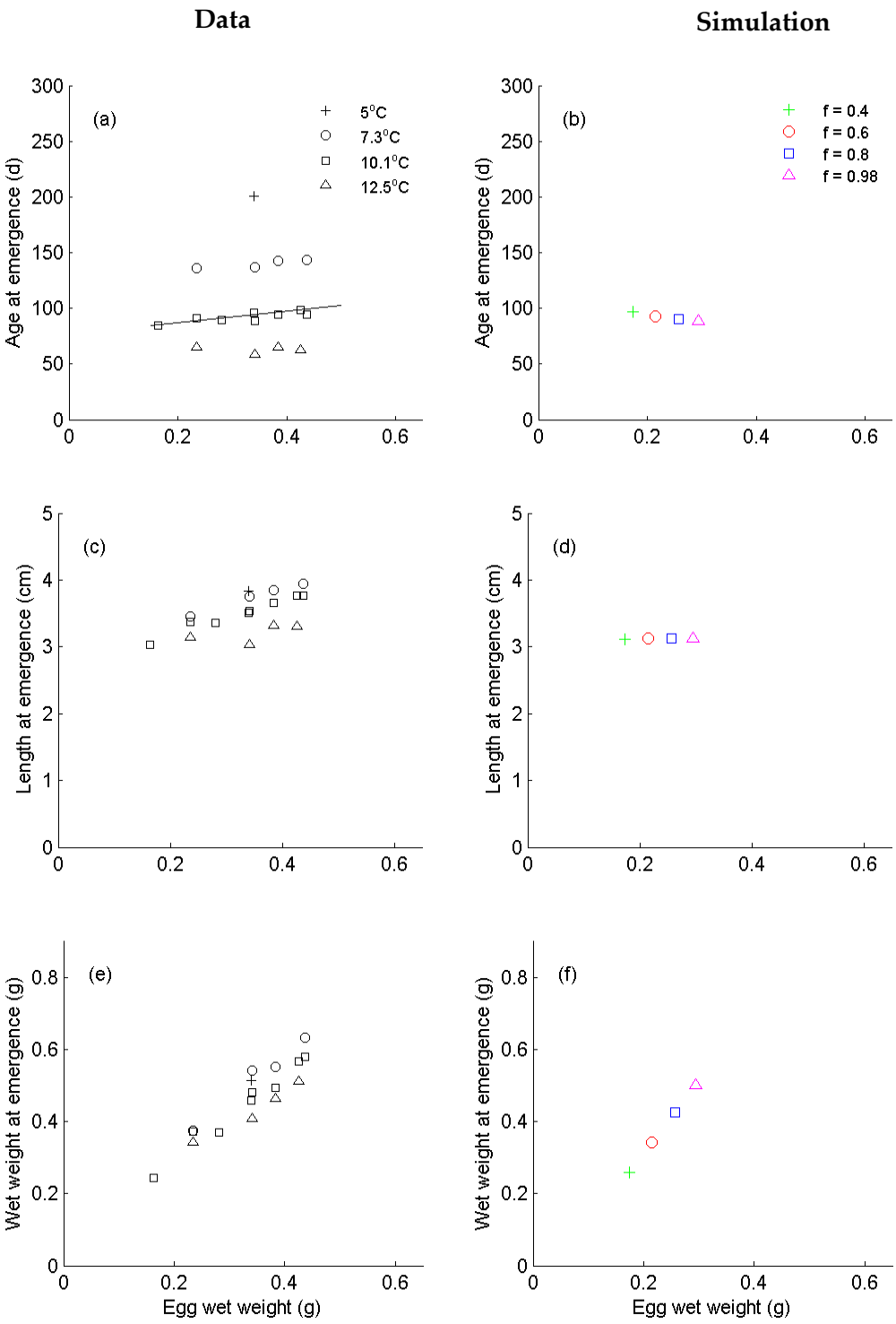

Figure 13: Chinook Embryo Stage. (a,b) Age at Emergence, (c,d) Length at Emergence and (e,f,) Weight at Emergence.

Data from Rombough 1985 and Heming 1982. Simulations with different scaled functional responses f.

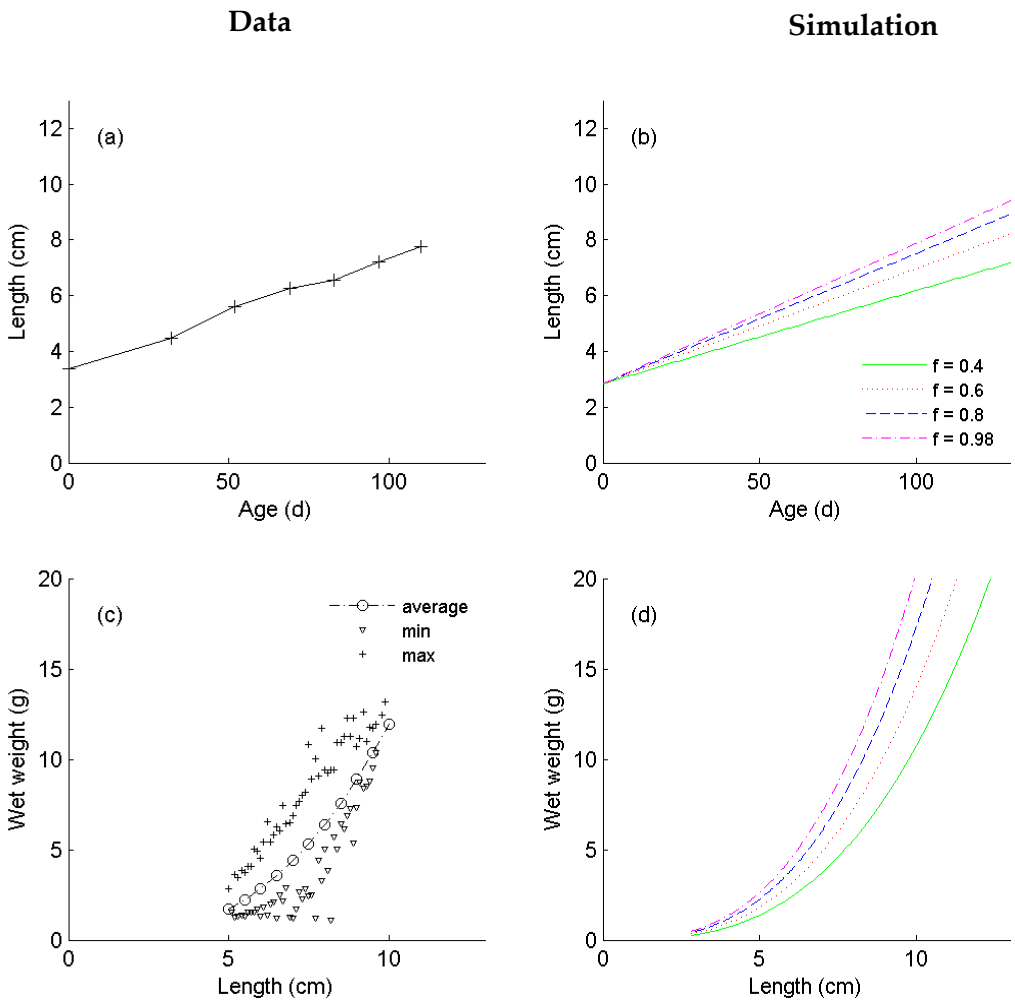

Figure 14: Chinook Juvenile Stage. (a, b) Growth in Length Since Emergence.

Data from Shrimpton et al.2007 . (c,d) weight-length relationship.
Data from Zabel et al. 2004. Simulations with different scaled functional responses f.

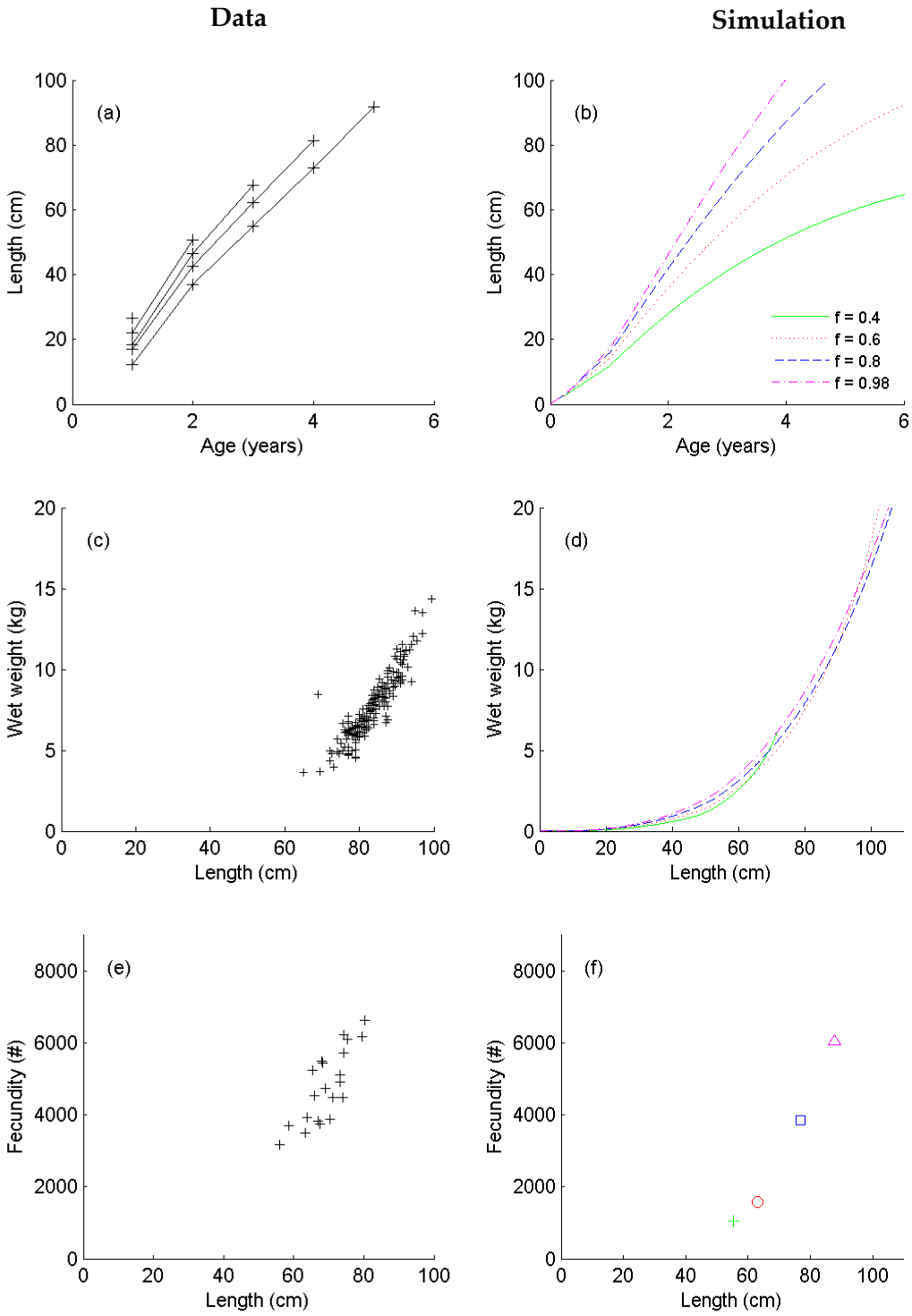

Figure 15: Adult Chinook Stage. (a,b) Growth in Length of Returning Adults of Different Ages.

Data from Parker and Larkin (1959) in Quinn (2005). (c,d) weight-length relationship. Data from Jasper and Evenson (2006), (e) fecundity as a function of length. Data from Einum et al. (2003) Simulations with different scaled functional response (f = 0.95 green, 0.75, red, 0.55 blue)

2.7 Future research

2.7.1 Chinook DEB model

The embryo-stage model for Chinook could be used to examine how temperature and oxygen stress impact survival and development. The equations of a DEB model can be written as macrochemical equations and take into account that oxygen is a limiting element. S. Lindley and his group (Southwest Fisheries Science Center, NOAA) have developed a high-resolution temperature and flow model for the Sacramento River that could be coupled to the Chinook embryo DEB model to examine how operation of Shasta Reservoir impacts incubating winter-run Chinook eggs in the reaches below the dam. The combined DEB-temperature-flow model could then be used immediately to guide operations of Shasta Reservoir on the Sacramento River (S. Lindley, pers. comm.).

In the present study, we considered the standard DEB model and added a limited number of parameters and rules to specify migration to and back from the ocean. Further work is required to better describe some specificities of the life cycle of Pacific salmon. The cost of osmoregulation for instance could be studied in this approach. These costs could be considered as additional (surface-area-specific) costs during the river stage, both as juveniles and adult migrating back to the spawning grounds.

Furthermore, further work is required to understand the effects of temperature on the physiological rates. For simplicity, we assumed an Arrhenius form (Eq. 2.10). Additional rules might be necessary to understand why the length at emergence decreases with increasing temperature Rombough (1985). In the standard DEB model, all rates have the same temperature dependence, which ensures that mass balances in a simple way Kooijman 2010a. Particular attention on how temperature affects the different mass fluxes will be necessary if we wish to include specific temperature effects on development or maintenance rates.

2.7.2 Population Growth Rate

Links between the outputs of DEB models for individuals and population dynamic processes have already been demonstrated for simpler systems (e.g., Nisbet et al. 2000). To relate the impact of flow regime on population levels to individual organisms described by a DEB model, we suggest using the concepts of sensitivity and elasticity analysis, widely used with matrix models in conservation biology (Caswell 2001). As originally developed for discrete time matrix models, sensitivity analysis characterizes the relative contributions to the growth rate of a population from an organism's stage-specific fecundities and survivorships. The results are easily used to determine the net effect of impacts on growth rates from environmental changes that affect multiple life-history features. Here, the objective would be to make statements of the form "an x% decrease in food delivery rate leads to a y% decrease in the fish population growth rate". Calculating how flow regime impacts food delivery rates is one long-term aim of the work described in Chapter 3. Recent work by de Roos (2008) defines the methodology for the calculations, with Appendix S6 of that paper containing MATLAB code for sensitivity analysis of precisely a type of model particularly appropriate for our proposed work – a continuous time DEB model for organisms with pulsed reproduction.

2.8 Conclusions

The main contribution of this work is the formulation of a "generic" model of all life stages of Pacific salmon that "closes" the life cycle in a realistic way. Because the model reproduced how female length determine egg size and how egg size influences fry size at the inter-and intra-species level, we are confident that the full life cycle of a Pacific salmon can be captured in the context of the DEB theory. Particular attention was devoted to modeling embryonic development, and this particular work was key for defining parameter-sparse rules for stage transitions relating to migration. One of the strengths of this approach is that particular stages can be studied more in details, e.g., the early-life stages in rivers, while ensuring that the main life-history traits of the other stages are also well reproduced.

The main features of the life cycle of Pacific salmon are thus captured by a limited addition of new rules compared to the standard DEB model, such that the full life cycle model still only requires a very limited number of parameters when compared to the number of patterns predicted. One additional stage was added that will permit the study of variable life-history strategies observed in Pacific salmon. Other changes compared with the standard DEB model included a change in food quality between the river and the ocean stage to take into account that growth rate are much faster during the ocean stage.

Further data such as the energy content of eggs of different sizes and the dry weight-wet weight relationship of eggs will allow us to further constrain the range of certain parameter values. Furthermore, data that includes the simultaneous measurement of both length and weight in controlled condition will be very useful.

Our approach combines features of both traditional bioenergetic models (Stewart and Ibarra 1991; Madenjian et al. 2004) and life-history models (Mangel 1994; Thorpe et al. 1998; Snover et al. 2005, 2006; Mangel and Satterthwaite 2008; Satterthwaite et al. 2009, 2010). As in traditional bioenergetic models, we can predict variation in weight as a function of variable food conditions, but we can also study the variability in life-history strategies. The main difference with the latter approach is that we do not make explicit use of evolutionary ideas to generate variable phenotypes and life-history strategies. Thus, our model could be used as a null model to study evolutionary processes and local adaptations of populations, as discussed further by Nisbet et al. (2000). This approach may ultimately connect to studies that focus on rapid evolution, e.g., unpublished work by M.L. Baskett (University of California, Davis).

We see two areas where our modeling approach is already ripe for application. First, recent work by Pecquerie (2008) demonstrates that DEB models can be used to determine environmental histories of fish using data from scales or otoliths, combined with knowledge of temperature variations. Thus it may be possible to use data from older juvenile fish to determine the history of (for example) food availability to fish in a river with altered flow. Second, there is a large body of methodology, described in Kooijman (2010) that enables calculation of other metabolic fluxes. Thus we anticipate in future being able to complement our work on embryonic development with calculations of the effects of oxygen stress.

CHAPTER 3:
Representing flow variability and invertebrate transport for length scale calculations in instream flow assessments

3.1 Abstract

Instream flow assessment methods for creating explicit links between changes in the distribution and availability of physical habitat, the availability and delivery rate of macroinvertebrates that comprise fish diets, and population dynamics of target fish species, are generally lacking. Recent theory addressing characteristic length scales provide a possible avenue for advancement, as they can describe the spatial scales over which variability in habitat and other processes regulate population dynamics of fish and their food. By quantifying the effects of spatial variability on processes important to instream populations, length scales can provide a useful means to compare the spatial scales of management effects to those that are relevant to preserve viability.

Characteristic length scales are likely to reflect a strong influence of flow conditions via drift dispersal. We propose simulations that can guide appropriate representations of flow-mediated dispersal and resulting distributions of benthic macroinvertebrates that comprise the major food source of salmon. Specifically, we use a 2-D hydraulic model of a restored section of the Merced River to describe the transport and settlement of macroinvertebrates. We found that the trajectories of simulated macroinvertebrates were dominated by a high velocity core under all discharge conditions. The 2D flow environment was collapsed into a 1D representation that allowed its use in population dynamic models for benthic invertebrates previously developed by two members of the project team. Cross-sectional averaged flow velocities in the 1D representation retained hydraulic structure of the 2D model. The 2D flow environment was collapsed into a 1D representation that allowed its use in population dynamic models for benthic invertebrates previously developed by two members of the project team. Cross-sectional averaged flow velocities in the 1D representation retained hydraulic structure including variation from riffle/pool sequences and sand bar development. We ran a stochastic simulation model incorporating the 1D flow representation and compared predicted transport and settlement dynamics with output from the 2D particle tracking model. Simulations yield distributions of macroinvertebrates that show a strong inverse relationship with flow velocity whose strength is set by other model parameters, namely the rate at which drift dispersal is initiated and the rate at which dispersers settle to the benthos. Surprisingly, these parameters had minimal effects on benthic distributions over the range of parameters examined. Estimates of dispersal distributions from the 1D and 2D models were compared and were qualitatively similar. One characteristic length scale, the average dispersal distance, was overestimated in the 1D model under most parameter combination. This result is likely owing to an incomplete representation of how dispersion in the 2D model influences settlement in the 1D model.

3.2 Introduction

Spatial variability in physical habitat can shape population dynamics by differentially affecting habitat selection, reproduction, and survival at different spatial scales. For example, small scale variation in foraging habitat will strongly affect the distribution of fish via habitat selection, while larger scale variation (i.e., total availability in a stream reach) will have stronger effects on total fish biomass via survival. Changes to flow regimes can profoundly alter both the spatial structure and total availability of physical habitat; traditional Instream Flow Assessment (IFA) methods (e.g., PHABSIM) focus on quantifying physical habitat and predicting how it will change given alterations in the flow regime. However, IFA methods for creating explicit links between changes in the distribution and availability of physical habitat and population dynamics of target species are generally lacking.

An additional complication is that physical habitat affects both target fish species directly via abiotic factors as well as indirectly via biotic ones. One of the frequently included components of fish bioenergetic models (including those proposed in Chapter 2) is food delivery rate, yet many studies assume that these rates are simple functions of discharge. Frequently missing are the known effects of physical habitat and flow on the dispersal and population dynamics of benthic macroinvertebrates (fish food) and feedbacks between fish and their prey.

Recent advances in theory have demonstrated that links between physical habitat, flow, and population response can be understood in terms of characteristic length scales (reviewed in Anderson et al. 2006). These length scales emerge as properties of a community of organisms interacting dynamically with their physical environment. Theory regarding characteristic length scales in rivers has generally addressed at least one of two themes: the minimal habitat required to sustain a viable population subject to downstream drift (Speirs and Gurney 2001; Lutscher et al. 2005; Pachepsky et al. 2005), and the spatial scale over which the local environment are strongly affected by upstream populations (Anderson et al. 2005; Anderson et al. 2006a; Nisbet et al. 2007; Diehl et al. 2008). The second of these, termed the "response length", additionally describes the spatial scales over which the distribution is driven largely by habitat selection shifts to the scales where the distribution is driven largely by survival and reproduction. These characteristic length scales form an important component of theory that predicts the distribution of organisms among different physical habitat types. For example, minimal habitat length calculations could allow assessment of the minimum amount of pool versus riffle habitat required to maintain viable populations of stream macroinvertebrates and the target fish that prey on them, while response lengths provide a means to predict how the distribution and abundance of both taxa change downstream of small scale habitat changes, such as a shift between riffle and pools, and larger scale changes such as downstream of dams.

Anderson et al. (2005) provided a recipe for calculating response lengths across a range of flow conditions using commonly collected data; this analysis was applied to multiple taxa in Diehl et al. (2008). Necessary data include invertebrate drift rates and consumption rates by fish (both with units of time) as well as the distribution of dispersal distances observed during a drift event; the latter is often referred to as the "dispersal kernel." Similar calculations were undertaken in the context of minimal habitat lengths by Speirs and Gurney (2001). However,

almost all discussion in the papers cited above and subsequent work was based on a one dimensional (1D) representation of flow: minimal habitat lengths and response lengths commonly predict characteristic lengths to scale directly with some "mean" river velocity. The validity of this representation has yet to be tested against more accurate two or three dimensional flow representations, much less empirically. Determining the validity of 1D representations of flow-mediated dispersal is an important step in advancing the utility of characteristic length scale concepts in practical settings and preparing them for empirical testing.

Below, we investigate the spatial dynamics of benthic macroinvertebrates that are important food sources for Chinook salmon in the Merced River using both parameterized 1D and 2D dispersal representations. We focus much of our efforts on dispersal kernels and how they alter with changes in flow. We demonstrate how results from computationally intensive 2D flow models can be used to construct simpler 1D representations, which we use in turn to explore invertebrate responses to spatial variability in flow across a range of discharge conditions. The results allow us to evaluate the validity of 1D representations of the spatial dynamics of the invertebrates that comprise the main diet of salmon under different hydrological conditions.

3.2.1 Study Site

To explore the relation between flow regime and the transport of invertebrates in the drift, we utilized a recently restored reach of the Merced River, CA. Our study utilized existing topographic and hydraulic data sets that were collected from the Robinson Reach of the Merced River with collaborator Tom Dunne (University of California, Santa Barbara). The Robinson Reach was restored as part of a larger effort to improve Chinook salmon habitat and channel-floodplain functionality following 150 years of gravel mining that had occurred at the site (CADWR, 2005). The re-engineered channel has a single-thread, meandering planform, with alternating deep pools and shallow riffles. The average bankfull width is 29.2 m and the bankfull discharge is 42.5 m^3/s, with a median grain-size of 52.5 mm.

3.3 2D hydrodynamic modeling methods

The MIKE 21 FM model was used in this study to characterize the two-dimensional (2D) flow field through the lower 1.7 km of the Robinson Reach. MIKE 21 FM is based on a numerical solution of the two-dimensional Reynolds-averaged form of the Navier-Stokes equations, and assumes that the flow is hydrostatic (DHI 2009a). The turbulence is modeled using the concept of an eddy viscosity, which is calculated in the vertical and horizontal directions. The vertical eddy viscosity comes from an assumed parabolic vertical distribution of eddy viscosity between the bed and the water surface, which results in a logarithmic velocity profile near the bed and a parabolic profile well away from the bed. The lateral eddy viscosity (LEV) parameter is used to represent horizontal momentum exchange due to turbulence not generated at the bed, but rather due to small-scale flow separation and eddies. The model runs utilized a mesh with a consistent grid node spacing of 1.0 m.

The model boundary conditions include input bed topography, specified upstream discharge and a downstream water surface elevation. The bed topography was surveyed using a total station, and the survey encompassed the active channel and roughly 10 m of the floodplain on either bank, with a mean cross section spacing of 7 m (20 percent of the channel width) and an average distance of 2 m between points along a transect. The topographic data was interpolated to form a continuous topographic surface using a specialized kriging method for curved channels developed by Legleiter and Kyriakidis (2008). The water surface elevations (WSE) were measured in the field at discharges of 32.6 m^3/s (~75 percent of the bankfull flow) and 6.4 m^3/s (baseflow conditions). Additional hydraulic data included 113 point measurements of velocity collected along six transects during a typical baseflow of 6.4 m^3/s. These data were obtained with an acoustic Doppler Velocimeter (ADV), which measured three-dimensional velocities for 60 s at a height above the bed equal to 40 percent of the local flow depth, approximating the depth-averaged velocity for an assumed logarithmic vertical profile, consistent with the hydrodynamic model.

The flow model was calibrated by adjusting the flow resistance, in the form of a drag coefficient, until the root mean square error (RMSE) was minimized between the measured and predicted water surface elevations. The model was validated by comparing the predicted vertically-averaged velocity magnitudes to measured values.

3.3.1 Particle tracking simulations

The goal of the model simulations was to assess how the travel distances of individual macroinvertebrates changed with flow discharge. To do this, we utilized a particle tracking module within MIKE 21 FM. The flow output from the hydrodynamic model provides the framework for the drift transport calculations, along with information on horizontal and vertical dispersion and the settling rates of individual organisms. The particle tracking algorithm uses a Lagrangian discretization to predict the discrete pathways and travel distances of individual particles. Transport of individual particles is predicted according to a drift regime, and dispersion can be introduced via a random walk approach (DHI, 2009b).

Individual "macroinvertebrates" were introduced into the upstream end of the flow model at a height that was 60 percent of the node depth. We selected to introduce invertebrates at 60 percent of the node depth to be consistent with the model predictions of the depth-integrated velocity, which is calculated at 60 percent of the flow depth. The concentration of organisms was computed at each node in the computational grid as the organisms were transported downstream. Drift transport was modeled at 6.4 m^3/s, a typical baseflow, and 32.5 m^3/s, which is 0.75 times the bankfull discharge. The effect of settling velocity (ω_s) and dispersion both play important roles on the pattern of drift transport, and these have been included in previous models of drift transport processes (Cibrowski 1983; Hayes et al. 2007). Settlement was implemented in the particle tracking module by computing the time an organism should settle given its settlement velocity, and removing it from the flow at the node it occupied after that time had been reached.

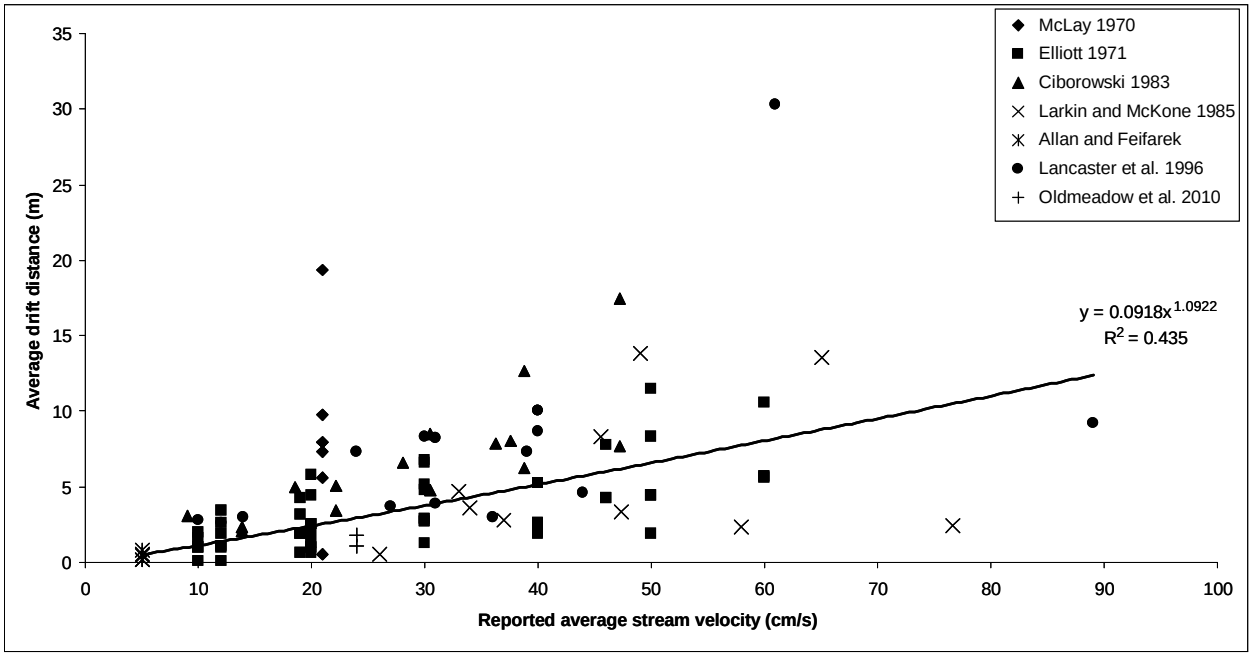

Figure 16: Values of Experimentally Measured Macroinvertebrate Drift Distances Summarized From the Literature.

Data are grouped by the study they were extracted from. Drift distances show a positive relationship with average stream velocity. This relationship is explained well by a power function as shown in the figure.

We choose to model drift transport using a synthetic range of settling velocity and dispersion values that were derived from the literature. We collected studies where drift distances were measured experimentally (McLay 1970; Elliott 1971; Ciborowski 1983; Larkin and McKone 1985; Allan and Feifarek 1989; Lancaster et al. 1996; Oldmeadow et al. 2010). Most of the organisms in these studies belonged to common stream macroinvertebrate taxa (i.e., mostly insects of the orders Ephemeroptera, Trichoptera, Plecoptera, Diptera, and Coleoptera, and crustaceans of order Amphipoda). Studies were conducted in many geographic regions, across a range of flow conditions, and under both field and laboratory experimental conditions. While this context-specific information no doubt profoundly influences the drift behavior of the organisms considered. Furthermore, these studies in no way represent a complete sample of relevant studies. However, our goal was to generate a first cut at reasonable parameter values for model comparisons and generating predictions for future empirical application (**see Section 3.5**). *Check!*

Our collected studies reported stream velocities, average drift distances (or its inverse, return rate), and stream depths. Consistent with the assumption of our particle tracking algorithm, macroinvertebrates in these studies collectively exhibited a strong positive relationship between their average distance traveled and stream velocity (Figure 17; $R^2 = 0.435$). In some cases, release heights were reported; if not, we assumed that the release height was 60 percent of the stream depth for consistency with our simulations. From these data, we were able to estimate settling rates σ (1/s) as (stream velocity/average distance traveled), and therefore settling velocity ω_s as settling rate x release height.

We estimated parameter values for 116 examples which spanned the range of settling velocities 0.11 m/s > ω_s > 0.0011 m/s. Most (93 percent) had settling velocities less than or equal to 0.01 m/s. The average of these values was 0.0087 m/s while the median was 0.0042 m/s. Therefore, in order to span what we felt were reasonable and common values of settling velocities, we used values of 0.0005, 0.005, and 0.05. While some organisms did have settling velocities higher than 0.05 m/s, we found that modeled particles in these ranges settled almost always in their release region in the 2D simulation, even in the presence of turbulent diffusion.

Similarly, we explored how drift transport patterns changed over a range of dispersion values, which we calculated as 1, 5 and 10 times the computed eddy viscosity. Table 6 provides the input values for 24 flow-drift simulations performed with the 2D model.

3.3.2 Model calibration

The model was calibrated by adjusting the roughness, as parameterized by a spatially explicit drag coefficient (C_d), until the root mean square error (*RMSE*) was minimized. We also assessed the goodness of fit between observed and predicted *WSE* values by examining profiles and observed versus predicted plots of the *WSE* (Figure 18). Overall agreement between modeled and measured elevations was close, as determined by the values of the *RMSE* (Table 18). To assess the accuracy of the flow model, predicted vertically-averaged velocity magnitudes were compared to measured values at six transects (Figure 19). Regression analyses (n = 113) were used to compare field measurements to predicted velocity magnitudes at a discharge of 6.4 m^3/s (Table 19). These analyses found that the coefficient of determination R^2 was 0.79 and *RMSE* between predicted and observed velocities was roughly 20 percent of the mean flow velocity. The good overall agreement suggests that the model is capable of reproducing the hydraulics at our field site.

Table 6: Input Values for the 2D Particle Tracking Simulations. Q = Channel Discharge; ωs = Settling Velocity; LEV = Lateral Eddy Viscosity; Dh and DV = Horizontal and Vertical Dispersion Coefficients.

Q (m^3/s)	ω_s (m/s)	LEV (m^2/s)	D_h and D_v (m^2/s)
6.4	0.0005	0.003	0
6.4	0.0005	0.003	0.003
6.4	0.0005	0.003	0.015
6.4	0.0005	0.003	0.03
6.4	0.005	0.003	0
6.4	0.005	0.003	0.003
6.4	0.005	0.003	0.015
6.4	0.005	0.003	0.03
6.4	0.05	0.003	0
6.4	0.05	0.003	0.003
6.4	0.05	0.003	0.015
6.4	0.05	0.003	0.03
32.5	0.0005	0.01	0
32.5	0.0005	0.01	0.01
32.5	0.0005	0.01	0.05
32.5	0.0005	0.01	0.1
32.5	0.005	0.01	0
32.5	0.005	0.01	0.01
32.5	0.005	0.01	0.05
32.5	0.005	0.01	0.1
32.5	0.05	0.01	0
32.5	0.05	0.01	0.01
32.5	0.05	0.01	0.05
32.5	0.05	0.01	0.1

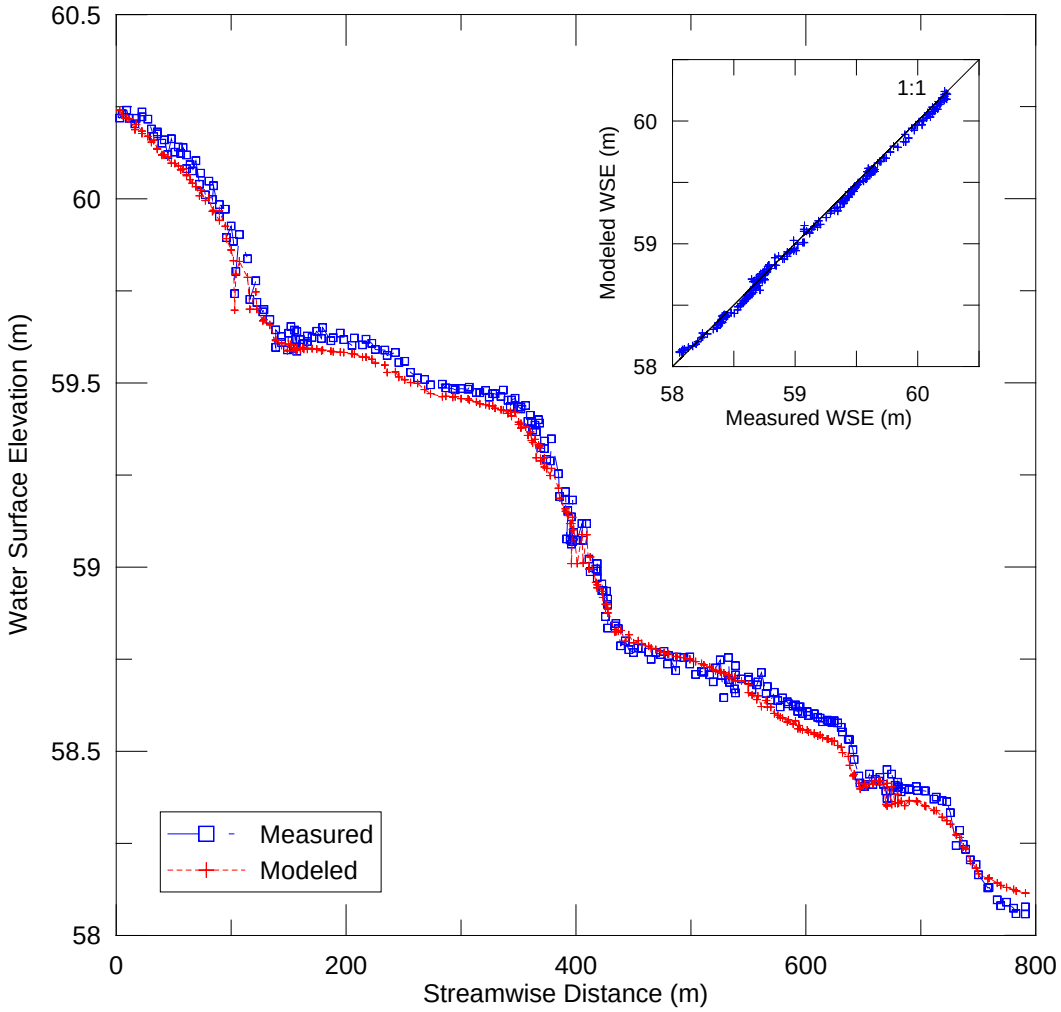

Figure 17: Comparison Between Measured and Modeled Water Surface Elevations for a Discharge of 6.4 m3/s.

The inset plot shows the observed versus predicted WSE and the minimal scatter about the 1:1 line.

3.3.3 Flow and drift transport results

Figure 20 shows a map of the spatial patterns in flow depth and velocity at the upstream end of the model reach, at a simulated baseflow of 6.4 m^3/s. Note that the flow is initially shallow and gradually deepens as the morphology transitions from the riffle into the pool. The velocity field is also more uniform throughout the riffle and a high velocity core develops as flow is converged by a point bar which is located on the inner bank of the meander bend. Flow decelerates as it moves through the pool due to the expansion in width at the pool exit, which creates a divergent flow field (Figure 20). Figure 20 provides a map of the depth and velocity at a discharge of 32.5 m^3/s. At this higher flow, a more well-developed high velocity core is present through the central portion of the riffle and through the pool thalweg, with velocities exceeding 1.0 m/s.

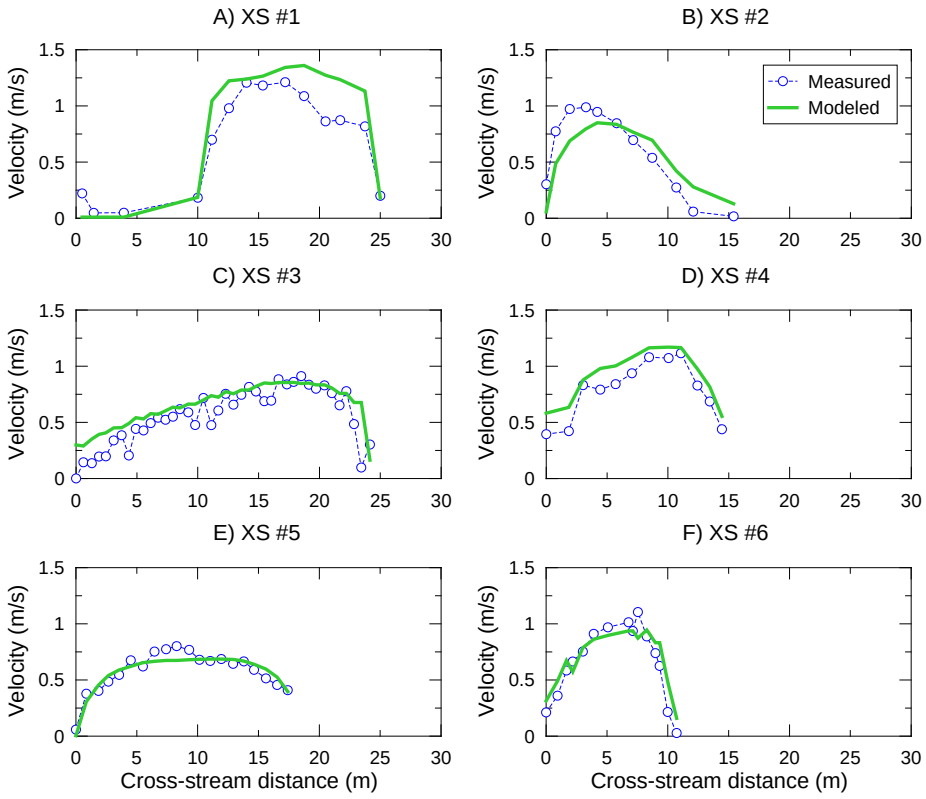

Figure 18: Comparison Between Measured and Modeled Velocity Magnitudes for a Discharge of 6.4 m3/s.

Using the output from the hydrodynamic model and the Lagrangian framework provided by the particle tracking module, we simulated invertebrate drift transport rates at baseflow and near-bankfull discharge flow conditions. At low flow, the predicted particle pathways follow the modeled velocity streamlines, as indicated by the largely parallel particle traces observed in the riffle, and convergent particle traces shown in the pool (Figure 3.6). Instantaneous particle velocities also reflect the local velocity conditions as the particles traveling near the channel margins tend to settle out of the drift while particles located in the central portion of the channel are swept into the high velocity core and transported through the pool. During high-flow events (Figure 3.7), the invertebrate drift transport pathway follows a similar trajectory along the high velocity core and the drift concentrations are greatest in the channel centerline, though the zone of invertebrate transport occupies a greater fraction of the channel width.

Table 7: MIKE21 FM Model Calibration and Water Surface Elevation Verification for Two Modeled Discharges (Q).

The drag coefficient (Cd) and lateral eddy visocity (LEV) values are provided for each flow. Disagreement between predicted and observed water surface elevations (WSE) is summarized in terms of the root mean square error (RMSE).

Q (m^3/s)	C_d (—)	*LEV* (m^2/s)	*WSE RMSE* (m)
6.4	0.017	0.003	0.038
32.5	0.011	0.01	0.037

The travel distances of individual particles were calculated and used to assess the distribution of dispersal distances observed during a drift event, referred to as the dispersal kernel. The distribution of drift distance can be extracted from the particle tracking algorithm by keeping track of the locations at each time step and summing the distances between these points.

Figure 24 shows that most particles that do not include a dispersion term settle out over a very small range of distances. The distances traveled unsurprisingly increase with increasing flow velocity and decrease with decreasing settlement velocity. The inclusion of dispersion works to increase the variance in dispersal distances. For all simulations with the highest settlement velocity ω_s and those with $\omega_s = 0.005$ and discharge at 6.4 m^3/s, dispersion works to also increase the average dispersal distance. This is likely due to horizontal dispersion moving particles into the high-velocity core that would otherwise be rapidly entrained in shallow areas near the upstream edge of the river model. In contrast, dispersion reduces the average dispersal distance for all other parameter combinations. In these cases, low settlement and high flow are enough to allow particle escape from the upstream area. Vertical dispersion is then likely more important by increasing the probability that a particle will hit the river bottom after traveling downstream a given distance. We intend to further explore the validity of the explanations in future work by independently varying the horizontal and vertical dispersion coefficients and examining the effects on average dispersal distances.

The increased variance from dispersion generates a distribution of dispersal distances that is closer to those observed in the literature, which are typically fit well by an exponential distribution (McLay 1970, Elliott 1971, Cibrowski 1983, Larkin and McCone 1985, Allan and Feifarek 1989, Lancaster et al. 1996). The inclusion of dispersion therefore points towards a qualitatively more accurate model, which should be considered in future empirical tests of invertebrate drift in the Merced River.

3.4 Representing in 1D

The 2D flow environment was collapsed into a 1D representation that could be used in our population dynamic models. Since results of our 2D modeling and previous empirical work suggest that velocity is a major determinant of downstream dispersal distances in macroinvertebrates, we choose to represent the dispersal environment using cross-section averaged velocities. Each cell in the 2D flow simulation has an area of 1 m x 1 m, which allowed

us to calculate the cross-sectional area for each 1m long stretch of river. Since discharge is conserved in our model, cross-sectional averaged velocity is therefore simply the input discharge (6.4 m^3/s or 32.5 m^3/s)/cross-sectional area. Resulting velocity profiles are show in Figure 3.9.

The overall structure of the 1D velocities mirror that of the full 2D model. The periodic patterns in velocity reflect the riffle/pool structure of the Robinson Reach and are conserved at the two discharge levels. In general, high velocity stretches correspond to riffle habitats. The slight increases in velocities over the last 200-300 m downstream reflect a restriction in cross-sectional area due to sandbar development. Harmonic means of the 1D velocity profiles are ~0.65 m/s and ~1.32 m/s for baseflow and 75 percent bankfull conditions, respectively.

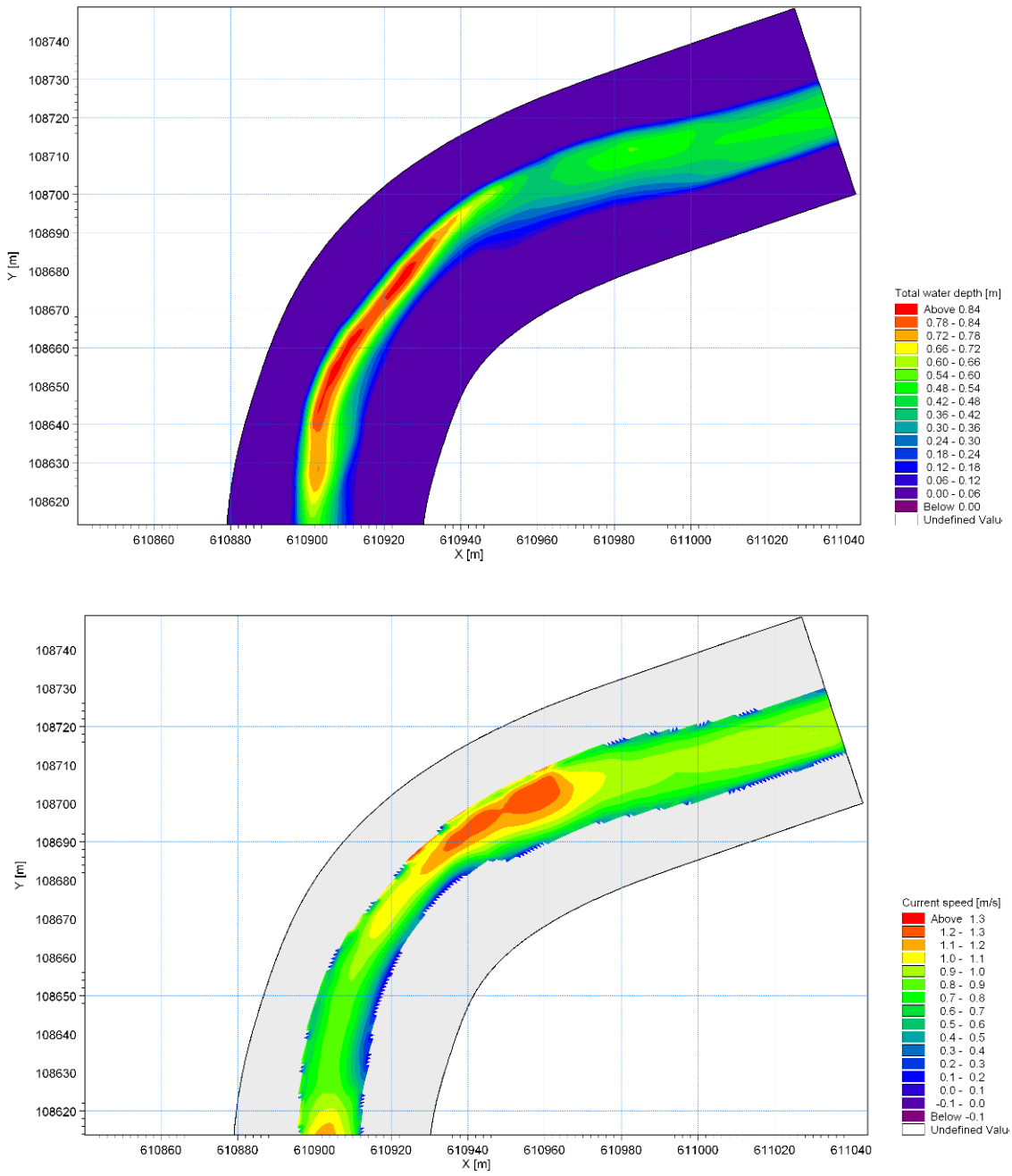

Figure 19: MIKE 21 FM Modeled Depth (Upper Panel) and Velocity (Lower Panel) for a Typical Pool-Riffle Sequence at a Baseflow of 6.4 m^3/s.

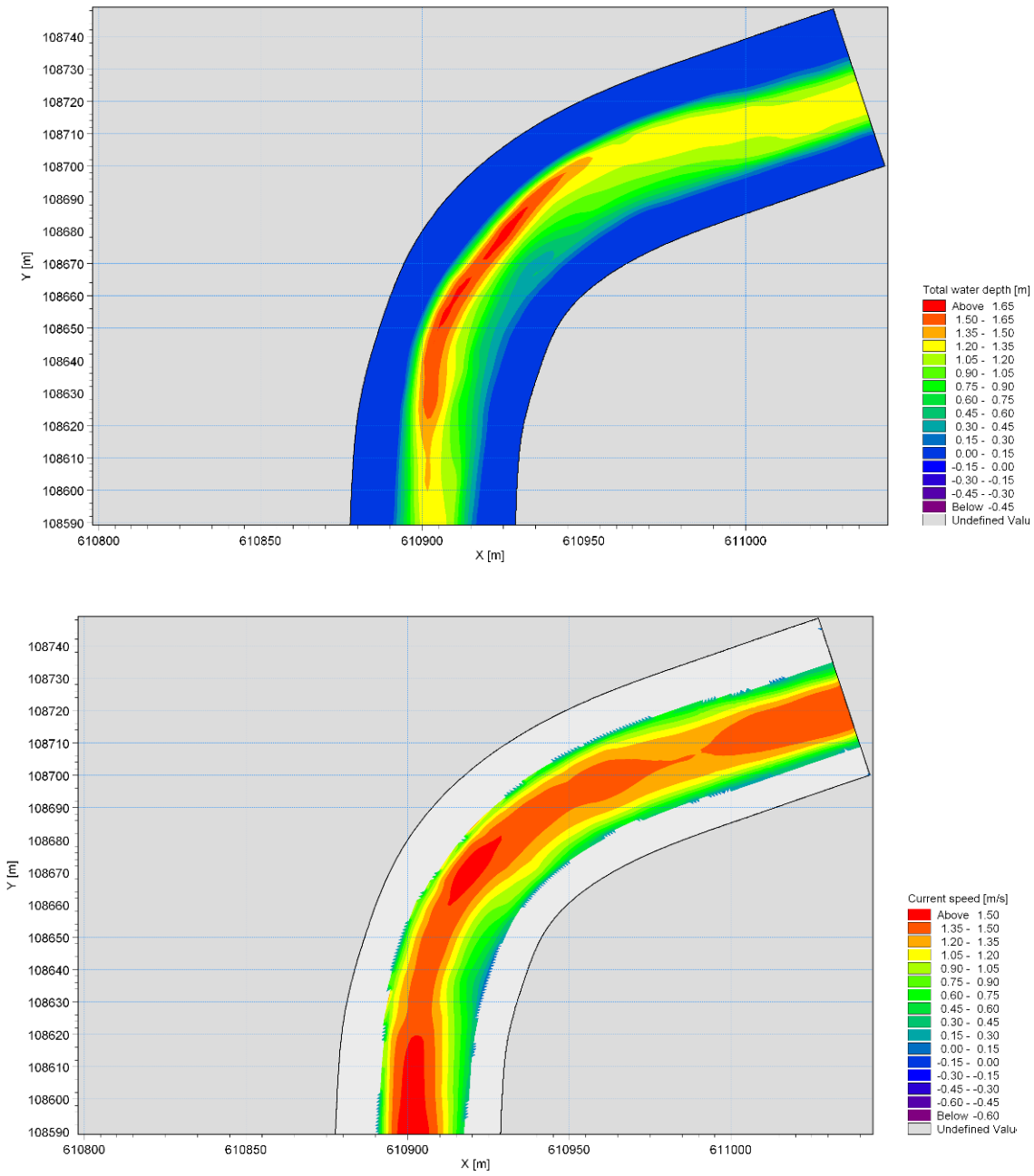

Figure 20: MIKE 21 FM Modeled Depth (Upper Panel) and Velocity (Lower Panel) for a Typical Pool-Riffle Sequence at a Baseflow of 32.5 m^3/s.

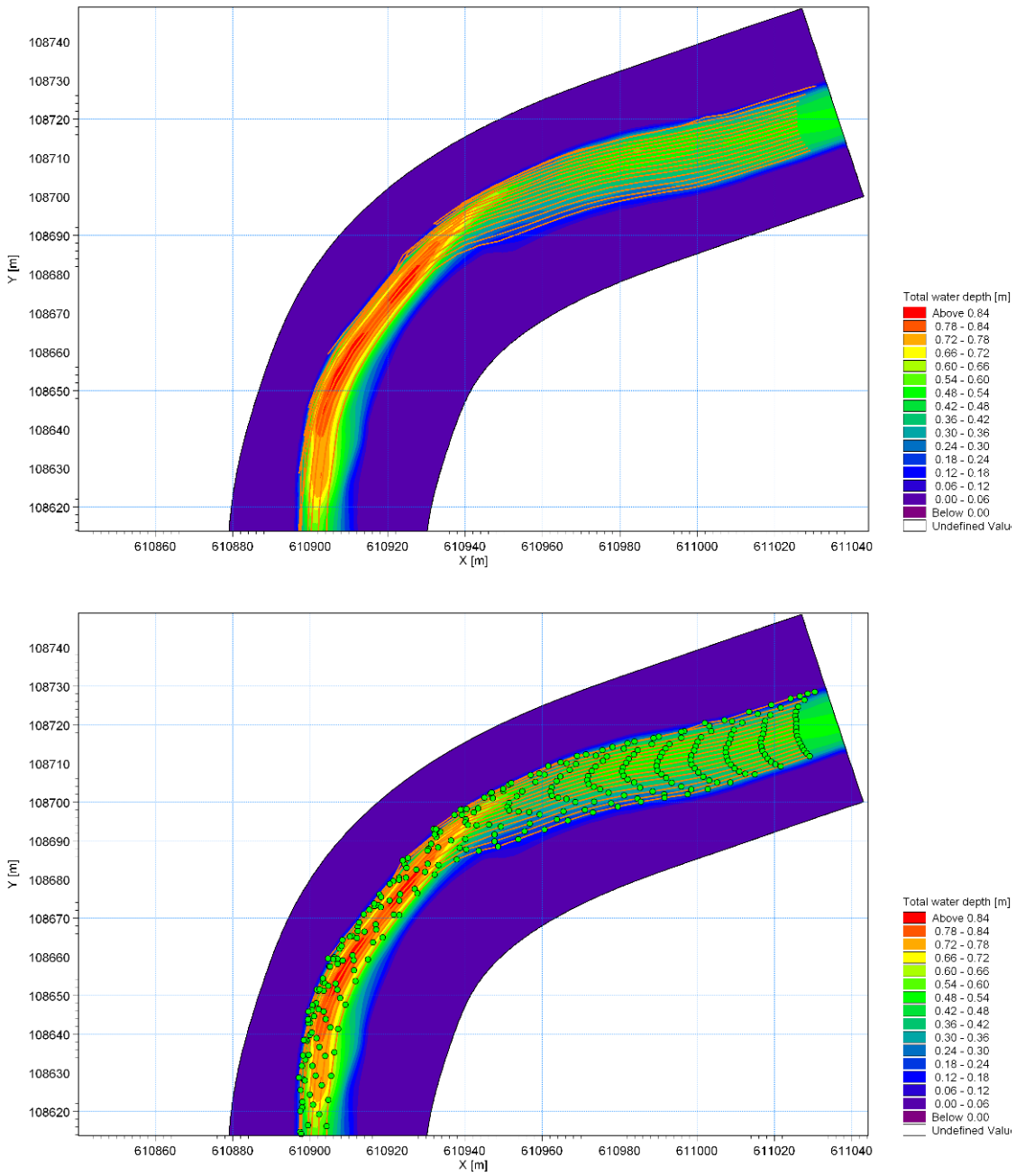

Figure 21: Modeled Particle Tracking Stream Traces (Upper Panel) and Instantaneous Particle Locations (Lower Panel), Overlain on a Contour Map of the Predicted Flow Depth. Discharge Equals 6.4 m^3/s.

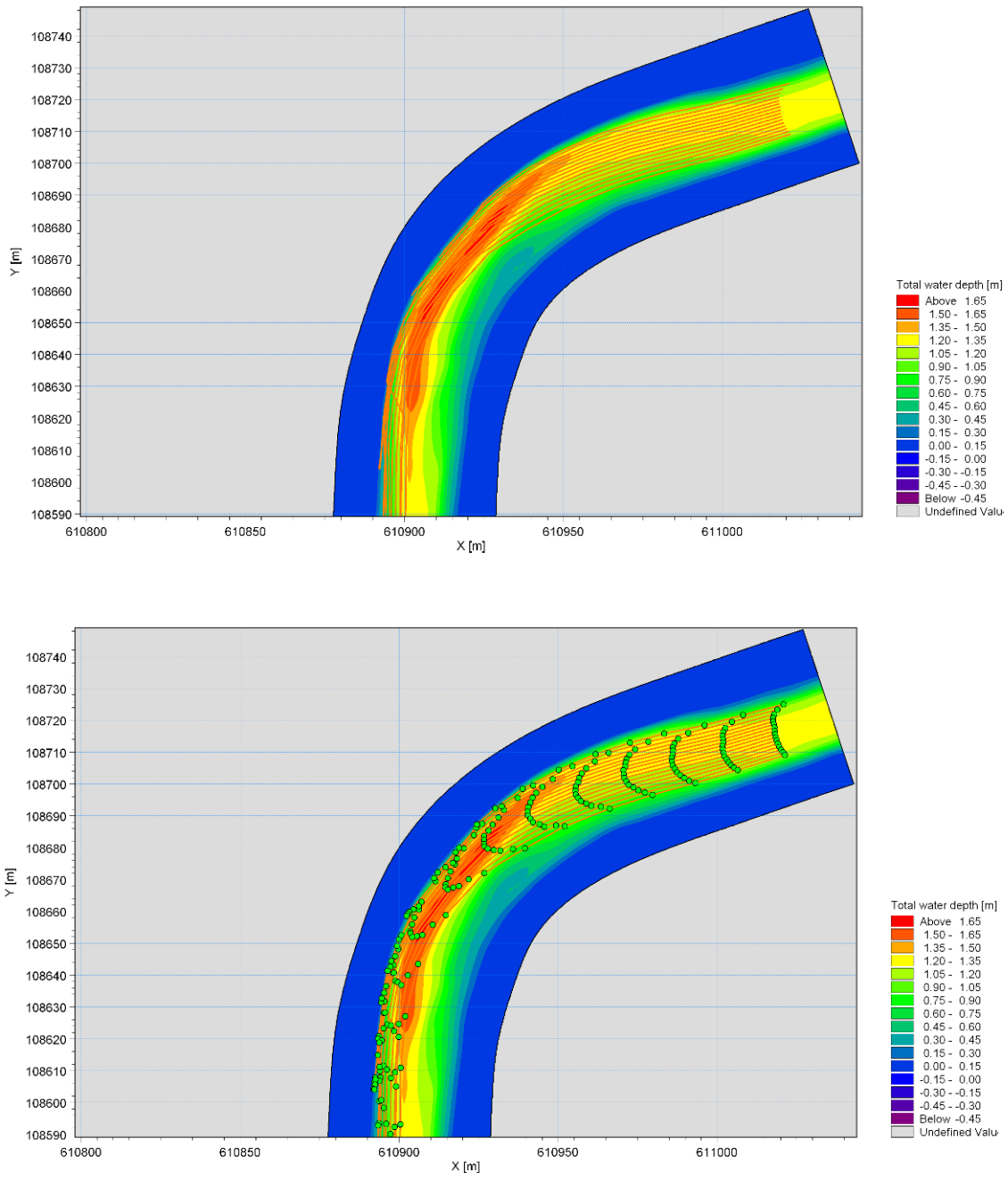

Figure 22: Modeled Particle Tracking Stream Traces (Upper Panel) and Instantaneous Particle Locations (Lower Panel), Overlain on a Contour Map of the Predicted Flow Depth. Discharge Equals 32.5 m^3/s.

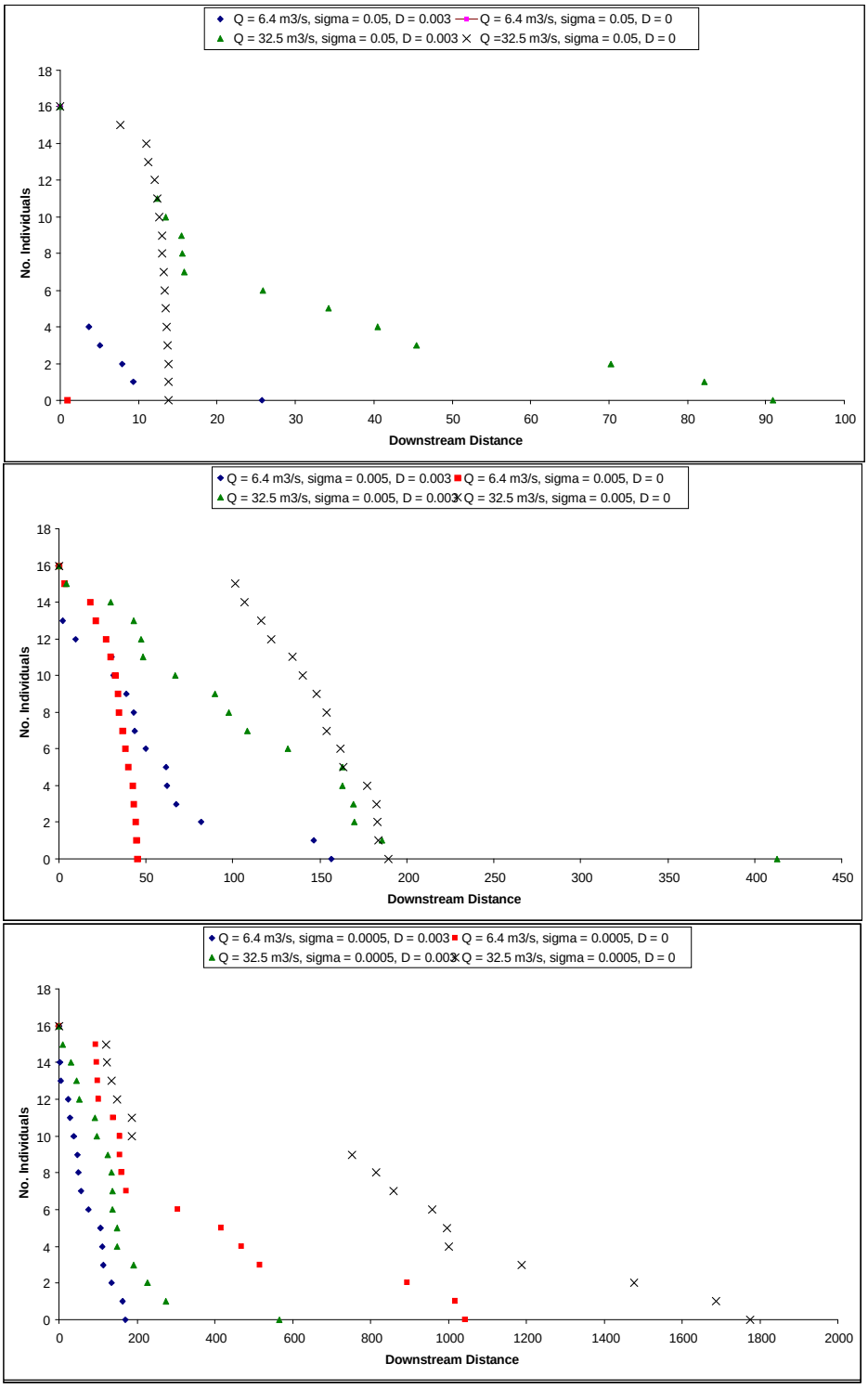

Figure 23: Particle Tracking Dispersal Results from the 2D Hydrological Model. Plots Give the Number of Individuals Remaining in the Drift as a Function of Drift Distance.

3.5 A drift/benthos model

Our approach to modeling movement dynamics of the 2D flow model particle tracking simulations in 1D is to use a spatially-explicit partial differential equation model. In our model, the population density of stream invertebrates consists of two coupled phases: an immobile phase where individuals reside on the habitat benthos, $N_B(x,t)$, and a dispersing phase where individuals are transported by stream flow, $N_D(x,t)$ (Lutscher *et al.* 2005; Pachepsky *et al.* 2005). Here, x is the location moving downstream and t is time. Macroinvertebrates emigrate from the benthos to the drift at per capita rate e_G (s^{-1}) while settlement from the drift to the benthos occurs at per capita rate σ (s^{-1}). Dispersal is accomplished through downstream advection at the velocity $v(x)$. The dynamics of the population are therefore described as

$$\begin{aligned}\frac{\partial N_D(x,t)}{\partial t} &= \underbrace{e_G N_B(x,t)}_{\text{emigration}} - \underbrace{\sigma N_D(x,t)}_{\text{resettlement}} - \underbrace{\frac{\partial}{\partial x}\left[v(x) N_D(x,t)\right]}_{\text{advection}} \\ \frac{\partial N_B(x,t)}{\partial t} &= -\underbrace{e_G N_B(x,t)}_{\text{emigration}} + \underbrace{\sigma N_D(x,t)}_{\text{resettlement}}\end{aligned} \quad . \quad (3.1)$$

The advection velocity $v(x)$ is given by the cross-sectional averaged velocity in Fig. 25 for the corresponding discharge. When $v(x)$ is made constant, Equation 3.1 predicts a distribution of dispersal distances given by a one-sided exponential where the average dispersal distance is equal to the velocity over the settlement rate, v/σ. Similar to the effects of diffusion in the 2D model, the resettlement process above introduces variance into the distances travelled in the drift.

We use the settling velocities ω_s calculated in 3.2.1 and the reach average depths for each discharge level to estimate settling rates. The reach average depths are 0.52 meters and 0.93 meters for discharges Q = 6.4 m^3/s and Q = 32.5 m^3/s, respectively. This yields settling rates of approximately 0.0962 $s^{-1} > \sigma > 0.000962$ s^{-1} for Q = 6.4 m^3/s and 0.0962 $s^{-1} > \sigma > 0.000962$ s^{-1} for Q = 32.5 m^3/s.

3.5.1 Stochastic simulation of the drift/benthos model

We simulate Equation (3.1) using the stochastic simulation algorithm (SSA) of Gillespie (2007) that was applied to a similar drift/benthos stream model by Kolpas and Nisbet (2010). In our stochastic version of Equation (3.1), we discretize space x into a set of k patches each with width Δx. Here, Δx is set to the mesh length 1 meter of the 2D flow model and the length of the system as the corresponding number of downstream patches when the 2D flow model is collapsed to its cross-sectional average, k = 1757.

We track the location of discrete individuals on the benthos in each patch j, N_{Bj}, whose location is altered only by movement. In order to simulate sample realizations of the stochastic movement process, we have to estimate properly distributed random variables for the time τ when the next movement event occurs. It is has been shown that the times between such

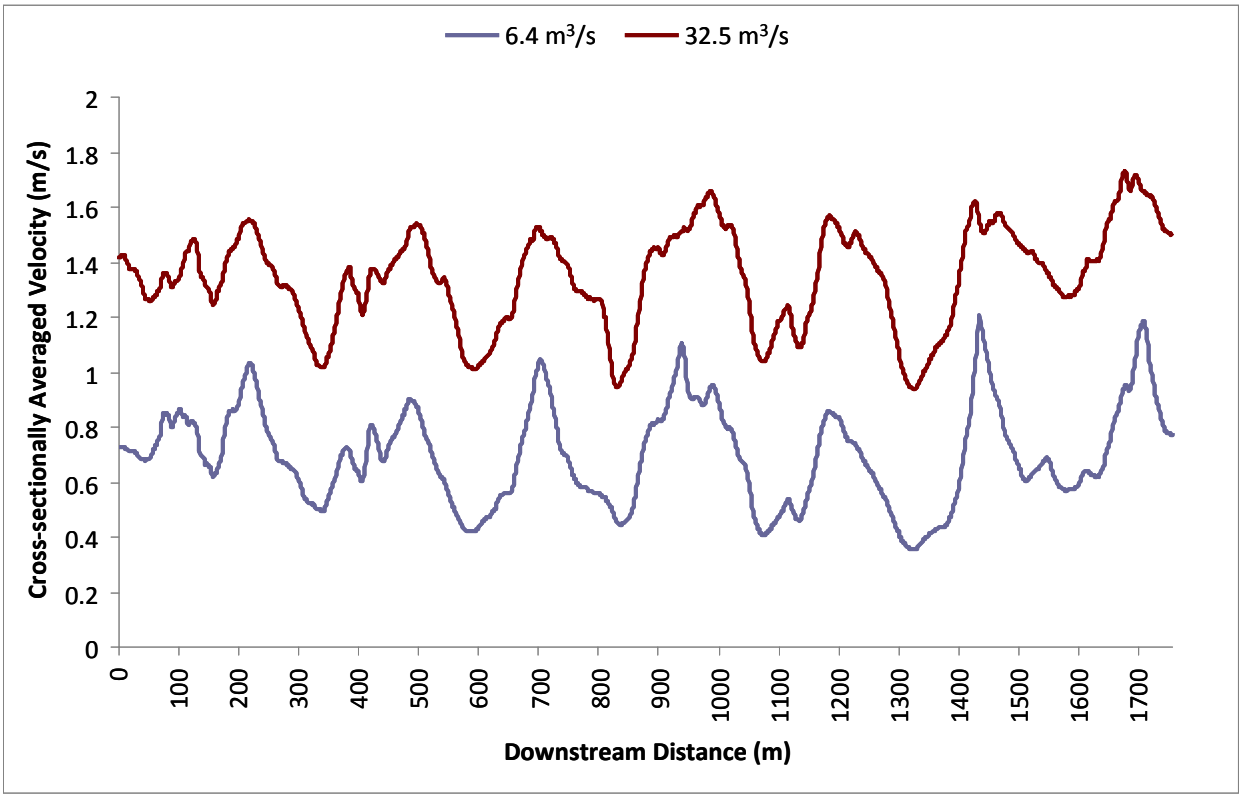

Figure 24: Cross-Sectional Averaged Velocities from the 2D Flow Model Simulated at Baseflow (6.4 m^3/s) and 75% Bankfull (32.5 m^3/s) Discharges.

discrete events are exponentially distributed (Gillespie 2007). Following Kolpas and Nisbet (2010), we implement the "first reaction" Monte Carlo method in order to generate simulated movement times. The idea behind the method is to generate M prospective event times τj by sampling the exponential distribution with rate constant equal to the per capita emigration rate eG and then choose the one that occurs first. It is this value that then determines when an organism leaves the benthos for the drift.

We simulate the advection-diffusion movement dynamics in the drift as a biased random walk process across the lattice of patches. While such a representation obviously ignores many deterministic aspects of macroinvertebrate drift behavior, it is often a good first approximation to estimating organism movement rates when such features are unmeasured (Turchin 1998). Once an individual is assigned a time for movement into the drift using the method above, it undertakes a series of downstream movements whose probabilities are determined by the advection velocity v(x). For the movement dynamics at the individual-based level to correspond to an advection process at the population level (Bailey 1964), we set the probability of moving downstream equal to $\Delta t\, v(x)/\Delta x$, with $\Delta t = 1$, $\Delta x = 1$. The velocity v(x) in each patch is the cross-sectionally averaged velocity in Figure 3.9 at the appropriate discharge.

We again sample from an exponential distribution to determine how long an individual undertakes a random walk, $p(t) = \sigma e^{-\sigma t}$, where σ is the settling rate from the drift and t is time.

The actual number of steps p(t) is then rounded to the nearest integer. Once this number of steps is completed, the individual returns to the benthos in the patch location where it ends its random walk.

Each simulation is started with an empty "river", and individuals are added to the initial upstream patch with probability b for all parameter combinations of eG and σ. The downstream end of the "river" in an absorbing boundary: if an individual crossed the downstream boundary, it is removed from the simulation.

The range of per emigration rates eG used in our simulations are estimated using observations on invertebrate drift rates and benthic densities collected in the Robinson Reach (Brad Caridinale and colleagues, unpublished data). The most prolific species in the Merced River are mayflies of the genus Baetis. Average drift densities of Baetis are ND ≈ 1/m3 and benthic densities are NB ≈ 1000/m2. As the depth in the Robinson Reach where the samples were taken was approximately 1 m deep on average, we can calculate the ratio of individuals in the drift to those in the benthos as depth x (ND/NB) = 0.001. From Equation (3.1), this ratio at equilibrium is the per capita emigration rate over the resettlement rate, eG/σ. Using values of σ from as described above, we estimate that eG is in the range of approximately 0.001-0.00001 s-1.

3.5.2 Stochastic simulation results

For each combination of parameter values (including with and without diffusion), simulations were run until a quasi-equilibrium in the total number of individuals in the system was achieved. The number of time steps required for each simulation to reach a quasi-equilibrium depended on the parameter values used, and could exceed 10^7 steps (this equates to a few "months" of simulated time). An example of the approach to quasi-equilibrium is shown in

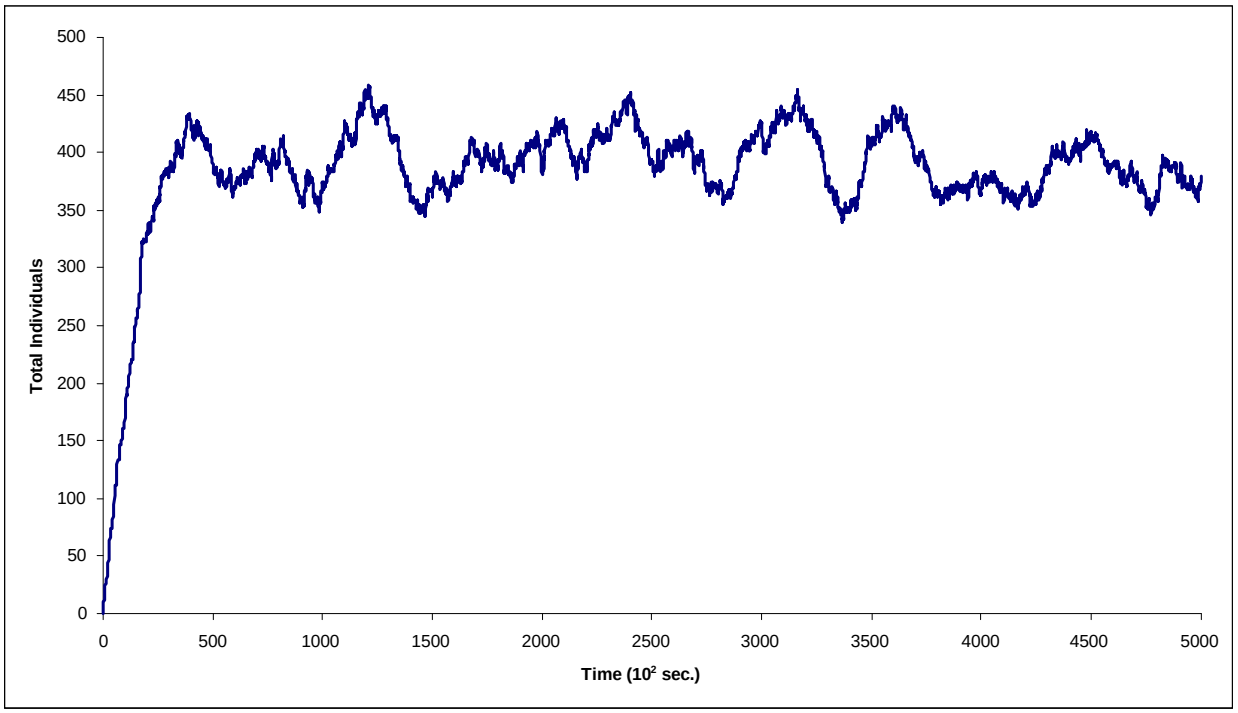

Figure 25: An Example of the Approach to Quasi-Equilibrium in a Replicate of the Stochastic Drift/Benthos Stream Simulation.

The example shown was run using velocities $v(x)$ from baseflow discharge conditions (6.4 m^3/s). Other parameters used were e_G = 0.001 and σ = 0.01.

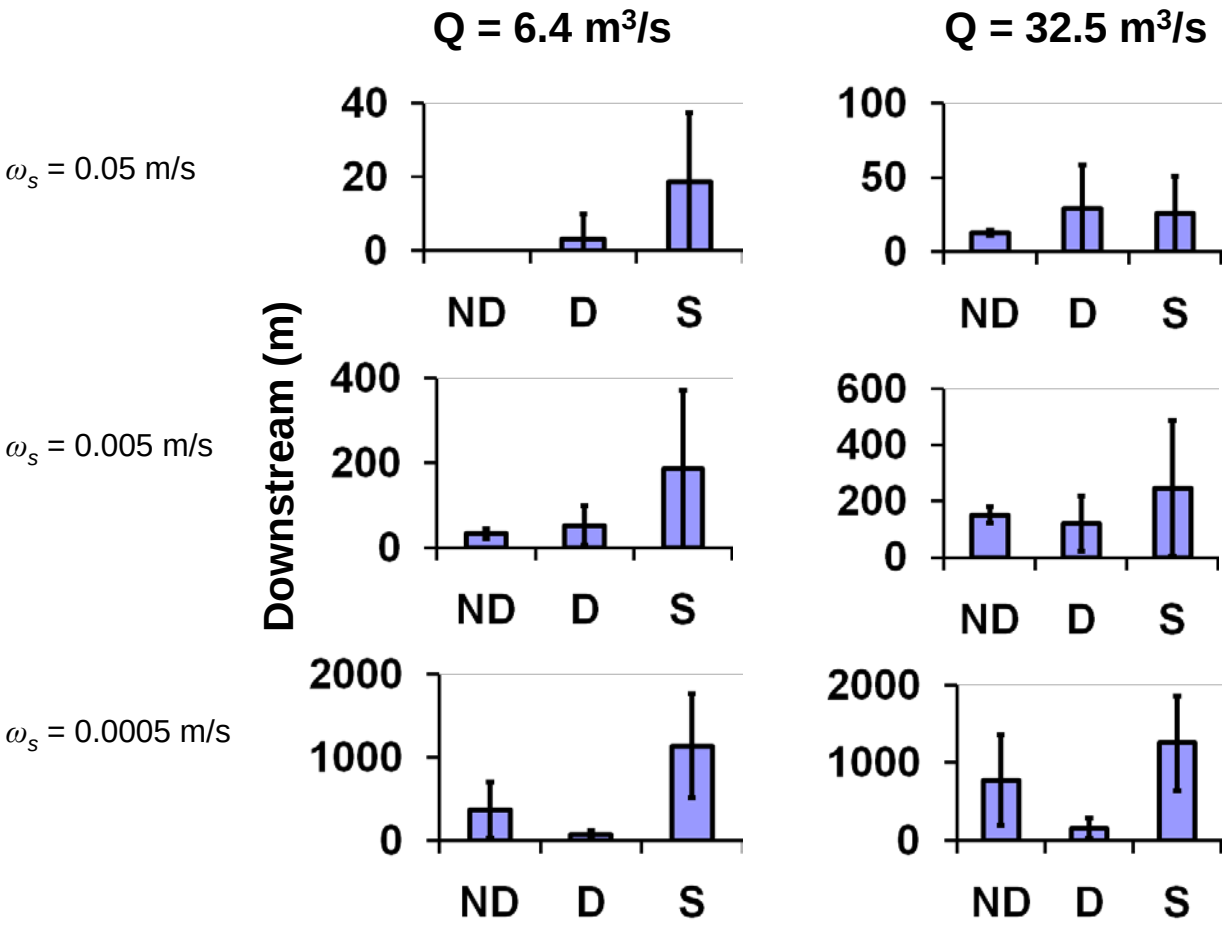

Figure 26: Average dispersal distances for simulated macroinvertebrates in 2D and 1D simulations.

Bars represent means and whiskers represent +/- one standard deviation. Results are presented for baseflow and 75% bankfull discharges Q and a range of settling velocities ωs. ND = no dispersion 2D simulation; D = dispersion (0.003 m2/s) 2D simulation; S = 1D simulation. Settling rates corresponding to the appropriate settling velocities are substituted for the 1D simulations

We begin by comparing a key characteristic length scale, the average dispersal distance traveled during a dispersal event. Figure 27 compares this value obtained from the 1D simulations with those obtained from the 2D hydrodynamic ones. Dispersal distances for the 1D simulations were calculated using individuals that were comparable to particles in the 2D simulations; i.e., those beginning a dispersal event at the initial upstream position. The number of individuals used varied among parameter combinations, but was never less than several hundred.

Similar to the 2D simulations, increased discharge and reduced settlement rates both worked to increase the average dispersal distance. Despite considerable flow variability, the distribution of dispersal distances was well approximated by an exponential distribution (data not shown) in every case. For such a distribution, the mean equals the variance (i.e., for p(x) = $\lambda e^{-\lambda x}$, mean = s.d. = 1/λ). This result is well reflected in the results of the 1D simulation and comparably better reflected than the results of the 2D particle tracking simulations. The substantial variance in the dispersal distances for the 1D simulations stems from the stochastic representation of

settlement. The only cases where the means and standard deviations of the 1D dispersal distances were not equal were for the lowest settling rates at each discharge. In these cases, dispersal of individuals was so far that many exited the downstream boundary, truncating the dispersal distribution.

In all parameter combinations except for settling velocity equal to 0.05 m/s at 32.5 m^3/s discharge, the 1D dispersal distances exceed those of both the no-dispersion and dispersion 2D simulations. It is likely that our parameterization of the 1D settlement rate does not accurately capture the settlement dynamics in the 2D model. One obviously missing component is dispersion. In one dimension, a 1D model with dispersion coefficient D (m^2/s) is

$$\frac{\partial N_D(x,t)}{\partial t} = \underbrace{e_G N_B(x,t)}_{\text{emigration}} - \underbrace{\sigma N_D(x,t)}_{\text{resettlement}} - \underbrace{\frac{\partial}{\partial x}\left[v(x) N_D(x,t)\right]}_{\text{advection}} + \underbrace{D\frac{\partial^2 N_D(x,t)}{\partial x^2}}_{\text{dispersion}}$$
$$\frac{\partial N_B(x,t)}{\partial t} = -\underbrace{e_G N_B(x,t)}_{\text{emigration}} + \underbrace{\sigma N_D(x,t)}_{\text{resettlement}} \quad . \quad (3.2)$$

The average dispersal distance for Equation 3.2 $v(x)$ is held constant at its average value is

$$\frac{2D}{v - \sqrt{v^2 + 4\sigma D}} \quad (3.3)$$

(see Lutscher et al. 2005 for a derivation). From Equation 3.3 it becomes clear that the addition of further dispersion would *increase* the average dispersal distance. This suggests that the mismatch between 1D and 2D simulations stems from the effects of dispersion on settlement in the 2D simulation, where it alters settlement dynamics by moving particles into and out of the high velocity core and speeding their contact with the benthos via vertical dispersion. Thus, the actual average settlement rate σ of particles in the 2D simulations diverges from that predicted by the settlement velocity ω_s and the reach average depth. Investigations of this hypothesis are ongoing.

Figure 28 presents the results of simulations across the range of parameter values. In each case, simulations are run for ten replicates, and average densities for each patch across each run were taken. Additionally, results are presented as proportional changes in density from the distributions spatial average value. For all parameter values, benthic densities of macroinvertebrates are strongly inversely proportional to flow velocity. This intuitive result also mirrors the results of the particle tracking algorithm, where individuals are more likely to settle in slow moving patches due to increased residence times in these areas. It is worth noting this result translate to drift densities as well, since benthic and drift ratios are directly proportional.

Somewhat surprising is that the proportional changes in densities are relatively insensitive to changes in emigration and settlement parameters over the range we have examined. It appears, then, that velocity variation drives the spatial pattern, while emigration and settlement rates work with the input rate to set the absolute densities in the system. Of course, we anticipate that

emigration and settlement rates would also vary with flow in natural systems, causing these parameters to exhibit a more dramatic impact on variability in benthic and drift densities.

In order to explore these results in the context of the actual population dynamics of aquatic macroinvertebrates, we introduce two new parameters to Equation 3.1, a recruitment term R (individuals/m) and a per capita morality rate m (s^{-1}). The recruitment term could represent hatching from egg banks laid by terrestrial adults, while the mortality term could represent

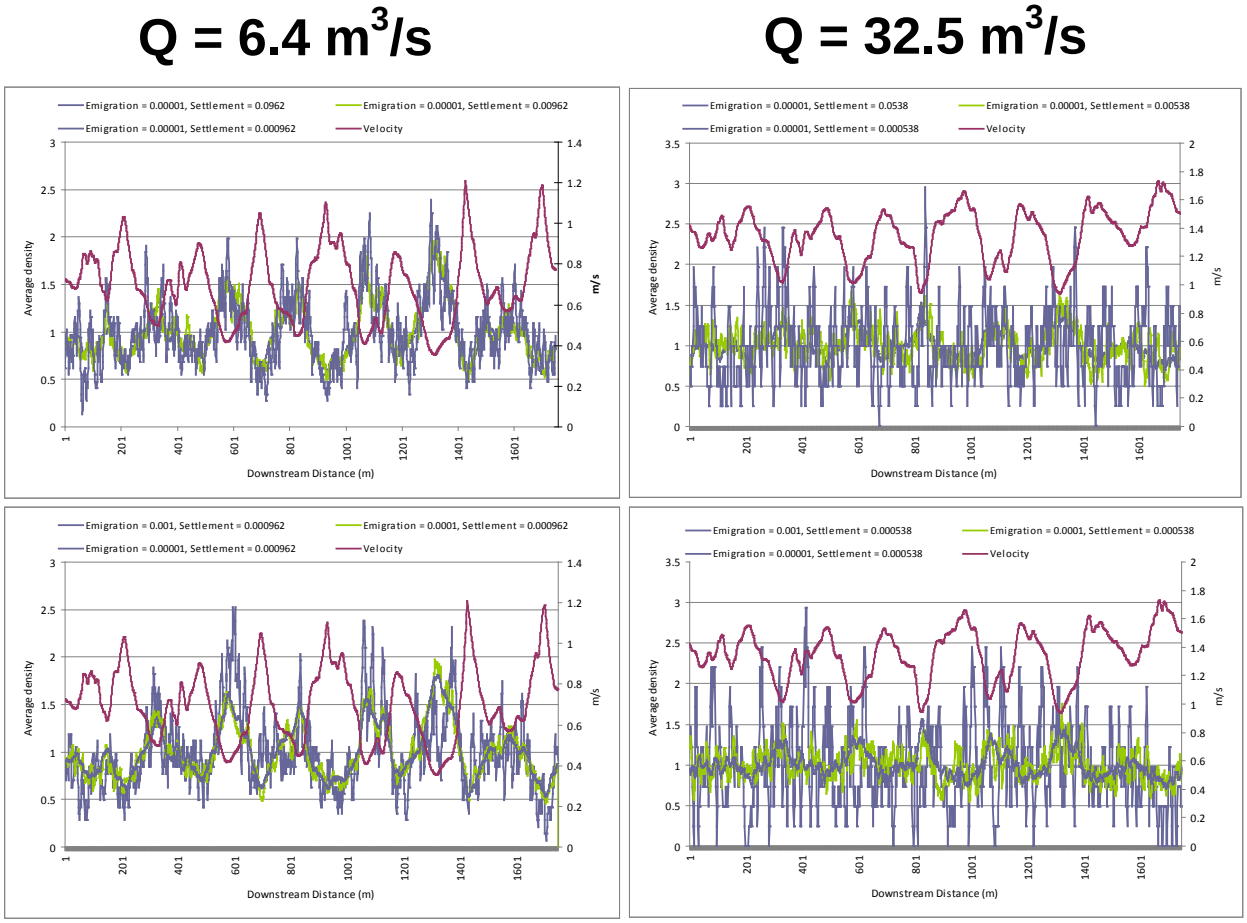

Figure 27: Spatial Variation in Average Benthic Densities and Flow Velocities in the 1D Simulations.

Benthic densities are presented as the average across ten replicate runs and as a proportion of their spatial average values. The input rate into the upstream patch is set to b = 0.001 s-1 for the upper two panels and 0.1 s-1 for the bottom two.

predation by salmon and other predators as well as other sources of mortality. While these terms likely vary in space, we assume here that they are constant. Progress towards understanding how variability in flow will influence these dynamics is facilitated by setting Equation (3.1) to equilibrium, recasting N_B, N_D, and v in terms of small changes from their spatial average values, $N_B(x,t) = \overline{N}_B + n_B$, $N_D(x,t) = \overline{N}_D + n_D$, and $v(x) = \overline{v} + \mu$, and ignoring products of spatially variable terms, yielding

$$0 = e_G n_B(x) - \sigma n_D(x) - \bar{v}\frac{\partial n_D(x)}{\partial x} - \bar{N}_D\frac{\partial \mu(x)}{\partial x} \quad . \qquad (3.3)$$
$$0 = -(e_G + m) n_B(x,t) + \sigma n_D(x,t)$$

Progress is further facilitated by the use of Fourier transforms,

$$\tilde{n}_B(k,t) = \int_{-\infty}^{\infty} n_B(x,t)\exp(-ikx)\,dx, \quad \tilde{n}_D(k,t) = \int_{-\infty}^{\infty} n_D(x,t)\exp(-ikx)\,dx, \quad . \ (3.4)$$
$$\tilde{\mu}(k,t) = \int_{-\infty}^{\infty} \mu(x,t)\exp(-ikx)\,dx$$

In our context, Fourier transforms are useful in that they allow us to represent spatial variability in flow velocity or population densities as the integral of sinusoids of different spatial frequencies *k*. Applying the Fourier transform to Equation 3.3 and conducting routine algebra yields a *transfer function* that describes how in the input of the Fourier transformed variability in flow velocity drives the output of the Fourier transformed variability in benthic densities as function of the spatial frequency *k*,

$$\frac{\tilde{n}_B}{\tilde{\mu}} = -\frac{1}{m}\frac{\bar{N}_D ik}{1 + \frac{\bar{v}}{\sigma}\left(1 + \frac{e_G}{m}\right)ik} \quad . \qquad (3.5)$$

Details of transfer function calculation and interpretation are given in Anderson et al. (2005) and Nisbet et al. (2007). However, this transfer function presents two immediate results. First, the negative sign in front of the function indicates that, as in Figure 28, positive changes in velocity leads to negative changes in benthic density (i.e., velocity and benthic density variation are anti-phase). Second, the addition of births and deaths causes the magnitude of benthic density response to be dependent on the spatial scale over which velocity is varying, where the spatial scale is denoted by the wavelength $L_E = 2\pi/k$. Variation in flow that fluctuates over very small spatial scales (high *k*, low L_E) has a very strong effect on benthic population variation. Much larger scale variation in flow has a much smaller effect.

A final note is that Anderson et al. (2005) demonstrate that the term $\frac{\bar{v}}{\sigma}\left(1 + \frac{e_G}{m}\right)$ is a characteristic lengths scale for the system, which they call the *response length*. Given that v/σ is the average dispersal distance per drift event, proper estimation of this value for linking drift variability to population dynamics becomes evident.

3.6 Conclusions

Accurately representing dispersal is a key challenge to the application of characteristic length scales in IFA settings. Here, we have combined several different modeling methods in an effort to determine the validity of simplified flow representations and their effects on drift dispersal. One-dimensional representations of flow variability retained key structural components of our full 2D hydraulic model. If we ultimately demonstrate our approach to be valid, it will provide the benefit that models based on 1D representations of flow require substantially less processing time and computer power relative to those that include full 2D representations. This

in turn allows flow data to be linked to separate models of population dynamics with a minimum of computational complexity.

The flow modeling in the current project demonstrated the feasibility of developing 1D approximations to invertebrate distributions in an artificially simple (engineered) river section. We view the Robinson Reach as a field-scale laboratory for investigating the relation between the flow and invert transport patterns in simple river system. In this sense our approach is similar to using a lab flume but conducted at field-scale. Despite this, we caution that both our modeling approach and the flow dynamics of the Robinson Reach introduce many simplifications that do not hold in "typical" river ecosystems. With this in mind, we suggest two modeling extensions of our work that would greatly add to its value.

First, some incorporation of behavior in the "particles" that represent the drifting animals would potentially expand the ability of our 1D representations to predict availability of macroinvertebrate food to young salmon. There are numerous candidate components to consider, including active swimming and settling in the drift (Oldmeadow et al. 2010), undirected and upstream-biased benthic crawling (Williams and Williams 1993), and emigration responses to local environmental conditions. The latter is especially important in the context of our simple prediction that benthic density should be inversely proportional to flow velocity. This result implies that most macroinvertebrates in the Merced River will be located in pools where salmon are abundant. However, invertebrates could increase their emigration rate in areas of unfavorable flow (Fonseca and Hart 1996) or predation pressure (Englund 2005). Strong emigration responses could therefore weaken or even invert the predictions we make regarding flow and benthic macroinvertebrate density. In addition, we recommend careful examination of the effects of introduction height on distances traveled. This parameter could strongly influence dispersal distances. Given the simplicity of the Merced River, the expected result of releasing particles at, say, the water surface would be a slight increase in the travel distance due to the higher velocity at the surface. However, this assumption remains to be tested and is a high priority for our future work.

The transfer function in Equation 3.5 illustrates how spatial variation can interact with dispersal to alter ecological dynamics across spatial scales. The output of Equation 3.5 is similar to dynamics observed in previous theory, where environmental variability influencing movement rates (e.g., emigration) has the strongest population response over small spatial scales and is weak or absent over much larger scales (Anderson et al. 2005; Nisbet et al. 2007; Anderson et al. 2008; Diehl et al. 2008). In contrast, variability influencing demographic rates such as births and mortality causes a stronger response over the largest spatial scales and a weaker response over smaller ones. Transfer functions for all of these relationships are straightforward to calculate, and can simultaneously explore the responses to multiple environmental drivers (Nisbet et al. 2007). For example, it should be possible to predict contrasting responses of flow variability on settlement, emigration, and mortality by predation indifferent flow regimes. We view incorporation of these factors into the modeling framework we have described as a fitting and exciting next step.

A second extension should consider the introduction of some small level of additional physical habitat complexity that could represent, for example, the region close to large woody debris. Creation of structural complexity is a common restoration strategy for streams and rivers, but one that has met with mixed success (Palmer et al. 2010). Modeling changes in flow and invertebrate transport could provide vital insight into the value of such strategies and/or the scale over which they must be undertaken to provide marked positive influence on fish habitat. Representing flow complexity in 1D that is introduced because of structural alterations could present additional technical challenges, but could again serve as an effective link between restoration effects on physical habitat and desired ecological endpoints.

Beyond model development, a crucial prerequisite for the application of characteristic length scale theory to river management is the empirical validation of key assumptions and predictions. A long-standing criticism of traditional habitat-based IFA methods is that they have been not been adequately tested (Anderson et al. 2006b; Locke et al. 2008). Developing theory based on ecological dynamics has great potential for IFAs, yet—like traditional methods—it requires empirical scrutiny before implementation. While particle tracking models have long-standing application in hydrogeomorphology and hydrological engineering, the simple fact that aquatic macroinvertebrates can alter their behavior in the drift (e.g., Oldmeadow et al. 2010) complicates application of particle tracking to ecological contexts. We have shown how key parameters (settling velocities and settling rates) can be extracted from studies of invertebrate drift behavior. When applied to a specific system, such studies could be informative when applied to the dominate prey taxa for focal fish species (e.g., Baetid mayflies for salmon in the Merced). This could include laboratory studies of settling velocities and drift behavior (e.g., Fonseca 1999; Hayes et al. 2007; Oldmeadow et al. 2010) or experimental drift releases in the field (e.g., Elliott 1971). Field validations of drift models should include standard sampling of drift and benthic densities. As an example, Hayes et al. (2007) included laboratory studies of settling velocities and field validations of drift densities to parameterize a pool-level model of drift delivery in a New Zealand river. Because of the central focus on flow needs, drift experiments and field validation should be conducted over range of flow conditions, as is standard in hydrogeomorphology (see section 3.2.2). Conducting such studies is a future goal of our collective research program.

CHAPTER 4:
Conclusions and Recommendations

4.1 Conclusions

This research rested on the premise that current approaches to environmental flow assessments should be complemented by methodology that takes account of ecological dynamics. Recognizing that the viability of salmon populations is a key concern in many California rivers, the research team focused on two related themes: development and testing of a dynamic energy budget model for salmon and study of the spatial scales of variation in the distribution of benthic invertebrates, essential food for young salmon. There were two broad objectives:

1. To formulate and evaluate a *full life cycle* model for Pacific salmon based on Dynamic Energy Budget (DEB) theory.
2. To perform simulations that can guide appropriate representations of flow-mediated dispersal and resulting distributions of benthic macroinvertebrates that comprise the major food source of salmon.

Nuanced descriptions of the findings from each study are in chapters 2 and 3; this chapter offers an overview of the findings that can be read without reference to the details.

4.1.1 Dynamic Energy Budget Model for salmon

Synthesis of data from five salmon species to test the assumptions and predictions of the DEB model

DEB theory makes predictions on how rates of physiological processes and transitions between life stages vary among taxonomically similar species. A number of these predictions were tested using literature data from five species: pink, chum, sockeye, coho and chinook. The research emphasized early life stages (egg, embryo, young juvenile), but data on returning adult females (length, fecundity and egg size) were also studied. Observed patterns both at the embryo stage and the spawning adult stage were well captured by the model. Initial discrepancies between data and model predictions for sockeye reproductive traits and coho development rates were resolved by adjusting one parameter value for both species, assuming these species-specific differences resulted from natural selection. The findings supported the validity of our approach to model all the different life stages of a Pacific salmon in a common framework, opening the new possibility to evaluate how the conditions experienced during the early life stages influences subsequent life stages.

Parameterization of the DEB model for Chinook salmon (Oncorhynchus tshawytscha)

The simulation results for chinook broadly agreed with experimental studies on chinook growth and development rates. However, the fecundity patterns that were initially predicted did not match the field data. The literature survey for other Pacific salmon species allowed us to identify models rules that led to better descriptions of the reproduction traits of chinook females. Further work will refine the parameter estimates with the new model assumptions (food availability and allocation to reproduction).

Calculations of sensitivity of salmon population growth rate to changes in food delivery rate

The methodology is in place, but the calculations require completion of the next round of parameter estimation for Chinook.

4.1.2 Simulations of flow-mediated dispersal and resulting distributions of benthic macroinvertebrates

2D hydraulic model of a restored section of the Merced River

A hydraulic model (MIKE 21 FM) was used to characterize the two-dimensional (2D) flow field through the lower 1.7 km of a restored region of the Merced River. The model was calibrated to match surface elevations and validated using vertically averaged flow measurements. Flow fields obtained from the model under baseflow and 75 percent bankfull discharge conditions indicated the presence of a high velocity core. A particle tracking module was added to describe the transport of benthic macroinvertebrates such as baetid mayflies that intermittently enter the drift and are transported downstream. The transport component was parameterized using a mix of literature data and measurements from previous studies in the Merced region. The trajectories of simulated macroinvertebrates were dominated by the high velocity core under all discharge conditions, though the zone of invertebrate transport occupied a greater fraction of the channel width under high discharge. Simulations where macroinvertebrate transport was determined solely by downstream velocity and sinking, produced settlement over a very small range of locations. The addition of random dispersion, modeled as proportional to eddy viscosity, introduced increased variance in settlement and generated distributions of dispersal distances qualitatively consistent with observations in the literature.

1D models of the transport and distribution of macroinvertebrates

The 2D flow environment was collapsed into a 1D representation that allowed its use in population dynamic models for benthic invertebrates previously developed by two members of the project team. Cross-sectional averaged flow velocities in the 1D representation retained hydraulic structure, including variation from riffle/pool sequences and sand bar development. We ran a stochastic simulation model incorporating the 1D flow representation and compared predicted transport and settlement dynamics with output from the 2D particle tracking model. Simulations yield distributions of macroinvertebrates that show a strong inverse relationship with flow velocity whose strength is set by other model parameters, namely the rate at which drift dispersal is initiated and the rate at which dispersers settle to the benthos. Surprisingly, these parameters had minimal effects on benthic distributions over the range of parameters examined.

Influences of flow variability on characteristic length scale calculations for the Merced River

Estimates of dispersal distributions from the 1D and 2D models were compared and were qualitatively similar. One characteristic length scale, the average dispersal distance, was overestimated in the 1D model under most parameter combination. This result is likely owing to an incomplete representation of how dispersion in the 2D model influences settlement in the 1D model.

4.2 Recommendations for Future Research

The research themes addressed in this study were identified in earlier work as a necessary step before process-based models can make a major contribution to instream flow assessments (IFA). These themes were also consistent with more recent recommendations on research priorities in publications from the Instream Flow Council (Locke et al., 2008).

The findings from this one year project represent incremental progress toward the broad goal of developing applicable process-based models. However there are two areas of immediate potential application of the DEB modeling, and a third, involving further flow modeling that would greatly extend our ability to model performance of young salmon:

Modeling embryonic development and early juvenile growth of young salmon

Flow regime influences egg viability in part through its effects on temperature and oxygen supply to redds. The DEB model here can be extended, using previously developed theory to describe the effects of both variables on egg viability and on the growth of fry. For example, a high-resolution temperature and flow model for the Sacramento River that could be coupled to the Chinook embryo DEB model to examine how operation of Shasta Reservoir impacts incubating winter-run Chinook eggs in the reaches of the Sacramento River below the dam.

Reconstructing environmental histories from otoliths or scales

The DEB model in this report projects the effect of a specified environment on the physiological performance of fish. The reverse process (inverse modeling) could be used to determine the history of some environmental variable (e.g., food supply), given information on temperature and on growth history (determined from otoliths or scales). This again would represent application of previously developed methodology.

Improved representations of food delivery to young salmon

The flow modeling in the current project demonstrated the feasibility of developing 1D approximations to invertebrate distributions in an artificially simple (engineered) river section. Two extensions of the work would greatly add to its value: some incorporation of behavior in the "particles" that represent the drifting animals, and introduction of some small level of additional flow complexity that could represent, for example, the region close to large woody debris.

Each of the above suggestions involves adapting existing, published theory for the particular problems associated with environmental flow assessments.

REFERENCES

Allan J.D. and Feifarek B.P. 1989. Distances traveled by drifting mayfly nymphs - factors influencing return to the substrate. *Journal Of The North American Benthological Society*, 8, 322-330

Anderson K.E., Nisbet R.M. and Diehl S. 2006a. Spatial scaling of consumer-resource interactions in advection-dominated systems. *The American Naturalist*, 168, 358-372

Anderson K.E., Nisbet R.M., Diehl S. and Cooper S.D. 2005. Scaling population responses to spatial environmental variability in advection-dominated systems. *Ecology Letters*, 8, 933-943

Anderson K.E., Nisbet R.M. and McCauley E. 2008. Transient responses to spatial perturbations in advective systems. *Bulletin Of Mathematical Biology*, 70, 1480-1502

Anderson K.E., Paul A.J., McCauley E., Jackson L.J., Post J.R. and Nisbet R.M. 2006b. Instream flow needs in streams and rivers: The importance of understanding ecological dynamics. *Frontiers in Ecology and the Environment*, 4, 309-318

Aydin K.Y., McFarlane G.A., King J.R., Megrey B.A. and Myers K.W. 2005. Linking oceanic food webs to coastal production and growth rates of Pacific salmon (*Oncorhynchus spp.*), using models on three scales. *Deep-Sea Research Part `II`-Topical Studies in Oceanography* 52, 757-780.

Bailey N.T.J. 1964. *The elements of stochastic processes*. Wiley, New York.

Ballantyne A.P., Brett M.T. and Schindler D.E. 2003. The importance of dietary phosphorus and highly unsaturated fatty acids for sockeye (*Oncorhynchus nerka*) growth in Lake Washington - a bioenergetics approach. *Canadian Journal of Fisheries and Aquatic Sciences* 60, 12-22.

Beacham T.D. and Murray C.B. 1990. Temperature, egg size, and development of embryos and alevins of 5 species of pacific salmon - a comparative-analysis. *Transactions of the American Fisheries Society*, 119, 927-945

Beacham T.D. and Murray C.B. 1993. Fecundity and egg size variation in North-American Pacific salmon (*oncorhynchus*). *Journal of Fish Biology*, 42, 485-508

Beauchamp D.A., Sergeant C.J., Mazur M.M., Scheuerell J.M., Schindler D.E., Scheuerell M.D., Fresh K.L., Seiler D.E. and Quinn T.P. 2004. Spatial-temporal dynamics of early feeding demand and food supply for sockeye salmon fry in Lake Washington. *Transactions of the American Fisheries Society* 133, 1014-1032.

Beckman B.R., Gadberry B., Parkins P., Cooper K.A. and Arkush K.D. 2007. State-dependent life history plasticity in Sacramento River winter-run chinook salmon (*Oncorhynchus tshawytscha*): interactions among photoperiod and growth modulate smolting and early male maturation. *Canadian Journal of Fisheries and Aquatic Sciences* 64, 256-271.

Bjornstad O.N., Nisbet R.M. and Fromentin J.-M. 2004. Trends and cohort resonant effects in age-structured populations. *Journal of Animal Ecology*, 73, 1157-1167

Brodeur R.D., Francis R.C. and Pearcy W.G. 1992. Food consumption of juvenile coho(*Oncorhynchus kisutch*) and chinook salmon (*O. tshawytscha*) on the continental shelf off Washington and Oregon. *Canadian Journal of Fisheries and Aquatic Sciences* 49, 1670-1685.

CADWR. 2005. The Merced River Salmon Habitat Enhancement Project: Robinson Reach Phase III, 159 pp., California Department of Water Resources, San Joaquin District, Fresno, CA.

Caswell H. 2001. *Matrix population models: Construction, analysis, and interpretation*. Sinauer Associates, Sunderland.

Cech J.J. and Myrick C.A. 1999. *Steelhead and Chinook Salmon Bioenergetics: Temperature, Ration, and Genetic Effects*. University of California Water Resources Center, Davis, CA.

Ciborowski J.J.H. 1983. Influence of current velocity, density, and detritus on drift of 2 mayfly species (ephemeroptera). *Canadian Journal Of Zoology-Revue Canadienne De Zoologie*, 61, 119-125

De Roos A.M. 2008. Demographic analysis of continuous-time life-history models. *Ecology Letters*, 11, 1-15

DHI. 2009a. MIKE 21 Flow Model FM. Horsholm, Denmark, 56 p.

DHI. 2009b. MIKE 21 Flow Model FM: Particle Tracking Module. Horsholm, Denmark, 48 p.

Diehl S., Anderson K. and Nisbet R.M. 2008. Population responses of drifting stream invertebrates to spatial environmental variability: New theoretical developments. In: *Aquatic insects: Challenges to populations* (eds. Lancaster J & Briers RA), p. In press. CABI Publishing

Einum S., Fleming I.A., Cote I.M. and Reynolds J.D. 2003. Population stability in salmon species: Effects of population size and female reproductive allocation. *Journal of Animal Ecology*, 72, 811-821

Elliott J.M. 1971. The distances travelled by drifting invertebrates in a lake district stream. *Oecologia*, 6, 350-379

Englund G. 2005. Scale dependent effects of predatory fish on stream benthos. *Oikos*, 105, 31-40

Fonseca D.M. 1999. Fluid-mediated dispersal in streams: Models of settlement from the drift. *Oecologia*, 121, 212-223

Fonseca D.M. and Hart D.D. 1996. Density-dependent dispersal of black fly neonates is mediated by flow. *Oikos*, 75, 49-58

Garner S.R., Heath J.W. and Neff B.D. 2009. Egg consumption in mature pacific salmon (*oncorhynchus spp.*). *Canadian Journal of Fisheries and Aquatic Sciences*, 66, 1546-1553

Gillespie D.T. 2007. Stochastic simulation of chemical kinetics. *Annual Review Of Physical Chemistry*, 58, 35-55

Groot C. and Margolis L. (eds.) 1991. *Pacific Salmon Life Histories*. UBC Press, Vancouver.

Groot C., Margolis L. and Clarke W.C. (eds.). 1995. *Physiological Ecology of Pacific Salmon*. UBC Press, Vancouver.

Hayes J.W., Hughes N.F. and Kelly L.H. 2007. Process-based modeling of invertebrate drift transport, net energy intake and reach carrying capacity for drift-feeding salmonids. *Ecological Modeling*, 207, 171-188

Heming T.A. 1982. Effects of temperature on utilization of yolk by chinook salmon (*oncorhynchus tshawytscha*) eggs and alevins. *Canadian Journal of Fisheries and Aquatic Sciences*, 39, 184-190

Jasper J.R. and Evenson D.F. 2006. Length-girth, length-weight, and fecundity of yukon river chinook salmon *oncorhynchus tshawytscha*. In: *Fishery Data Series. Tech. rept.* Alaska Department of Fish and Game. Divisions of Sport Fish and Commercial Fisheries

Kolpas A. and Nisbet R.M. 2010. Effects of demographic stochasticity on population persistence in advective media. *Bulletin Of Mathematical Biology*, 72, 1254-1270

Kooijman S.A.L.M. 2009. What the egg can tell about its hen: Embryonic development on the basis of dynamic energy budgets. *Journal of Mathematical Biology*, 58, 377-394

Kooijman S.A.L.M. 2010a. *Dynamic energy budget theory for metabolic organization*. 3rd edn. Cambridge University Press.

Kooijman S.A.L.M. 2010b. *Dynamic energy budget theory for metabolic organization.* 3rd edn. Cambridge University Press, Cambridge, MA.

Kooijman S.A.L.M., Sousa T., Pecquerie L., van der Meer J. and Jager T. 2008. From food-dependent statistics to metabolic parameters, a practical guide to the use of Dynamic Energy Budget theory. *Biological Reviews* 83, 533-552.

Lancaster J., Hildrew A.G. and Gjerlov C. 1996. Invertebrate drift and longitudinal transport processes in streams. *Can. J. Fish. Aquat. Sci*, 53, 572-582

Larkin P.A. and McKone D.W. 1985. An evaluation by field experiment of the mclay model of stream drift. *Can. J. Fish. Aquat. Sci*, 42, 909-918

Legleiter, C. J., and P. C. Kyriakidis. 2008. Spatial prediction of river channel topography by kriging, *Earth Surface Processes and Landforms* 33, 841-867.

Lika K., Freitas V., van der Veer H.W., van der Meer J., van der Wijsman J.W.M., Pecquerie L., Kearney M.R. and Kooijman S.A.L.M. 2011. Capturing species diversity with the parameters of the standard DEB model; the covariation method of estimation. *Journal of Sea Research* (submitted).

Locke A., Stalnaker C., Zellmer S., Williams K., Beecher H., Richards T., Robertson C., Wald A., Paul A. and Annear T. 2008. *Integrated approaches to riverine resource management: Case studies, science, law, people, and policy*. Instream Flow Council, Cheyenne, WY.

Lutscher F., Lewis M. and McCauley E. 2006. Effects of heterogeneity on spread and persistence in rivers. *Bulletin of Mathematical Biology*, 68, 2129

Lutscher F., McCauley E. and Lewis M.A. 2007. Spatial patterns and coexistence mechanisms in systems with unidirectional flow. *Theoretical Population Biology*, 71, 267-277

Lutscher F., Pachepsky E. and Lewis M.A. 2005. The effect of dispersal patterns on stream populations. *SIAM Rev.*, 47, 749-772

Madenjian C.P., O'Connor D.V., Chernyak S.M., Rediske R.R. and O'Keefe J.P. 2004. Evaluation of a chinook salmon (*Oncorhynchus tshawytscha*) bioenergetics model. *Canadian Journal of Fisheries and Aquatic Sciences* 61, 627-635.

Mangel M. 1994. Climate-Change and Salmonid Life-History Variation. *Deep-Sea Research Part `II`-Topical Studies in Oceanography* 41, 75-106.

Mangel M. and Satterthwaite W.H. 2008. Combining proximate and ultimate approaches to understand life history variation in salmonids with application to fisheries, conservation, and aquaculture. *Bulletin of Marine Science* 83, 107-130.

McLay C. 1970. A theory concerning the distance traveled by animals entering the drift of a stream. *Journal of the Fisheries Research Board of Canada*, 27, 359-370

Nisbet R.M., Anderson K., McCauley E. and Lewis M.A. 2007. Response of equilibrium states to spatial environmental hetergeneity in advective systems. *Math. Biosci. Eng.*, 4, 1-13

Nisbet R.M., Muller E.B., Lika K. and Kooijman S.A.L.M. 2000a. From molecules to ecosystems through dynamic energy budget models. *Journal of Animal Ecology*, 69, 913-926

Nisbet R.M., Muller E.B., Lika K. and Kooijman S.A.L.M. 2000b. From molecules to ecosystems through dynamic energy budget models. *Journal of Animal Ecology*, 69, 913-926

Oldmeadow D.F., Lancaster J. and Rice S.P. 2010. Drift and settlement of stream insects in a complex hydraulic environment. *Freshwater Biology*, 55, 1020-1035

Pachepsky E., Lutscher F., Nisbet R.M. and Lewis M.A. 2005. Persistence, spread and the drift paradox. *Theoretical Population Biology*, 67, 61

Palmer M.A., Menninger H.L. and Bernhardt E. 2010. River restoration, habitat heterogeneity and biodiversity: A failure of theory or practice? *Freshwater Biology*, 55, 205-222

Parker R.R. and Larkin P.A. 1959. A concept of growth in fishes. *J. Fish. Res. Board Can.*, 16, 721-745

Pecquerie L. 2008. Bioenergetic modelling of the growth, development and reproduction of a small pelagic fish: The bay of biscay anchovy. In. Vrije Universiteit

Peterseni J.H., Deangelas D.L. and Paukert C.P. 2008. An overview of methods for developing bioenergetic and life history models for rare and endangered species. *Transactions of the American Fisheries Society* 137, 244-253.

Quinn T.P. 2005. *The behavior and ecology of pacific salmon and trout*. University of Washington Press, Seattle.

Quinn T.P., Hendry A.P. and Wetzel L.A. 1995. The influence of life history trade-offs and the size of incubation gravels on egg size variation in sockeye salmon (oncorhynchus nerka). *Oikos*, 74, 425-438

Rand P.S. and Hinch S.G. 1998. Swim speeds and energy use of upriver-migrating sockeye salmon (oncorhynchus nerka): Simulating metabolic power and assessing risk of energy depletion. *Canadian Journal of Fisheries and Aquatic Sciences*, 55, 1832-1841

Rombough P.J. 1985. Initial egg weight, time to maximum alevin wet weight, and optimal ponding times for chinook salmon (*oncorynchus tshawytscha*). *Canadian Journal of Fisheries and Aquatic Sciences*, 42, 287-291

Rosenfeld J. 2003. Assessing the habitat requirements of stream fishes: An overview and evaluation of different approaches. *Transactions of the American Fisheries Society*, 132, 953-968

Satterthwaite W.H., Beakes M.P., Collins E.M., Swank D.R., Merz J.E., Titus R.G., Sogard S.M. and Mangel M. 2009. Steelhead Life History on California's Central Coast: Insights from a State-Dependent Model. *Transactions of the American Fisheries Society* 138, 532-548.

Satterthwaite W.H., Beakes M.P., Collins E.M., Swank D.R., Merz J.E., Titus R.G., Sogard S.M. and Mangel M. 2010. State-dependent life history models in a changing (and regulated) environment: steelhead in the California Central Valley. *Evolutionary Applications* 3, 221-243.

Snover M.L., Watters G.M. and Mangel M. 2005. Interacting effects of behavior and oceanography on growth in salmonids with examples for coho salmon (*Oncorhynchus kisutch*). *Canadian Journal of Fisheries and Aquatic Sciences* 62, 1219-1230.

Snover M.L., Watters G.M. and Mangel M. 2006. Top-down and bottom-up control of life-history strategies in coho salmon (*Oncorhynchus kisutch*). *American Naturalist* 167, E140-E157.

Shrimpton J.M., Zydlewski J.D. and Heath J.W. 2007. Effect of daily oscillation in temperature and increased suspended sediment on growth and smolting in juvenile chinook salmon, *oncorhynchus tshawytscha*. *Aquaculture*, 273, 269-276

Sousa T., Domingos T., Poggiale J.C. and Kooijman S. 2010. Dynamic energy budget theory restores coherence in biology introduction. *Philosophical Transactions of the Royal Society B-Biological Sciences*, 365, 3413-3428

Speirs D.C. and Gurney W.S.C. 2001. Population persistence in rivers and estuaries. *Ecology*, 82, 1219-1237

Stewart D.J. and Ibarra M. 1991. Predation and Production by Salmonine Fishes in Lake-Michigan, 1978-88. *Canadian Journal of Fisheries and Aquatic Sciences* 48, 909-922.

Thorpe J.E., Mangel M., Metcalfe N.B. and Huntingford F.A. 1998. Modelling the proximate basis of salmonid life-history variation, with application to Atlantic salmon, *Salmo salar* L. *Evolutionary Ecology* 12, 581-599.

Trudel M., Geist D.R. and Welch D.W. 2004. Modeling the oxygen consumption rates in pacific salmon and steelhead: An assessment of current models and practices. *Transactions of the American Fisheries Society* 133, 326-348.

Trudel M., Tucker S., Morris J.F.T., Higgs D.A. and Welch D.W. 2005. Indicators of energetic status in juvenile coho salmon and chinook salmon. *North American Journal of Fisheries Management* 25, 374-390.

Turchin P. 1998. *Quantitative analysis of movement: Measuring and modeling population redistribution in animals and plants*. Sinauer, Sunderland, Mass., USA.

van der Veer H.W., Kooijman S.A.L.M. and van der Meer J. 2003. Body size scaling relationships in flatfish as predicted by dynamic energy budgets (deb theory): Implications for recruitment. *Journal of Sea Research*, 50, 257-272

Weatherley A.H. and Gill H.S. 1995. Growth. In: *Physiological ecology of pacific salmon* (eds. Groot C, Margolis L & Clarke WC), pp. 101-158. UBC Press, Vancouver

Williams D.D. and Williams N.E. 1993. The upstream/downstream movement paradox of lotic invertebrates: Quantitative evidence from a welsh mountain stream. *Freshwater Biology*, 30, 199-218

Wootton R.J. 1984. Introduction: Strategies and tactics in fish reproduction. In: *Fish reproduction: Strategies and tactics* (eds. Potts GW & Wootton RJ), pp. 1-12. Academic Press, London

Zabel R.W. and Achord S. 2004. Relating size of juveniles to survival within and among populations of chinook salmon. *Ecology* 85, 795-806.

APPENDIX A:
Standard DEB model equations

$$\frac{d}{dt}M_E = \dot{J}_{EA} - \dot{J}_{EC} \quad \text{(A.1)}$$

$$\frac{d}{dt}M_V = \dot{J}_{VG} = (\kappa \dot{J}_{EC} - \dot{J}_{EM})y_{VE} \quad \text{(A.2)}$$

$$\frac{d}{dt}M_H = (1-\kappa)\dot{J}_{EC} - \dot{J}_{EJ} \quad \text{if } M_H < M_H^p \quad \text{, else } \frac{d}{dt}M_H = 0 \quad \text{(A.3)}$$

$$\frac{d}{dt}M_{ER} = 0 \quad \text{if } M_H < M_H^p \quad \text{, else } \frac{d}{dt}M_{ER} = (1-\kappa)\dot{J}_{EC} - \dot{J}_{EJ} \quad \text{(A.4)}$$

with $\dot{J}_{EA} = c(T) f(X) \{\dot{J}_{EAm}\} L^2$ if $M_H \geq M_H^b$ else $\dot{J}_{EA} = 0$ (A.5)

$$\dot{J}_{EC} = c(T)\{\dot{J}_{EAm}\} L^2 \frac{ge}{g+e}\left(1 + \frac{L}{gL_m}\right) \quad \text{(A.6)}$$

$$\dot{J}_{EM} = c(T)[\dot{J}_{EM}] L^3 \quad \text{(A.7)}$$

$$\dot{J}_{EJ} = c(T)\dot{k}_J M_H \quad \text{(A.8)}$$

$$f(X) = \frac{X}{X+K} \quad \text{(A.9)}$$

$$c(T) = \exp\left(\frac{T_A}{T_1} - \frac{T_A}{T}\right) \quad \text{(A.10)}$$

Post Orbital Hyprual (POH) is the measurement that is taken from the rear of the eye opening to the end of the hypural plate, which is the last vertebrae, at the base of the tail.